

60,000 YEAR CLIMATE AND VEGETATION HISTORY OF SOUTHEAST ALASKA

By

Paul S. Wilcox, M.Sc.

A Dissertation Submitted in Partial Fulfillment of the Requirements
for the Degree of

Doctor of Philosophy

In

Geology

University of Alaska Fairbanks

August 2017

©2017 Paul S. Wilcox

APPROVED:

Sarah Fowell, Committee Chair
Nancy Bigelow, Committee Member
Daniel Mann, Committee Member
Jeffrey Dorale, Committee Member
Paul McCarthy, Chair

Department of Geosciences

Paul Layer, Dean

College of Natural Science and Mathematics

Michael Castellini, *Dean of the Graduate School*

Abstract

Sedimentological and palynological analyses of lacustrine cores from Baker Island, located in Southeast Alaska's Alexander Archipelago, indicate that glaciers persisted on the island until ~14,500 cal yr. BP. However, the appearance of tree pollen, including *Pinus cf. contorta ssp. contorta* (shore pine) and *Tsuga mertensiana* (mountain hemlock) immediately following deglaciation suggests that a forest refugium may have been present on ice-free portions of neighboring islands or the adjacent continental shelf. Sedimentological and palynological analyses indicate a variable climate during the Younger Dryas interval between ~13,000 and ~11,500 cal yr. BP, with a cold and dry onset followed by ameliorating conditions during the latter half of the interval. An eight cm-thick black tephra dated to $13,500 \pm 250$ cal yr. BP is geochemically distinct from the Mt. Edgecumbe tephra and thus derived from a different volcano. Based on overall thickness, multiple normally graded beds, and grain size, I infer that the black tephra was emplaced by a large strombolian-style paroxysm. Because the dominant wind direction along this coast is from the west, the Addington Volcanic Field on the continental shelf, which would have been subaerially exposed during the eruption, is a potential source. The similarity in timing between this eruption and the Mt. Edgecumbe eruption suggests a shared trigger, possibly a response to unloading as the Cordilleran Ice Sheet retreated. To complement the Baker Island lacustrine record, a speleothem paleoclimate record based on $\delta^{13}\text{C}$ and $\delta^{18}\text{O}$ values spanning the interval from ~60,000 yr. BP to ~11,150 yr. BP was recovered from El Capitan Cave on neighboring Prince of Wales Island. More negative $\delta^{13}\text{C}$ values are attributed to predominance of angiosperms in the vegetation above the cave at ~22,000 yr. BP and between ~53,000 and ~46,000 yr. BP while more positive $\delta^{13}\text{C}$ values in speleothem EC-16-5-F indicate the presence of gymnosperms. These data suggest limited or no ice cover above El Capitan Cave for the duration of the record, possibly indicating that this region was a nunatak during glacial periods.

Table of Contents

	Page
Title Page.....	i
Abstract.....	iii
Table of Contents.....	v
List of Figures.....	ix
List of Tables.....	xi
Acknowledgments.....	xiii
Appendix.....	xv
Chapter 1 Introduction.....	1
1.1 References.....	4
Chapter 2 Variable Younger Dryas Based on Palynological and Sedimentological Analyses of Lacustrine Cores from Baker Island, Southeast Alaska	7
2.1 Abstract.....	7
2.2 Introduction.....	8
2.3 Study Area.....	9
2.4 Methods.....	9
2.5 Results.....	12
2.5.1 Core Lithology and Chronology.....	12
2.5.2 Pollen.....	15
2.6 Discussion.....	18
2.6.1 Vegetation History Immediately After Deglaciation and Evidence for Refugia.....	18
2.6.2 Climate History.....	21
2.6.2.1 Pre-Younger Dryas.....	21
2.6.2.2 Younger Dryas.....	22
2.6.2.3 Post Younger Dryas.....	26
2.6.3 Broader Younger Dryas Connections: European/Alaska/British Columbia Records.....	29
2.7 Conclusions.....	31
2.8 References.....	32
2.9 Figures.....	38

2.10 Tables.....	45
2.11 Acknowledgments.....	46
2.12 Appendix.....	47
Chapter 3 13,500 cal yr. BP Black Tephra From Baker Island, Southeast Alaska.....	49
3.1 Abstract.....	49
3.2 Introduction.....	50
3.3 Material and Methods.....	50
3.3.1 Chronology.....	51
3.3.2 Analytical Methods.....	52
3.4 Results.....	53
3.5 Discussion.....	54
3.6 Conclusions.....	59
3.7 References.....	60
3.8 Figures.....	64
3.9 Tables.....	74
3.10 Acknowledgements.....	76
Chapter 4 A Speleothem Paleoclimate Record of Southeast Alaska from 60 to 11 ka.....	77
4.1 Abstract.....	77
4.2 Introduction.....	77
4.3 Site Location.....	79
4.4 Climate and Vegetation.....	79
4.5 Methods.....	80
4.6 Results.....	81
4.6.1 Uranium-Series Dating.....	81
4.6.2 Stable Isotopes.....	81
4.7 Discussion.....	82
4.7.1 $\delta^{13}\text{C}$ Record.....	83
4.7.2 $\delta^{18}\text{O}$ Record.....	83
4.7.3 Overlapping records of EC-16-5-F and Baker Island lake core.....	84
4.7.4 EC-16-5-F $\delta^{13}\text{C}$ Extrapolation.....	86

4.7.5 Evidence for Refugia.....	87
4.8 Conclusions.....	88
4.9 References.....	89
4.10 Figures.....	93
4.11 Acknowledgments.....	98
Chapter 5 Conclusion.....	99
5.1 References.....	101

List of Figures

	Page
Figure 2.1: Map showing location of Baker Island.....	38
Figure 2.2: Bathymetry of Bonsai Lake.....	39
Figure 2.3: Baker Island sediment core analyses.....	40
Figure 2.4: Pollen and spore percentage diagram from Baker Island.....	41
Figure 2.5: Pollen and spore influx from Baker Island.....	42
Figure 2.6: Map showing initial pollen arrival patterns.....	43
Figure 2.7: Summary Figure.....	44
Figure A-1: Baker Island Pollen Concentration.....	47
Figure 3.1: Map showing location of Baker Island/Bathymetry.....	64
Figure 3.2: Baker Island core stratigraphy.....	65
Figure 3.3: Age-depth diagram of cores from Baker Island	66
Figure 3.4: Sediment core with tephra unit magnified and highlighted	67
Figure 3.5: Na ₂ O + K ₂ O vs. SiO ₂ of black tephra.....	68
Figure 3.6: Scanning electron image of black tephra.....	69
Figure 3.7: Distribution map of tephtras in western Canada and Alaska.....	70
Figure 3.8: Plot of median diameter versus sorting coefficient.....	71
Figure 3.9: Location of Addington volcanic field/artificial sun-illuminated seafloor map.....	72
Figure 3.10: Map of proposed tephra limits.....	73
Figure 4.1: Site Location of El Capitan Cave and Goliath's Wake Cave/map of El Capitan Cave.....	93
Figure 4.2: Photo of speleothem with U/Th sampling sites and possible unconformities.....	94
Figure 4.3: Age and depth of δ ¹³ C and δ ¹⁸ O samples.....	95
Figure 4.4: Overlapping records of EC-16-5-F and Baker Island lake core.....	96
Figure 4.5: Vegetation interpreted from δ ¹³ C in EC-16-5-F and Goliath's Wake Cave	97

List of Tables

	Page
Table 2.1: List of radiocarbon dates used for chronology on Baker Island.....	45
Table 3.1: List of radiocarbon dates used for chronology on Baker Island.....	74
Table 3.2: Geochemical results from tephra from Baker Island.....	75

Acknowledgments

I would like to thank my Dad who provided constant support throughout this process. I would also like to thank my friends who were willing to adventure with me in the Alaska backcountry. Finally, I would like to thank Pandora's Sugar Ray radio station for providing solid tunes from the late 90's/early 2000's while doing endless hours of pollen processing/pollen identification.

Appendix

Figure A-1: Baker Island Pollen Concentration.....43

Chapter 1: Introduction

There has been much debate over the past 50 years regarding the timing and magnitude of climate events following the last glacial maximum (LGM) and the deterioration of the Cordilleran Ice Sheet ~20,000 yr. BP in Southeast Alaska (e.g. Klein, 1965; Rausch, 1969; Warner et al., 1982; Heaton et al., 1996; Hansen and Engstrom, 1996; Kaufman and Manley, 2004; Lacourse and Mathewes, 2005). The nature of these debates often stems from the possible presence of ice free refugia in the region as well as climate fluctuations during the Younger Dryas (YD) interval. Klein (1965) states that the coastal regions of Alaska were virtually completely overridden by ice during the LGM and the modern flora and fauna became established after the recession of ice. A study of Kodiak Island mammals also discounted Ice Age refugia in favor of postglacial colonization (Rausch, 1969). In addition, a glacial geologic map compiled from numerous reports of statewide glacier extents shows Southeast Alaska completely covered in ice during the LGM (Kaufman and Manley, 2004). However, others suggest that ice free areas existed in the region and supported refugia (Warner et al., 1982; Heaton et al., 1996; Hansen and Engstrom, 1996; Lacourse and Mathewes, 2005).

Refugia in Southeast Alaska would have allowed a habitat suitable for animals and plants to survive the encroachment of the vast Cordillera Ice Sheet during the height of the ice age, possibly including migrating humans (Fagundes, 2008). Ancient bones from bears with genetically distinct DNA from mainland bears have been dated to ~30,000 years BP and to ~13,000 years BP, which hints that a refugium existed (Heaton et al., 1996). In addition, pollen evidence collected from Southeast Alaska's Pleasant Island, which was covered under the Cordillera Ice Sheet during the LGM, indicate that pine woodland was present immediately after deglaciation, which suggests survival within a nearby refugium (Hansen and Engstrom, 1996). Furthermore, a palynological record from sea-cliff exposures of late Pleistocene sediment and peat from the Queen Charlotte Islands spans the last ~18 ka and indicates that at least a portion of Queen Charlotte Island was ice free throughout the late Wisconsin (Warner et al.,

1982; Mathewes et al. 1993; Mandryk et al. 2001). Beyond these hints, there is no definitive evidence that such a refugia existed in the region.

The Younger Dryas (YD) is a cold interval between ~12,800 and ~11,500 cal yr. BP (Alley, 2000) linked to breakdown of thermohaline circulation in the North Atlantic (Broecker et al., 1989). This resulted in severe cooling of the North Atlantic region (Bohncke, 1993; Clark et al., 1999; Isarin and Renssen, 1999). Modeling experiments (Mikolajewicz et al., 1997; Okumura et al., 2009) and foraminiferal oxygen isotope records from the Gulf of Alaska (Praetorius and Mix, 2014) indicate cooling of the North Pacific as well, both by oceanic and atmospheric pathways. Paleovegetation records from coastal Alaska record a subtle change during the YD (Cwynar, 1990; Ager and Rosenbaum, 2007; Ager et al., 2010), while records from central and northern Alaska may record little or no change at all (Kokorowski et al., 2008). Consequently, there is no clear consensus regarding the impact of the YD on the climate or vegetation of Alaska.

To test if refugia existed in the region and develop a consensus on climate during the YD, I employ a suite of proxies including palynology, sedimentology, and speleology. From the present to 13,500 yr. BP, my reconstruction is based on palynological and sedimentological analyses of a sediment core collected from a lake on Baker Island (N 55.281232°, W 133.637559°, 107 m above sea level). Multiple analyses including $\delta^{13}\text{C}$ values, carbon/nitrogen ratios, loss-on-ignition, magnetic susceptibility, and grain size were used for the reconstruction. This resulted in the first palynological evidence for a variable climate throughout the YD in Southeast Alaska, beginning cold and dry but becoming warmer and more humid during the latter half. Results also suggest the possible presence of local refugium based on first arrivals of plant taxa.

From 11,100 to 60,000 yr. BP, the reconstruction is based on a speleothem record from El Capitan Cave on Prince of Wales Island (N 56.162°, W 133.319°, 74 m a.s.l.). $\delta^{13}\text{C}$ and $\delta^{18}\text{O}$ values from the speleothem

were used to determine past climate and vegetation. Because the El Capitan speleothem record overlapped with the Baker Island sediment core record between 11,100 and 13,500 yr. BP, the Baker Island sediment core provided evidence regarding the nature of vegetation changes that drive changes in the speleothem $\delta^{13}\text{C}$ record. The results provide a rare glimpse into climate and vegetation of Southeast Alaska during and prior to the LGM and suggest that areas above the cave may have served as a refugium based on isotope values which indicate that ice above the cave was minimal or absent and vegetation was present throughout the record.

A tephra identified in the Baker Island sediment core was determined to be distinct from other eruptions in the region, such as Mt. Edgecumbe, and therefore unique. The submerged Addington Volcanic Field, which may have been subaerially exposed during the eruption, is consistent with the available data and may have produced the black tephra found in the Baker Island sediment core. Geochemical analyses, grain size, bedding thickness, tephra grain texture, and wind direction were used to determine the likelihood of an Addington Volcanic Field eruption. The age of the tephra, which was deposited during interglacial warming $\sim 13,500$ cal yr. BP, can be used to help calibrate radiocarbon ages among other sites in the region, which can subsequently assist in determining arrival times of key plant taxa.

In this dissertation, I organized logistics for field work, conducted the field research, completed all lab work (except for grain size analyses in Chapter 2), interpreted the data, and developed the main conclusions. Raphael Dreier completed the grain size analyses, seen in chapter 2, as part of an undergraduate research project.

1.1 References

- Ager, T.A. and Rosenbaum, J.G., 2007. Late glacial-Holocene pollen-based vegetation history from Pass Lake, Prince of Wales Island, southeastern Alaska (No. 1760-G). US Geological Survey.
- Ager, T.A., Carrara, P.E., Smith, J.L., Anne, V., Johnson, J., 2010. Postglacial vegetation history of Mitkof Island, Alexander Archipelago, southeastern Alaska. *Quaternary Research* 73(2), 259-268.
- Alley, R.B., 2000. The Younger Dryas cold interval as viewed from central Greenland. *Quaternary science reviews* 19(1), 213-226.
- Bohncke, S. J. P., 1993. Lateglacial environmental changes in the Netherlands: Spatial and temporal patterns. *Quaternary Science Reviews* 12, 707– 717.
- Broecker, W.S., Kennett, J.P., Flower, B.P., Teller, J.T., Trumbore, S., Bonani, G., Wolfli, W., 1989. Routing of meltwater from the Laurentide Ice Sheet during the Younger Dryas cold episode. *Nature* 341, 318-321.
- Clark, P.U., Alley, R.B. and Pollard, D., 1999. Northern Hemisphere ice-sheet influences on global climate change. *Science* 286(5442), 1104-1111.
- Cwynar, L.C., 1990. A late Quaternary vegetation history of Lily Lake, Chilkat Peninsula, southeast Alaska: *Canadian Journal of Botany* 68, 1106-1112.
- Fagundes, N. J., Kanitz, R., Bonatto, S. L., 2008. A reevaluation of the Native American mtDNA genome diversity and its bearing on the models of early colonization of Beringia. *PLoS One* 3(9), e3157.
- Hansen, B.C.S., Engstrom, D.R., 1996. Vegetation history of Pleasant Island, southeastern Alaska, since 13,000 yr B.P. *Quaternary Research* 46, 161-175.
- Heaton, T.H., Talbot, S.L., Shields, G.F., 1996. An ice age refugium for large mammals in the Alexander Archipelago, southeastern Alaska. *Quaternary Research* 46, 186-192.
- Isarin, R.F., Renssen, H., 1999. Reconstructing and modelling Late Weichselian climates: The Younger Dryas in Europe as a case study. *Earth-Science Reviews* 48(1), 1-38.
- Kaufman, D.S., Manley, W.F., 2004. Pleistocene maximum and Late Wisconsinan glacier extents across Alaska, USA. *Developments in Quaternary Sciences* 2, 9-27.
- Klein, D. R., 1965. Postglacial distribution patterns of mammals in the southern coastal regions of Alaska. *Arctic* 18, 7–20.
- Kokorowski, H.D., Anderson, P.M., Mock, C.J., Lozhkin, A.V., 2008. A re-evaluation and spatial analysis of evidence for a Younger Dryas climatic reversal in Beringia. *Quaternary Science Reviews* 27(17), 1710-1722.

- Lacourse, T., Mathewes, R. W., 2005. Terrestrial paleoecology of Haida Gwaii and the continental shelf: Vegetation, climate, and plant resources of the coastal migration route. *Haida Gwaii: Human History and Environment from the Time of Loon to the Time of the Iron People*, 38-58.
- Mandryk, C.A.S., Josenhans, H., Fedje, D.W., Mathewes, R.W., 2001. Quaternary paleoenvironments of Northwestern North America: implications for inland versus coastal migration routes. *Quaternary Science Reviews* 20, 301-314.
- Mathewes, R.W., Heusser, L.E., Patterson, R.T., 1993. Evidence for a Younger Dryas-like cooling event on the British Columbia coast. *Geology* 21, 101-104.
- Mikolajewicz, U., Crowley, T.J., Schiller, A., Voss, R., 1997. Modelling teleconnections between the North Atlantic and North Pacific during the Younger Dryas. *Nature*, 388(6642), 602.
- Okumura, Y.M., Deser, C., Hu, A., Timmermann, A., Xie, S.P., 2009. North Pacific climate response to freshwater forcing in the subarctic North Atlantic: Oceanic and atmospheric pathways. *Journal of Climate* 22(6), 1424-1445.
- Praetorius, S. K., Mix, A. C., 2014. Synchronization of North Pacific and Greenland climates preceded abrupt deglacial warming. *Science* 345, 444-448.
- Rausch, R. L., 1969. Origin of the Terrestrial Mammalian Fauna of the Kodiak Archipelago. *The Kodiak Island Refugium: its Geology, Flora, Fauna and History*. Boreal Institute, University of Alberta, Ryerson Press, 216-234.
- Warner, B.G., Mathewes, R.W., Clague, J.J., 1982. Ice-free conditions on the Queen Charlotte Islands, British Columbia, at the height of late Wisconsin glaciation. *Science* 218(4573), 675-677.

Chapter 2: Variable Younger Dryas Based on Palynological and Sedimentological Analyses of Lacustrine Cores from Baker Island, Southeast Alaska¹

2.1 Abstract

Sedimentological and palynological analyses of lacustrine cores from Baker Island, located in southeast Alaska's Alexander Archipelago, indicate that glaciers persisted on the island until ~14,500 cal yr. BP. However, the appearance of tree pollen, including *Pinus* cf. *contorta* ssp. *contorta* (shore pine) and *Tsuga mertensiana* (mountain hemlock) immediately following deglaciation suggests that forested refugia may have been present on ice-free portions of neighboring islands or the adjacent continental shelf. Influx of *Pinus* and *Tsuga mertensiana* at ~13,500 cal yr. BP suggest establishment of pine parkland following ice retreat. A subsequent decline in the percentages of *Pinus* and *Tsuga mertensiana* accompanied by an increase in *Alnus* pollen and fern spores suggests lowered treeline at the onset of the Younger Dryas (YD), at ~13,000 cal yr. BP. Increasing percentages of *Pinus* at ~12,400 cal yr. BP suggest an increase in temperature and humidity. Conditions continued to ameliorate during the latter half of the YD, between ~12,200 cal yr. BP and ~11,500 cal yr. BP, when percentages of *Pinus* pollen decrease, percentages of *Picea* (spruce) increase, and *Abies* (fir) appears. At ~6,000 cal yr. BP an increase in pollen of the forest taxa *Pinus* and *Abies*, the bog taxon *Lysichiton americanus* (skunk cabbage), and spores of *Sphagnum* indicate cooler temperatures and paludification. Increasing abundances of Cupressaceae (cf. *Juniperus*) pollen accompanied by a decrease in *Lysichiton americanus*, Ericaceae (heath), fern and *Sphagnum* spores at ~5,400 cal yr. BP may be driven by Neoglacial cooling.

¹ Wilcox, P.S., Fowell, S.J., Bigelow, N.H., Baichtal, J.F., Raphael Dreier. 2017. Variable Younger Dryas Based on Palynological and Sedimentological Analyses of Lacustrine Cores from Baker Island, Southeast Alaska. Prepared for submission in the Journal of Palaeogeography, Palaeoclimatology, Palaeoecology.

2.2 Introduction

The Younger Dryas (YD) is a cold interval between ~12,800 and ~11,500 cal yr. BP (Alley, 2000) linked to breakdown of thermohaline circulation in the North Atlantic (Broecker et al., 1989). This resulted in severe cooling of the North Atlantic region (Bohncke, 1993; Clark et al., 1999; Isarin and Renssen, 1999). Modeling experiments (Mikolajewicz et al., 1997; Okumura et al., 2009) and foraminiferal oxygen isotope records from the Gulf of Alaska (Praetorius and Mix, 2014) indicate cooling of the North Pacific as well, both by oceanic and atmospheric pathways.

Paleovegetation records of the YD from the North Atlantic region, in the vicinity of northwest and central Europe, show a sharp transition from a forested landscape during the preceding Late-Glacial interstadial to more open vegetation with tundra and steppe elements (Bohncke, 1993; Madeyska and Kozłowski, 1995; Walker, 1995). Paleovegetation records from coastal Alaska record a more subtle change during the YD (Cwynar, 1990; Ager and Rosenbaum, 2007; Ager et al., 2010), while records from central and northern Alaska may record little or no change at all (Kokorowski et al., 2008). Consequently, there is no clear consensus regarding the impact of the YD on the climate or vegetation of Alaska. For example, in coastal regions of Alaska and British Columbia, Peteet and Mann (1994) identify a fern gap between ~12,700 and ~11,400 cal yr. BP on Kodiak Island, which they interpret as a result of cold, dry YD conditions. Reconstruction of similar conditions on Pleasant Island and Queen Charlotte Island are based on a shift from forest to open, herb-rich vegetation (Mathewes, 1993; Hansen and Engstrom, 1996). Conversely, on Vancouver Island, pre-YD vegetation of *Pinus contorta* and *Alnus*, is replaced by *Tsuga mertensiana* and *Tsuga heterophylla* at ~13,200 cal yr. BP. This is interpreted as a change from relatively cool and dry conditions prior to the YD to cool and humid conditions during the YD (Hebda, 1983). Either there are considerable regional differences in the impact of the YD across the northern Pacific or these studies record different phases of a variable YD. High-resolution palynological and sedimentological analyses of cores from an unnamed lake on Baker Island (Fig. 2.1), in the western Alexander Archipelago

(N 55.281232°, W 133.637559°, 107 m a.s.l.), indicate that climate was cool and dry at the onset of the YD, followed by an increase in both temperature and humidity during the latter half of the interval.

2.3 Study Area

The informally named 'Bonsai' lake (Fig. 2.1) is located in a granitic glacial valley (Ayuso et al., 2005) with steep slopes on the northwest and southeast sides where there is evidence of recent landslides. The lake is in a closed catchment and is bedrock dammed, with a maximum depth of 27 m.

Regionally, common tree species are western hemlock (*Tsuga heterophylla*) and Sitka spruce (*Picea sitchensis*). Mountain hemlock (*Tsuga mertensiana*) is more common in upland forests. Also present are shore pine (*Pinus contorta* ssp. *contorta*), yellow cedar (*Chamaecyparis nootkatensis*), and occasional red cedar (*Thuja plicata*). Red alder trees (*Alnus rubra*) are common in lowlands, while Sitka alder shrubs (*Alnus crispa* ssp. *sinuata*) often form dense thickets along rocky coastlines and stream banks, in avalanche scars, at forest edges, and in the subalpine zone (Pawuk and Kissinger, 1989).

2.4 Methods

A preliminary bathymetric survey was conducted using a Humminbird Matrix 47 3D sonar/GPS unit to map the lakebed and identify optimal coring sites (Fig. 2.2). Cores were collected from a modular raft using a Livingstone piston corer. A 5.3 m core was extracted from 10.19 m of water at site BBL4, near the northeastern end of the lake, and a 3.6 m core was extracted from 7.4 m of water at site BBL6, on the southwestern side of the lake (Fig. 2.2). Both cores terminate in blue-grey clay (Fig. 2.3). A Bolivia corer was used to recover the sediment-water interface at a third site, BBL1, located three meters from site BBL4. Given their proximity, the surface core from BBL1 is combined with the core from BBL4 to create a composite record (Fig. 2.3).

Whole cores were encased in PVC tubing and transported to the National Lacustrine Core Facility (LacCore) in Minneapolis, MN where detailed imaging was performed on a digital line scanner, producing a ~50 MB single image per 1.5 m core section at a resolution of 10 pixels per millimeter. Magnetic susceptibility analyses were conducted with a Geotek MSCL-XYZ core scanner at a resolution of 0.5 cm (Fig. 2.3). Half of the core is archived at LacCore, while the other half was transported to the University of Alaska for further sampling and analyses.

The cores from sites BBL4 and BBL6 cover correlative intervals (Fig. 2.3), but the core from site BBL4 is 1.7 m longer. Therefore this higher-resolution record was selected for detailed palynological and sedimentological analyses. Pollen processing at the University of Alaska Fairbanks followed a modified version of the standard methods described in Traverse (1988). 1 cc of sediment was collected every 2 cm from 475 cm to 425 cm, every 4 cm from 425 cm to 260 cm, and every 8 cm from 260 cm to 0 cm. A tablet containing ~9,660 *Lycopodium* spores was added to each 1cc sample in order to estimate palynomorph concentrations. Assemblage data are based on identification of at least 300 terrestrial pollen grains per sample. Spores were not included in this total. Therefore, the total number of pollen and spores exceeds 300 grains. Percentages of pollen taxa (Fig. 2.4) were calculated based on the sum of all pollen types, excluding spores. Percentages of spores were calculated using the sum of pollen and spores. Pollen and spore influx for each taxon (Fig. 2.5) is calculated by the equation: $((\text{number of grains counted} * 9,660 / \text{exotic } Lycopodium \text{ counted}) / \text{sample vol.}) * (\text{sedimentation rate})$, to determine grains/cm²/year (Faegri et al., 1989). Influx data are used to assess changes in the abundance of each taxon independent of increases or decreases in the other taxa (Faegri et al., 1989). Percentages and concentrations were calculated by means of Tilia software, version 1.7.16 (Grimm, 2011).

The vast majority of fern spores in the Baker Island cores are monolete and psilate. The absence of the perine precludes identification of genera or families (Moore et al., 1991). Pollen grains placed within the Cupressaceae family typically lacked diagnostic gemmae, but the gemmae of *Juniperus* are known to be

deciduous (Faegri et al., 1989). Identifications of cf. *Juniperus* are based on the presence of faint reticulate sculpturing visible on type specimens of *Juniperus* that have lost the gemmae. Reference type slides that were used for identification were created from specimens curated by the University of Alaska Museum of the North herbarium. These slides are available in the paleoecology laboratory at the University of Alaska Fairbanks.

Loss-on-ignition (% organics) was performed at the Arctic Coastal Geoscience Lab (ACGL) at the University of Alaska Fairbanks following standard lab procedures. LOI is calculated using the equation: $LOI_{550} = ((DW_{100} - DW_{550})/DW_{100}) * 100$, where LOI_{550} represents LOI at 550 °C (as a percentage), DW_{100} represents the dry weight of the sample before combustion, and DW_{550} represents the dry weight of the sample after heating to 550 °C (Heiri et al., 2001). 1 cc of sediment was sampled every 1 cm from 475 cm to 425 cm, every 2 cm from 425 cm to 310 cm, and every 4 cm from 310 cm to 0 cm. The influx of inorganic sediment (clastic influx) was calculated by multiplying sedimentation rate (cm/yr) by the mass of sample remaining after heating at 550° C for 90 minutes.

Grain size analysis was performed at the ACGL using a Beckman Coulter Counter LS 320. Samples of sediment were collected every 1 cm from 510 cm to 425 cm and every 2 cm from 425 cm to 0 cm. A gravel unit at 430 cm was too large to analyze in the Coulter Counter.

Carbon and nitrogen stable isotopes were processed using a ThermoFinnigan Continuous Flow Isotope Ratio Mass Spectrometer at the Alaska Stable Isotope Facility at the University of Alaska Fairbanks. 2 to 15 mg of bulk sediment, untreated with acid fumigation/acid washing, was sampled every 4 cm from 470 cm to 430 cm, every 10 cm from 430 to 400 cm, and every 25 cm from 400 to 0 cm. Mass of bulk sediment varied depending on organic content, with smaller masses collected at organic-rich depths determined by loss-on-ignition.

The chronology is based on radiocarbon dates of nine wood fragments and one pollen separate (Table 2.1). One wood fragment was extracted from the center of core BBL6 at 307 cm and eight additional wood fragments were collected from core BBL4 at depths of 55 cm, 120 cm, 180 cm, 227 cm, 320 cm, 380 cm, 422 cm, and 455 cm. Extraction of palynomorphs from a sediment sample at 455 cm provides a duplicate date for this horizon. Due to the location of the lake in a granite basin, macrofossils and pollen collected for Accelerator Mass Spectrometry (AMS) dating have little chance of contamination by old, bedrock-derived carbon.

In preparation for dating, pollen collected at 455 cm in core BBL 4 was separated from 1cc of bulk sediment. Processing followed a procedure modified from Brown et al., (1989): Sieving through 250 μm mesh, treating with 10% HCL, 10% KOH, 48% HF, and 12M H_2SO_4 , and sieving again at 20 μm , resulting in an organic residue consisting primarily of *Picea* pollen.

Samples were cleaned with de-ionized water and sent to Livermore National Laboratory for AMS dating on an HVEC 10 MV Model FN Tandem Van de Graaff Accelerator. AMS ages were calibrated using CALIB 7.0 software with 2σ range (Stuiver et al., 2013). Median ages were calculated from CALIB 7.0 software. Ages of layers between dated horizons are estimated via linear interpolation (Fig. 2.3).

2.5 Results

2.5.1 Core Lithology and Chronology

The basal sediment in cores BBL4 and BBL6 consists of blue-grey clay with a median grain size of $\sim 8 \mu\text{m}$ and high magnetic susceptibility ($\sim 500 \text{ SI } 10^{-5}$) (Fig. 2.3). This is overlain by a black tephra with a median grain size ranging from 25 μm to 120 μm (Fig. 2.3), arranged in multiple fining upward units. Within this unit, magnetic susceptibility spikes to $670 \text{ SI } 10^{-5}$ in BBL4 and $500 \text{ SI } 10^{-5}$ in BBL6 (Fig. 2.3). Assuming a constant rate of sedimentation between dated horizons at 455 cm and 420 cm, the black tephra was deposited $\sim 13,500$ cal yr. BP. In core BBL 4 the black tephra is overlain by 35 cm of silt with a layer of

gravel towards the top of the unit, at 430 cm. A similar gravel layer is found in BBL6 at 322 cm (Fig. 2.3). Above the silt, the remaining 4.05 m of core BBL4 is primarily comprised of organic-rich silt. The organic silt is interrupted at 350 cm by a series of small silt layers extending to 300 cm, distinguished by a lighter color than the surrounding organic silt, with each silt layer no more than 4 cm thick.

$\delta^{13}\text{C}$ and Carbon/Nitrogen (C/N) ratios

$\delta^{13}\text{C}$ is more positive (-25.4‰) early in the record at ~13,500 cal yr. BP (Fig. 2.3). It becomes more negative at ~13,000 cal yr. BP, decreasing to -27.3‰. At ~12,400 cal yr. BP, $\delta^{13}\text{C}$ increases to -25.8‰ and then decreases to -26.8‰ by ~12,200 cal yr. BP. It then gradually increases through the remainder of the record to -25.9‰. The C/N ratio is 14.1 at ~13,500 cal yr BP and increases to 15.0 by ~13,000 cal yr. BP (Fig. 2.3). Ratios decrease to 14.0 at ~12,500 cal yr. BP, increase sharply to 20.7 by ~11,500 cal yr. BP, and fluctuate between 17.9 and 23.0 for the remainder of the record.

Loss-on-ignition (% Organics)

Loss-on-ignition (LOI) is a measure of % organic matter (Heiri et al., 2001). Organic matter percentages are low (~5 %) early in the record at ~13,500 cal yr. BP (Fig. 2.3). They increase to 23% by ~13,000 cal yr. BP and then decrease to ~6% by ~12,500 cal yr. BP. At ~11,800 cal yr. BP, the percentage rises to 32%, gradually drops to 18% at ~9,000 cal yr. BP, rises slightly to ~25% by ~5,500 and remains near this level for the remainder of the record.

Grain size

Median grain sizes are predominantly silt-sized (~8 μm) early in the record at ~14,000 cal yr. BP (Fig. 2.3). They rise to ~98 μm at ~13,500 cal yr. BP and then decline to ~38 μm at ~13,200 cal yr. BP. Afterwards, grain size increases to ~115 μm at ~12,900 cal yr. BP and then decrease to ~40 μm at ~12,500 cal yr. BP. Grain size increases sharply to ~160 μm at ~11,900 cal yr. BP and stays at ~160 μm for

the remainder of the record, except for a small decrease to $\sim 110 \mu\text{m}$ between $\sim 8,000$ cal yr. BP and $\sim 5,600$ cal yr. BP. Because no hydrogen peroxide or a deflocculant were used in the analyses, organic matter was not removed and there was clumping of finer grains, resulting in a grain size increase to sand-sized particles ($\sim 160 \mu\text{m}$), even though no sand grains are evident.

2.5.2 Pollen

Pollen and spore assemblages from the Baker Island core are divided into five zones initially identified by Tilia software, version 1.7.16, and modified based on visual inspection (Fig. 2.4). These zones are described from oldest to youngest.

Zone 5, *Pinus-Alnus* (475 – 456 cm, ~13,500 – 12,900 cal yr. BP).

Pinus initially dominates assemblages in this zone, with 75% of total pollen grains (~8,000 grains/cm²/year) (Fig. 2.4, 2.5). Throughout the zone, *Pinus* decreases to 10% (~300 grains/cm²/year) while *Alnus* increases from 15% to 70% (~1,000 to ~5,000 grains/cm²/year). Fern spores also increase from an initial 20% to 65% (~3,000 to ~12,000 grains/cm²/year). *Picea* first appears in the pollen record at ~13,000 cal yr. BP (455 cm) with 10% of total pollen grains (~100 grains/cm²/year). This zone represents the only period during the record where *Tsuga mertensiana* is consistently present, comprising ~10-15% of total pollen grains (~200-800 grains/cm²/year).

Zone 4, *Pinus-Picea-Alnus* (454 – 412 cm, ~12,800 – 11,500 cal yr. BP). *Pinus* constitutes only 10% of the total pollen at the beginning of this zone (~300 grains/cm²/year) but increases to 20% (~2,000 grains/cm²/year) at ~12,400 cal yr. BP (436 cm). Afterwards, *Pinus* decreases to minor amounts (5%, <300 grains/cm²/year). *Picea* comprises 10% of the basal assemblages (~400 grains/cm²/year) and increases to a zone maximum of 40% (~6,000 grains/cm²/year) at ~12,000 cal yr. BP (430 cm). *Alnus* reaches its peak frequency early in the zone at ~12,700 cal yr. BP (450 cm) with 75% total pollen grains (10,000 grains/cm²/year) and decreases to 55% by the end of the zone (~2,500 grains/cm²/year). Ferns are initially abundant (70%, ~22,500 grains/cm²/year), but decline to 35% (~10,000 grains/cm²/year) by ~11,900 cal yr. BP. (420 cm) and then increase to 65%. However, the increase in the percentage of ferns at the end of this zone is not reflected in the influx data, which decreases to ~9,000 grains/cm²/year.

Fungal spores increase from 10% to 20% throughout the zone (~100 to ~300 grains/cm²/year). *Abies* and *Sphagnum* first appear in very low frequencies at the end of this zone at ~11,700 cal yr. BP (413 cm).

Zone 3, *Picea-Tsuga heterophylla-Alnus* (410 – 352 cm, ~11,400 – 8,300 cal yr. BP). *Picea* remains abundant, with 35% total pollen grains, but influx decreases significantly (between ~10,00 and ~1,500 grains/cm²/year) relative to the previous zone. *Tsuga heterophylla* first appears in small amounts (5%) at ~10,800 cal yr. BP (390 cm), increasing to 15% by the end of the zone. *Tsuga heterophylla* influx is relatively constant at ~500 grains/cm²/year. *Alnus* frequencies vary between 50% and 65% (~500 and ~2,500 grains/cm²/year). Fern spores have consistently high percentages of ~65%, and fungal spores are most abundant during this zone with values ranging from 15% to 20%. Influx estimates reveal decreasing values for both fern and fungal spores throughout the zone, from ~9,000 to ~2,000 grains/cm²/year and ~800 to ~200 grains/cm²/year, respectively.

Zone 2, *Pinus-Picea-Tsuga heterophylla-Alnus* (350 – 255 cm, ~8,200 – 5,500 cal yr. BP). *Pinus* frequencies are low (<5%) except for a small increase to 10% (~1,000 grains/cm²/year) at ~6,000 cal yr. BP (320 cm). *Picea* percentages drop from 35% at the end of zone 3 to 20% at ~8,200 cal yr. BP (350 cm), the beginning of zone 2. *Picea* remains at ~20% for the duration of zone 2; however, influx records an increase from ~1,000 to ~4,000 grains/cm²/year. *Tsuga heterophylla* is most successful during this zone with percentages rising from 15% to 30% at ~8,200 cal yr. BP. The influx of *Tsuga heterophylla* also increases throughout this zone from ~500 to ~5,700 grains/cm²/year. *Alnus* frequencies range from 40-60%, while influx rises from ~500 to ~12,000 grains/cm²/year. *Abies* initially constitutes 10% of total pollen at ~8,200 cal yr. BP but declines to <5% by ~6,000 cal yr. BP. Conversely, the influx of *Abies* rises from ~100 to ~500 grains/cm²/year. *Lysichiton americanus* first appears in the pollen record at ~8,200 cal yr. BP with frequencies of ~5%. *Betula* appears at ~8,200 cal yr. BP and is represented throughout this zone, but with minimal percentages (<5%). Cyperaceae increases in frequency to ~10% beginning at ~5,700 cal yr. BP (270 cm). *Saxifraga* and *Botrychium* first appear in the pollen record at ~8,200 cal yr. BP

and ~6,500 cal yr. BP (325 cm), respectively, with frequencies less than 5%. *Lysichiton americanus*, Ericaceae, and *Sphagnum* are most successful in this zone with frequencies of ~5%. Fern spores drop from 55% to 45% at the onset of the zone, followed by a return to 55% at ~7,500 cal yr. BP (340 cm). Fungal spore percentages drop from 20% to 10% at ~8,200 cal yr. BP.

Zone 1, *Picea-Tsuga heterophylla-Alnus-Cupressaceae* (cf. *Juniperus*) (250 – 0 cm, ~5,400 cal yr. BP – present). *Picea* frequencies range from 10% to 20% throughout the zone, but influx values decrease from ~5,000 to <200 grains/cm²/year. *Tsuga heterophylla* is the dominant arboreal taxon, ranging from 30% to 40% (~1,000 to ~5,000 grains/cm²/year). *Alnus* gradually decreases from an initial frequency of 50% to 20% (~10,000 to ~2,000 grains/cm²/year), its lowest frequency in the record. Cupressaceae first appears in the pollen record at ~5,400 cal yr. BP (250 cm) with low frequencies (3%) but eventually increases to 15% (~200 to ~800 grains/cm²/year). Fern spores show an opposite trend, decreasing from 50% to 15% (~50,000 to <5,000 grains/cm²/year) at ~5,400 cal yr. BP.

2.6 Discussion

2.6.1 Vegetation History Immediately After Deglaciation and Evidence for Refugia

In order to determine arrival times of key taxa during the late Pleistocene, we compiled first post-glacial appearances of three forest taxa, *Pinus*, *Picea*, and *Tsuga mertensiana*, recorded in palynological records from southeast Alaska (Fig. 2.6). As tree taxa typically appear immediately above a glacial clay unit, it seems likely that their arrival is controlled largely by the timing of regional glacial retreat. Initial arrival dates in Fig. 2.6 are based on radiocarbon ages as reported in the literature. All ^{14}C ages were converted to calibrated ages using CALIB 7.0 software (Stuiver et al., 2013).

Because no attempt was made to reassess or revise published dates, large uncertainties in the chronologies are reflected in large uncertainties in arrival times. For example, Hansen and Engstrom (1996) applied an 850-year correction to bulk dates from Pleasant Island because they are older than adjacent AMS dates on conifer needles by 800 to 1000 years. They attribute this error to inputs of ^{14}C -depleted carbon derived from carbonate-rich tills in the catchment. In addition, dates reported by Cwynar (1990) and Peteet (1991) have large uncertainties ranging from ± 210 to ± 450 years, respectively, for ^{14}C basal ages. AMS dates from Queen Charlotte Island (Lacourse et al., 2005), Prince of Wales Island (Ager and Rosenbaum, 2007), and Mitkof Island (Ager et al., 2010) used in Fig. 2.6 have relatively small uncertainties with no mention of a reservoir effect.

Pinus appears on Baker Island at $\sim 13,500 \pm 100$ cal yr. BP, approximately coeval with its appearance on nearby Prince of Wales Island at $\sim 13,700 \pm 100$ cal yr. BP (Ager and Rosenbaum, 2007) and two millennia after its $\sim 15,600 \pm 740$ cal yr. BP arrival on the Queen Charlotte Islands to the south (Lacourse et al., 2005) (Fig. 2.6). North of Baker Island, *Pinus* arrived more recently. For example, *Pinus* appeared on Mitkof Island near Petersburg at $\sim 12,900 \pm 90$ cal yr. BP (Ager et al., 2010), on the Chilkat Peninsula $\sim 12,800 \pm 410$ cal yr. BP (Cwynar, 1990), and in the Yakutat region $\sim 11,800 \pm 590$ cal yr. BP (Peteet,

1991). Younger arrivals to the north support the hypothesis of a northward migration along the coast. However, *Pinus* first appeared on Pleasant Island, approximately 3° of latitude north of Baker Island, at $\sim 14,500 \pm 500$ cal yr. BP (Hansen and Engstrom, 1996), at least four centuries earlier than Baker Island. If this date is correct, it seems that pine trees expanded outward from multiple locations following deglaciation, rather than merely migrating northward. This would require the presence of glacial refugia north of Baker Island and/or on the emergent continental shelf.

Picea appeared on Baker Island at $\sim 13,000 \pm 100$ cal yr. BP after arriving on Queen Charlotte Island at $\sim 13,400 \pm 175$ cal yr. BP (Lacourse et al., 2005). Dates of first appearances on islands to the north do not support northward migration, as first arrivals show no clear trend in a north-south direction. *Picea* colonized the region around Pass Lake, on adjacent Prince of Wales Island at $\sim 11,900 \pm 90$ cal yr. BP (Ager and Rosenbaum, 2007), following a slightly earlier appearance further north, on Mitkof Island, at $\sim 12,200 \pm 180$ cal yr. BP (Ager et al., 2010). *Picea* arrived even earlier, $13,106 \pm 91$ cal yr. BP, on Kruzof Island, where a tree trunk was found in-situ among volcanic flows (Baichtal, 2014). Later arrivals are reported further north. On Pleasant Island and the Chilkat Peninsula, the first arrivals of *Picea* are reported at $\sim 10,850 \pm 290$ cal yr. BP (Hansen and Engstrom, 1996) and $\sim 10,800 \pm 400$ cal yr. BP (Cwynar, 1990), respectively. In the Yakutat region, *Picea* arrives at $\sim 11,800 \pm 590$ cal yr. BP (Peteet, 1991). This irregular spatiotemporal pattern suggests dispersal from multiple locations.

The first appearance of *Tsuga mertensiana* on Baker Island occurs at $\sim 13,500 \pm 100$ cal yr. BP. The relative abundance (10 -15%) of this taxon, which is underrepresented in the pollen rain (Hebda, 1983), is strong evidence for local presence as opposed to long-distance transport. Nevertheless, *Tsuga mertensiana* does not appear at Pass Lake, on adjacent Prince of Wales Island until $\sim 11,920 \pm 90$ cal yr. BP (Ager and Rosenbaum, 2007). *Tsuga mertensiana* arrived on Queen Charlotte Island to the south at $\sim 13,200 \pm 175$ cal yr. BP (Lacourse and Mathewes, 2005), a few centuries after it colonized Baker Island. To the North, sites on Mitkof Island do not record *Tsuga mertensiana* until $\sim 11,200 \pm 70$ cal yr. BP (Ager

et al., 2010). Earlier arrival times on Pleasant Island interrupt the apparent northward migration trend. *Tsuga mertensiana* appears on Pleasant Island at $\sim 15,260 \pm 500$ cal yr. BP, the oldest recorded arrival in southeast Alaska (Hansen and Engstrom, 1996). The early arrival and relative abundance of *Tsuga mertensiana* on Baker Island and Pleasant Island may be indicative of glacial refugia west of the islands on the emergent continental shelf. Alternatively, the ages reported by Hansen and Engstrom (1996) may be too old due to a reservoir effect on Pleasant Island.

Carrara et al. (2007) attempted to use geomorphology to map the extent of ice cover in southeast Alaska during the LGM. Whereas this map indicates that western Baker Island was ice free (Carrara et al., 2007), the presence of blue-gray clay at the base of the cores from 'Bonsai' Lake indicates that glaciers were present in the drainage until $\sim 14,500$ cal yr. BP. Nevertheless, unglaciated areas on the continental shelf to the west, which would have been subaerially exposed during the late Pleistocene (Carrara et al., 2003, 2007; Hetherington et al., 2004; Lacourse et al., 2005; Lacourse and Mathewes, 2005), may have supported refugia. The presence of forested ice age refugia on the emergent continental shelf is supported by a high degree of faunal endemism (Heusser, 1989); 24 mammalian species or subspecies are considered endemic to the Alexander Archipelago (Cook et al., 2001). Early postglacial appearance of *Tsuga mertensiana* on Baker Island, prior to its arrival further south, further supports this hypothesis.

2.6.2 Climate History

Climate histories are based on vegetation reconstruction from pollen analysis as well as geochemical and sedimentological aspects of the core, such as $\delta^{13}\text{C}$ values and the percentage of sedimentary organic matter determined by loss-on-ignition (LOI) (Fig. 2.7). Due to variable sedimentation rates, influx values were calculated for both pollen and clastic material in order to facilitate interpretation. We divide the core into three primary climate zones: Pre-Younger Dryas, Younger Dryas, and Post-Younger Dryas.

2.6.2.1 Pre-Younger Dryas (13,500 – 13,000 cal yr. BP)

In order to better constrain paleoclimate parameters, we assume that *Pinus* pollen in our record was produced primarily by *Pinus contorta* ssp. *contorta* and base our reconstructions on the modern limitations of this taxon (Hultén, 1968). This assumption is supported by the fact that *Pinus contorta* ssp. *contorta* is the only subspecies of the genus found in SE Alaska today (Viereck and Little, 2007; Ager and Rosenbaum, 2007). In addition, *Pinus* pollen appears immediately following glacier retreat on Baker Island, and *Pinus contorta* ssp. *contorta* is an early successional taxon on modern outwash sand and gravel (Viereck and Little, 2007).

Today, *Pinus contorta* ssp. *contorta* occupies cool, wet maritime environments in southeast Alaska with a mean annual temperature range of ~ 0.8 °C to 6.6 °C (Thompson et al., 2006). Therefore the abundance (75 %) of *Pinus contorta* ssp. *contorta* early in the Baker Island record at $\sim 13,500$ cal yr. BP may be indicative of cool and wet conditions. Dominance of this taxon could also indicate the presence of sand and gravel in the substrate (Viereck and Little, 2007; Benn and Evans, 2014) immediately following glacial retreat. The abundance (15%) of *Tsuga mertensiana* also suggests that humid conditions prevailed at $\sim 13,500$ cal yr BP as this taxon is characteristic of humid subalpine environments (Hebda, 1983).

An increase in the influx of clastic sediment ($17 \text{ mg/cm}^2/\text{yr}$) at $\sim 13,500$ cal yr. BP could be indicative of increased precipitation and sediment run-off or sediment input from retreating glaciers. It could also be attributed to sparse vegetation, resulting in decreased slope stabilization and allowing more sediment to enter the lake. Magnetic susceptibility is positively correlative with in-washed, inorganic allochthonous material in lake cores (Thompson et al., 1975). Therefore, the increase in magnetic susceptibility ($200 \text{ MS } 10^{-5}$) at $\sim 13,500$ cal yr. BP is further evidence for an increase in the influx of clastic sediment at this time.

Sparse vegetation following deglaciation may account for the relatively low organic fraction, with the region covered in a pine parkland setting similar to that described by Engstrom et al. (1990) for Pleasant Island. The reduced organic fraction may also be the result of decreased primary productivity within the lake, due to cold temperatures or increased clastic influx resulting in limited light penetration (Guildford et al., 1987). Relatively low C/N ratios indicate minor contributions of terrestrial organic matter to the lake (Meyers and Ishiwatari, 1993), further supporting a sparsely vegetated landscape. More positive $\delta^{13}\text{C}$ values suggest conifers were present on the landscape, as they have significantly enriched $\delta^{13}\text{C}_{\text{leaf}}$ values compared to co-occurring angiosperms and aquatic material (DeLucia et al. 1988; DeLucia and Schlesinger 1991; Lajtha and Barnes 1991; Marshall and Zhang 1994; Van de Water et al., 2002; McCallister and Giorgio, 2008).

2.6.2.2 Younger Dryas (13,000 – 11,500 cal yr. BP)

The decrease in *Pinus* at $\sim 13,000$ cal yr. BP is attributed to cooling associated with the onset of the YD, as it represents a major change in the vegetation in this and numerous other coeval records from southeast Alaska (Engstrom et al., 1990; Hansen and Engstrom, 1996; Ager and Rosenbaum, 2007) and coastal British Columbia (Mathewes, 1993; Lacourse et al., 2005).

Rapid vegetation changes can also be a result of succession and soil development (Chapin et al., 1994). If the decrease in *Pinus* pollen at sites throughout southeast Alaska and coastal British Columbia is due to primary succession, then this change should be asynchronous due to differences in arrival times (Fig. 2.6). On the other hand, if the decrease of *Pinus* is climate driven, it should be synchronous throughout the region. A comparison of published records reveals a decrease in *Pinus contorta* at $12,600 \pm 290$ cal yr. BP on Pleasant Island (Hansen and Engstrom, 1996), at $12,800 \pm 100$ cal yr. BP on Prince of Wales Island (Ager and Rosenbaum, 2007), at $13,000 \pm 175$ cal yr. BP on Queen Charlotte Island (Lacourse et al., 2005), and at $13,000 \pm 100$ cal yr. BP on Baker Island (this study). Therefore, *Pinus* declined synchronously across the region $\sim 12,900$ cal yr. BP. We therefore suggest that the vegetation change at $\sim 13,000$ cal yr. BP on Baker Island is driven by cooler temperatures associated with the onset of the YD. At $\sim 13,000$ cal yr. BP, *Pinus* is replaced by an assemblage of *Alnus* pollen and fern spores comparable to the modern pollen rain at treeline in the Malaspina Glacier District near Yakutat, southeast Alaska (Peteet, 1986). This transition provides further support for the onset of YD. In response to cooler temperatures, the elevation of tree line decreased and the pine parkland disappeared. The modern treeline vegetation of the Malaspina Glacier District is comprised of thick stands of *Alnus crispa* ssp. *sinuata* with ferns of the genus *Dryopteris* in the understory (Peteet, 2017, pers. comm.). An increase in *Alnus* pollen and fern spores follows a decrease in *Pinus* pollen at other sites in southeast Alaska (Cwynar, 1990; Hansen and Engstrom, 1996; Ager and Rosenbaum, 2007), which suggests a regional decrease in the elevation of tree line associated with the YD.

Decreases in the influx of clastic sediment ($7 \text{ mg/cm}^2/\text{yr}$) and magnetic susceptibility ($20 \text{ MS } 10^{-5}$) at $\sim 13,000$ cal yr. BP may indicate limited sediment runoff due to arid conditions or colder temperatures. However, as glacial flour is not evident in the lake core after $\sim 13,500$ cal yr. BP, we infer that glaciers were small or altogether absent from the watershed during the YD.

More negative $\delta^{13}\text{C}$ values at the onset of the YD indicate that the organic matter in the lake was derived from algal or angiosperm sources, as lacustrine algae and *Alnus* have similarly depleted $\delta^{13}\text{C}$ values (algal = -28.4 to -32.5‰ (McCallister and Giorgio, 2008), *Alnus* = -29.2 to -31‰ (Simenstad and Wissmar, 1985) with respect to conifers (-26‰ to -27‰ (Kloepfel et al., 1998; Choi et al., 2005)). It is difficult to constrain the $\delta^{13}\text{C}$ values of the ferns in this record, as the psilate, monoete spores were probably contributed by multiple genera. However, a shade tolerant fern species growing beneath the *Alnus* canopy would be expected to have depleted $\delta^{13}\text{C}$ values due to decreased light intensity (Ehleringer et al., 1986; Medina et al., 1991). Regardless, low C/N ratios indicate minor terrestrial organic input. Therefore, the increase in sedimentary organic matter is attributed to an increase in lacustrine primary productivity, possibly driven by increased light penetration as a result of limited clastic input (Guildford et al., 1987).

Whereas ferns increase during this apparently cold and dry interval, the opposite trend is recorded on Kodiak Island, where a decrease in ferns is thought to represent the onset of cold, dry conditions associated with the YD (Peteet and Mann, 1994). These seemingly contradictory interpretations are a result of the stark difference in pre-YD vegetation at these two sites. On Kodiak Island, the post-glacial vegetation includes ferns but does not include any trees, and the only shrubs consistently present are *Ericales* (Peteet and Mann, 1994). Because of these preceding vegetation differences, ferns responded differently to the cooler and drier YD climate at these two sites.

A 13% increase in *Pinus* pollen during the middle of the YD at ~12,400 cal yr. BP and a coincident decline in *Alnus* pollen and fern spores indicate warmer and more humid conditions. Because *Pinus* is characteristically overrepresented in the pollen record, the low percentages (~20%) suggest that it may not have been locally present (MacDonald and Cwynar, 1985). However, $\delta^{13}\text{C}$ values are nearly identical to those for the pre-YD pine parkland, supporting the presence of conifers in the drainage (Fig. 2.7). Furthermore, the increase in *Pinus* to frequencies of 20% to 30% at ~12,400 cal yr. BP is present in other

records from southeast Alaska and coastal British Columbia (Cwynar, 1990; Hansen and Engstrom, 1996; Lacourse et al., 2005; Ager and Rosenbaum, 2007; Ager et al., 2010) and may be indicative of regional climate amelioration. Rising humidity is supported by increased clastic influx and magnetic susceptibility during this time, possibly due to increased precipitation and sediment runoff. Alternatively, increased clastic influx could be the result of sparse vegetation and increased erosion. Relatively low C/N ratios indicate minor contributions of terrestrial organic matter to the lake (Meyers and Ishiwatari, 1993), further supporting a sparsely vegetated landscape.

The simultaneous decrease in *Pinus contorta* ssp. *contorta* and increase in *Picea sitchensis* pollen at ~12,200 cal yr. BP is indicative of an increase in temperature and/or humidity as *Picea sitchensis* occupies modern-day temperate rainforests in southeast Alaska (Viereck and Little, 2007). Hansen and Engstrom (1996) suggest that an increase in *Picea sitchensis* pollen on Pleasant Island at 11,400 cal yr. BP indicates both rising temperatures and the presence of mineral-rich soils, since *Picea sitchensis* is an edaphically demanding tree that does not prosper on water-saturated, peaty soils. The simultaneous transition to more negative $\delta^{13}\text{C}$ values suggests either a shift to a more closed canopy (Ehleringer et al., 1986; Medina et al., 1991), or a change in the dominant vegetation. We favor development of a more closed canopy at this time, since *Picea sitchensis* has similar $\delta^{13}\text{C}$ values to *Pinus contorta* ssp. *contorta*; They belong to the same family and have $\delta^{13}\text{C}$ values between approximately -26‰ and -27‰ (Kloppel et al., 1998; Choi et al., 2005). C/N ratios increase drastically during this period and remain high for the duration of the record, indicating a predominantly terrestrial signal and limited lacustrine primary productivity in the lake (Meyers and Ishiwatari, 1993).

A layer of gravel that accumulated at ~12,000 cal yr. BP provides further evidence of increased precipitation during the latter part of the YD. Gravel was found in sediment cores extracted from opposite ends of the lake, 4 km apart, indicating a regional increase in landslide or snow avalanche activity or a large single event. Whereas this may have been a stochastic event, it is also possible that

increased landslide activity was a result of greater precipitation. An increase in precipitation would also explain the increase in the influx of predominantly terrestrial organic material between ~12,200 cal yr. BP and ~11,800 cal yr. BP.

Today, southeast Alaska represents the northernmost range limit of *Abies* (Thompson et al., 2006). An increase in this taxon's pollen at ~11,700 cal yr. BP suggests that temperatures approached modern levels near the end of the YD. Conditions during the latter part of the YD thus appear to have been somewhat similar to modern based on the abundance of *Picea sitchensis*, the arrival of *Abies*, minor amounts of *Pinus contorta* ssp. *contorta* pollen, relatively low percentages of fern spores, high percentages of organic matter, and high C/N ratios.

The climate during the YD on Baker Island can thus be divided into three stages. Stage one represents the onset of the YD, when conditions were cool and dry with low percentages of *Pinus*, a predominance of *Alnus* and ferns, high C/N ratios, and low $\delta^{13}\text{C}$ values. Stage 2 represents warmer and more humid conditions during the middle of the YD, when percentages of *Pinus contorta* ssp. *contorta* pollen increase temporarily as percentages of *Alnus* pollen and fern spores decrease, and both clastic influx and $\delta^{13}\text{C}$ values increase. Stage three indicates that the end of the YD was warmer and more humid. *Pinus contorta* ssp. *contorta* was replaced by *Picea sitchensis* and *Abies* and clastic influx suggests an increase in landslide activity.

2.6.2.3 Post Younger Dryas (11,500 cal yr. BP – modern)

Immediately after the YD, between ~11,500 cal yr. BP and ~11,000 cal yr. BP, percentages of *Picea sitchensis* pollen are high, percentages of *Pinus contorta* ssp. *contorta* are low, and there are minimal amounts of bog taxa such as Ericaceae and *Sphagnum*. A gradual replacement of *Picea sitchensis* by *Tsuga heterophylla* that takes place between ~11,000 cal yr. BP and ~6,000 cal yr. BP may indicate rising temperatures as *Tsuga heterophylla* has a slightly higher mean temperature threshold than *Picea*

sitchensis (Thompson et al., 2006). However, primary succession may also be contributing to the replacement of *Picea sitchensis* by *Tsuga heterophylla* in Southeast Alaska (Mann and Hamilton, 1995).

Substantial decrease in clastic sediment influx to 2 mg/cm²/yr after the YD interval may indicate drier conditions resulting in less sediment runoff. However, the decrease in clastic sediment influx may also be due to increased vegetation and slope stabilization.

Warm and dry conditions are seen in other records in southeast Alaska during this period. Hebda (1983) reports warmer and drier conditions at Bear Cove Bog on Vancouver Island between 10,000 cal yr. BP and 7,000 cal yr. BP based on the increase in *Pseudotsuga*, which does not extend that far north today. Heusser et al. (1985) reports similar dry and warm conditions on the North Pacific coast around 8,700 cal yr. BP. Based on pollen-climate transfer functions that relate modern pollen assemblages to temperature and precipitation records from sites between the Aleutian Islands and California, Heusser et al. (1985) estimates an increase in mean July temperature to 3°C above modern and a decrease in mean annual precipitation of 200 mm. On Pleasant Island, initial peat accumulation and the replacement of *Picea sitchensis* by *Tsuga heterophylla* between ~9,500 cal yr. BP and ~8,800 cal yr. BP is considered evidence of increased temperatures (Hansen and Enstrom, 1996). On Queen Charlotte Island, local presence of *Tsuga heterophylla* between ~10,800 cal yr. BP and ~9,900 cal yr. BP suggests a climate warmer than today. However, climate deterioration is indicated shortly afterwards, between ~9,800 cal yr. BP and ~8,150 cal yr. BP, based on a decrease in *Tsuga heterophylla* and increasing percentages of *Tsuga mertensiana* (Pellatt and Mathewes, 1997).

From ~6,000 cal yr. BP to ~4,500 cal yr. BP, there are significant increases in bog taxa such as Ericaceae, *Sphagnum*, and *Lysichiton americanus*, suggesting increased precipitation and paludification (Neiland, 1971). Humid conditions are also indicated by an increase in *Abies* (Thompson et al., 2006). An increase in percentages of *Pinus contorta* ssp. *contorta* at ~6,000 cal yr. BP, from <5 to 10%, may also suggest

increased humidity and possibly cooler temperatures, as small amounts of *Pinus contorta* ssp. *contorta* are only found above 300 m on Baker Island today (Robinson, 1946).

A significant decrease in fern spore percentages at ~5,400 cal yr. BP in the Baker Island record is associated with a 15% rise in Cupressaceae and decreases in percentages of *Lysichiton americanus*, Ericaceae, and *Sphagnum*. Modern representatives of the Cupressaceae in Southeast Alaska include *Thula plicata* (Red Cedar), *Chamaecyparis nootkatensis* (Yellow Cedar), and *Juniperus communis* (Common Juniper) (Viereck and Little, 2007). Adams (2008) noted that specimens of *Juniperus communis* from southeast Alaska and British Columbia are molecularly and physically distinct from other *Juniperus* species. In these regions, *Juniperus* is confined to low-lying muskeg bogs near the ocean in areas that were glaciated during the LGM (Adams, 2008). Cupressaceae pollen from Baker Island shows characteristics consistent with type specimens of *Juniperus communis* that have lost their gemmae, such as size (~28 µm) and low-relief, reticulate sculpture with narrow muri. As *Juniperus communis* can tolerate the lowest mean temperature range of all other conifers in this region (Thompson et al., 2006), increased abundance may be a result of Neoglacial cooling.

Because of the deciduous gemmae, fossil *Juniperus* pollen is difficult to identify, possibly resulting in undercounting of this taxon (Faegri et al., 1989). Nevertheless, Late Holocene increases in Cupressaceae percentages are reported from other pollen records in southeast Alaska and northern British Columbia (Pellatt and Mathewes, 1997; Ager and Rosenbaum, 2007; McLaren, 2008; Ager et al., 2010). In southeast Alaska, small increases (<5%) are reported at ~2,300 cal yr. BP on Mitkof Island (Ager et al., 2010) and at ~6,000 cal yr. BP at Pass Lake (Ager and Rosenbaum, 2007). On Queen Charlotte Island, Pellatt and Mathewes (1997) report percentages of Cupressaceae similar to those in the Baker Island record (~15%) following its first appearance at ~7,400 cal yr. BP. Higher percentages of Cupressaceae are reported from Dundas Island, ~75 km northeast of Queen Charlotte Island, where values reach ~40% at ~5,000 cal yr. BP (McLaren, 2008). These authors attribute the rise in Cupressaceae to the spread of

cedar, indicating decreasing temperature and/or increasing precipitation. Based on subtle sculptural features and overall size, shape, and exine thickness, we attribute the increase in Cupressaceae primarily to the spread of *Juniperus communis*, which is also indicative of cooler temperatures.

Evidence for wetter and/or cooler conditions have been cited by various authors as a result of Neoglacial cooling sometime after ~6,000 cal yr. BP. Wetter conditions between ~6,300 cal yr. BP and ~4,500 cal yr. BP are represented on Queen Charlotte Island by the initiation and expansion of bog taxa (Hebda, 1995). Increased paludification and abrupt *Pinus* expansion (from 1 to 30%) is reported on Pleasant Island between ~7,700 cal yr. BP and ~4,100 cal yr. BP, possibly as a result of a change in climate (Hansen and Engstrom, 1996). However, Hansen and Engstrom (1996) suggest that the increase in bog taxa could also be due to changing edaphic conditions as soils stabilized. On Mitkof Island and the Chilkat Peninsula, *Pinus* percentages increase at ~7,100 cal yr. BP and ~7,600 cal yr. BP, respectively (Ager et al., 2010; Cwynar, 1990). Coeval increases in the percentages of Cyperaceae and *Sphagnum* on Mitkof Island are interpreted to reflect a shift to wetter conditions (Ager et al., 2010). Along the North Pacific coast, mean July temperatures fell by ~4° C and mean annual precipitation increased by ~1,200 mm at ~5,700 cal yr. BP based on pollen-climate transfer functions (Heusser et al., 1985). On Queen Charlotte Island, the minor percentages of *Tsuga heterophylla* and *Picea* at ~3,400 cal yr. BP suggest cooling and associated lowering of tree line (Pellatt and Mathewes, 1994). In the Malaspina Glacier District, wet conditions are cited at ~3,400 cal yr. BP, evidenced by increases in percentages of *Tsuga heterophylla* and *Pinus* (Peteet, 1986).

2.6.3 Broader Younger Dryas Connections: European/Alaska/British Columbia Records

The subdivision of the YD described from Baker Island, starting cold but becoming warmer and more humid during the latter half of the interval, is observed in several European records that show an initial phase of maximum cold followed by a warmer phase (Atkinson et al., 1987; Berglund et al., 1994;

Vandenbergh, 1995). A cold maximum early in the YD is also suggested by $\delta^{18}\text{O}$ values from Greenland ice cores (Stuiver et al., 1995). Bohncke (1993) indicates that this cold maximum in Europe may have taken place between ~12,800 cal yr. BP and ~12,400 cal yr. BP, roughly correlative with the coldest period from the Baker Island record between ~13,000 cal yr. BP and ~12,400 cal yr. BP. In Alaska, Evidence of increased moisture midway through the YD is observed at Discovery Pond in south-central Alaska based on increases in *Pediastrum boryanum* var. *longicorne* and *Pediastrum boryanum* var. *boryanum*, known to respond positively to higher precipitation (Kaufman et al., 2010). In addition, Kaufman et al. (2010) interpret an increase in the minerogenic component of the lake sediment during the latter half of the YD as evidence of increased moisture.

The difference in YD signals in Alaska, with central and northern Alaska showing limited or no vegetation change during the YD and southern Alaska exhibiting more variability in the magnitude and nature of vegetation changes (Kokorowski et al., 2008), is due in part to regional differences in the interstadial vegetation prior to the YD. In order for the YD to be expressed in pollen records, taxa intolerant to YD cooling must have been established during the preceding warm interstadial. For example, *Pinus* is abundant in southern Alaska during interstadial warmth but declines throughout the region at the onset of the YD. *Pinus* was not present in central and northern Alaska. Vegetation in these regions had wider temperature and/or precipitation tolerances, allowing the interstadial taxa to persist during the onset of the YD. Persistence of interstadial vegetation during the YD in portions of northern Europe such as Ireland, England, and Sweden (Isarin and Bohncke, 1999) results in a similarly subtle change in the pollen record.

Sampling resolution may explain differences between records from coastal Alaska and British Columbia that characterize the YD as either dry (Mathewes, 1993; Hansen and Engstrom, 1996) or humid (Hebda, 1983), in that lower resolution sampling may have captured only one phase of the YD.

Pollen and sediment records from Baker Island largely support a synchronization of the North Pacific and North Atlantic climates during the YD based on the similar timing of the event. Praetorius and Mix (2014) also found evidence for synchronization of North Pacific and North Atlantic climates in foraminiferal oxygen isotope records from the Gulf of Alaska. However, based on the decline of *Pinus* at ~13,000 cal yr BP, the onset of the YD occurs ~200 years earlier on Baker and Queen Charlotte Islands (Lacourse et al., 2005) than it does in North Atlantic records (Alley, 2000), suggesting an earlier onset in the North Pacific. Additional sites with well-constrained ages and high resolution pollen reconstructions are needed to confirm this result.

2.7 Conclusions

1. Glaciers remained on Baker Island until ~14,500 cal yr. BP, but the early presence and irregular migration patterns of *Pinus*, *Picea*, and *Tsuga mertensiana* suggest adjacent refugia, possibly on the continental shelf.
2. The decrease in *Pinus* is a key indicator of YD climate cooling in Southeast Alaska. The decline at ~13,000 on Baker Island indicates a slightly (~200 year) earlier onset of the YD than in the North Atlantic.
3. Climate during the YD in Southeast Alaska begins cold and dry based on increases in *Alnus* and ferns and a decrease in clastic influx (~13,000 to ~12,400 cal yr. BP), but becomes warmer and more humid based on increases in *Pinus*, *Picea*, and *Abies* and an increase in clastic influx and landslide activity (~12,400 to ~11,500 cal yr. BP).

2.8 References

- Adams, R.P., 2008. Taxonomy of *Juniperus communis* in North America: Insight from variation in nrDNA SNPs. *Phytologia* 90(2), 181-197.
- Ager, T.A., Rosenbaum, J.G., 2007. Late glacial-Holocene pollen-based vegetation history from Pass Lake, Prince of Wales Island, southeastern Alaska. US Geological Survey Professional Paper 1760-G. US Dept. of the Interior, US Geological Survey.
- Ager, T.A., Carrara, P.E., Smith, J.L., Anne, V., Johnson, J., 2010. Postglacial vegetation history of Mitkof Island, Alexander Archipelago, southeastern Alaska. *Quaternary Research* 73(2), 259-268.
- Alley, R.B., 2000. The Younger Dryas cold interval as viewed from central Greenland. *Quaternary science reviews* 19(1), 213-226.
- Ayuso, R.A., Karl, S.M., Slack, J.F., Haeussler, P.J., Bittenbender, P.E., Wandless, G.A., Colvin, A.S., 2005. Oceanic Pb-isotopic sources of Proterozoic and Paleozoic volcanogenic massive sulfide deposits on Prince of Wales Island and vicinity, southeastern Alaska. *Studies by the US Geological Survey in Alaska*, 1-20.
- Atkinson, T. C., Briffa, K. R., Coope, G. R., 1987. Seasonal temperatures in Britain during the past 22,000 years, reconstructed using beetle remains. *Nature* 325, 587–591.
- Baichtal, J.F., 2014. The Buried Forest of Alaska's Kruzof Island: A Window into the Past. U.S. Department of Agriculture. Retrieved from <https://www.usda.gov/media/blog/2014/03/7/buried-forest-alaskas-kruzof-island-window-past> (accessed 04.05.13).
- Benn, D., Evans, D.J., 2014. *Glaciers and glaciation*. Routledge, London and New York.
- Berglund, B. E., Björck, S., Lemdahl, G., Bergsten, H., Nordberg, K., Kolstrup, E., 1994. Late Weichselian environmental change in southern Sweden and Denmark. *Journal of Quaternary Science* 9, 127–132.
- Bohncke, S. J. P., 1993. Lateglacial environmental changes in the Netherlands: Spatial and temporal patterns. *Quaternary Science Reviews* 12, 707– 717.
- Broecker, W.S., Kennett, J.P., Flower, B.P., Teller, J.T., Trumbore, S., Bonani, G., Wolfli, W., 1989. Routing of meltwater from the Laurentide Ice Sheet during the Younger Dryas cold episode. *Nature* 341, 318-321.
- Brown, T. A., Nelson, D. E., Mathewes, R. W., Vogel, J. S., Southon, J. R. 1989. Radiocarbon dating of pollen by accelerator mass spectrometry. *Quaternary Research* 32, 205-212.
- Carrara, P.E., Ager, T.A., Baichtal, J.F., VanSistine, P.D., 2003. Map of glacial limits and possible glacial refugia in the southern Alexander Archipelago, Alaska, during the late Wisconsin glaciation: U.S. Geological Survey Miscellaneous Field Studies Map MF-2424, scale 1:500,000, with text.

- Carrara, P.E., Ager, T.A., Baichtal, J.F., 2007. Possible refugia in the Alexander Archipelago of southeastern Alaska during the late Wisconsin glaciation. *Canadian Journal of Earth Sciences* 44, 229-244.
- Chapin, F. S. I., Walker, L. R., Fastie, C. L., Sharman, L. C., 1994. Mechanisms of primary succession following deglaciation at Glacier Bay, Alaska. *Ecological Monographs* 64, 149-175.
- Cook, J.A., Bidlack, A.L., Conroy, C.J., Demboski, J.R., Fleming, M.A., Runck, A.M., Stone, K.D., MacDonald, S.O., 2001. A phylogeographic perspective on endemism in the Alexander Archipelago of southeast Alaska. *Biological Conservation* 97(2), 215-227.
- Choi, W.J., Chang, S.X., Curran, M.P., Ro, H.M., Kamaluddin, M., Zwiazek, J.J., 2005. Foliar $\delta^{13}\text{C}$ and $\delta^{15}\text{N}$ response of lodgepole pine and Douglas-fir seedlings to soil compaction and forest floor removal. *Forest Science* 516, 546-555.
- Clark, P.U., Alley, R.B., Pollard, D., 1999. Northern Hemisphere ice-sheet influences on global climate change. *Science* 286(5442), 1104-1111.
- Cwynar, L.C., 1990. A late Quaternary vegetation history of Lily Lake, Chilkat Peninsula, southeast Alaska: *Canadian Journal of Botany* 68, 1106-1112.
- DeLucia, E.H., Schlesinger, W.H., 1991. Resource-use efficiency and drought tolerance in adjacent Great Basin and Sierran plants. *Ecology* 72, 51-58
- DeLucia, E.H., Schlesinger, W.H., Billings, W.D., 1988. Water relations and the maintenance of Sierran conifers on hydrothermally altered rock. *Ecology* 69, 303-311
- Ehleringer, J.R., Field, C.B., Lin, Z.F., Kuo, C.Y., 1986. Leaf carbon isotope and mineral composition in subtropical plants along an irradiance cline. *Oecologia* 70(4), 520-526.
- Engstrom, D.R., Hansen, B.C.S., Wright Jr, H.E., 1990. A possible Younger Dryas record in southeastern Alaska. *Science* 250(4986), 1383.
- Fægri, K., Kaland, P.E., Krzywinski, K., 1989. *Textbook of pollen analysis* (No. Ed. 4). John Wiley & Sons Ltd.
- Guildford, S.J., Healey, F.P., Hecky, R.E., 1987. Depression of primary production by humic matter and suspended sediment in limnocorral experiments at Southern Indian Lake, northern Manitoba. *Canadian Journal of Fisheries and Aquatic Sciences* 44(8), 1408-1417.
- Grimm, E.C., 2011. TILIA software version 1.7.16.
- Hansen, B.C.S., Engstrom, D.R., 1996. Vegetation history of Pleasant Island, southeastern Alaska, since 13,000 yr B.P. *Quaternary Research* 46, 161-175.
- Hebda, R. J., 1983. Late-glacial and postglacial vegetation history at Bear Cove Bog, northeast Vancouver Island, British Columbia. *Canadian Journal of Botany* 61, 3172-3192.

- Hebda, R., 1995. British Columbia vegetation and climate history with focus on 6 ka BP. *Géographie physique et Quaternaire* 49(1), 55-79.
- Heiri, O., Lotter, A.F., Lemcke, G., 2001. Loss on ignition as a method for estimating organic and carbonate content in sediments: reproducibility and comparability of results. *Journal of paleolimnology* 25(1), 101-110
- Hetherington, R., Barrie, J.V., Reid, G.B., MacLeod, R., Smith, D.J., 2004. Paleogeography, glacially induced crustal displacement, and late Quaternary coastlines on the continental shelf of British Columbia, Canada. *Quaternary Science Reviews* 23, 295-318.
- Heusser, C.J., Heusser, L.E., Peteet, D.M., 1985. Late-Quaternary climatic change on the American North Pacific coast. *Nature*, 315(6019), 485-487.
- Heusser, C. J., 1989. North Pacific coastal refugia—the Queen Charlotte Islands in perspective. *The Outer Shores, Proceedings of the Queen Charlotte Islands First International Symposium* (G. G. E. Scudder and N. Gessler, Eds.). University of British Columbia, Vancouver.
- Hultén, E., 1968. *Flora of Alaska and neighboring territories: a manual of the vascular plants*. Stanford University Press: Stanford, CA.
- Isarin, R.F., Renssen, H., 1999. Reconstructing and modelling Late Weichselian climates: The Younger Dryas in Europe as a case study. *Earth-Science Reviews* 48(1), 1-38.
- Isarin, R.F., Bohncke, S.J., 1999. Mean July temperatures during the Younger Dryas in northwestern and central Europe as inferred from climate indicator plant species. *Quaternary Research* 51(2), 158-173.
- Kaufman, D.S., Anderson, S.R., Hu, F.S., Berg, E., Werner, A., 2010. Evidence for a variable and wet Younger Dryas in southern Alaska. *Quaternary Science Reviews* 29(11), 1445-1452.
- Kloepfel, B.D., Gower, S.T., Treichel, I.W., Kharuk, S., 1998. Foliar carbon isotope discrimination in *Larix* species and sympatric evergreen conifers: a global comparison. *Oecologia* 114(2), 153-159.
- Kokorowski, H.D., Anderson, P.M., Mock, C.J., Lozhkin, A.V., 2008. A re-evaluation and spatial analysis of evidence for a Younger Dryas climatic reversal in Beringia. *Quaternary Science Reviews* 27(17), 1710-1722.
- Lacourse, T., Mathewes, R.W., Fedje, D.W., 2005. Late-glacial vegetation dynamics of the Queen Charlotte Islands and adjacent continental shelf, British Columbia, Canada. *Palaeogeography, Palaeoclimatology, Palaeoecology* 226, 36-57.
- Lacourse, T., Mathewes, R.W., 2005. Terrestrial paleoecology of Haida Gwaii and the continental shelf: Vegetation, climate, and plant resources of the coastal migration route, In: *Haida Gwaii: Human History and Environment from the Time of Loon to the Time of the Iron People*. UBC Press, Vancouver and Toronto, pp. 38-58.

- Lajtha K, Barnes FJ., 1991. Carbon gain and water use in pinyon pine-juniper woodlands of northern New Mexico: field versus phytotron chamber measurements. *Tree Physiology* 9, 59- 67.
- MacDonald, G.M., Cwynar, L.C., 1985. A fossil pollen based reconstruction of the late Quaternary history of lodgepole pine (*Pinus contorta ssp. latifolia*) in the western interior of Canada. *Canadian Journal of forest Research* 6, 1039-1044.
- Madeyska, T., Kozłowski, S.K., 1995. Human settlement and paleoenvironmental changes in Poland 20,000-8,000 years ago. *Biuletyn Peryglacjalny* 34.
- Mann, D.H., Hamilton, T.D., 1995. Late Pleistocene and Holocene paleoenvironments of the North Pacific coast. *Quaternary Science Reviews* 14(5), 449-471.
- Marshall J.D., Zhang J., 1994. Carbon isotope discrimination and water-use efficiency in native plants of the north-central Rockies. *Ecology* 75, 1887-1895.
- Mathewes, R.W., 1993. Evidence for Younger Dryas age cooling on the North Pacific coast of America: *Quaternary Science Reviews* 12, 321-331.
- McCallister, S.L., Giorgio, P.A.D., 2008. Direct measurement of the $\delta^{13}\text{C}$ signature of carbon respired by bacteria in lakes: Linkages to potential carbon sources, ecosystem baseline metabolism, and CO₂ fluxes. *Limnology and oceanography* 53(4), 1204.
- McLaren, D., 2008. Sea level change and archaeological site locations on the Dundas Island Archipelago of North Coastal British Columbia. Doctoral dissertation, University of Victoria.
- Medina, E., Sternberg, L., Cuevas, E., 1991. Vertical stratification of $\delta^{13}\text{C}$ values in closed natural and plantation forests in the Luquillo mountains, Puerto Rico. *Oecologia* 87(3), 369-372.
- Meyers, P.A., Ishiwatari, R., 1993. Lacustrine organic geochemistry—an overview of indicators of organic matter sources and diagenesis in lake sediments. *Organic geochemistry* 20(7), 867-900.
- Mikolajewicz, U., Crowley, T.J., Schiller, A., Voss, R., 1997. Modelling teleconnections between the North Atlantic and North Pacific during the Younger Dryas. *Nature* 388(6642), 602.
- Moore, P.D., Webb, J.A., Collison, M.E., 1991. Pollen analysis. Blackwell scientific publications.
- Neiland, B.J., 1971. The forest-bog complex of southeast Alaska. *Vegetatio* 22(1-3), 1-64.
- Okumura, Y.M., Deser, C., Hu, A., Timmermann, A., Xie, S.P., 2009. North Pacific climate response to freshwater forcing in the subarctic North Atlantic: Oceanic and atmospheric pathways. *Journal of Climate* 22(6), 1424-1445.

- Pawuk, W.H., Kissinger, E.J., 1989. Preliminary plant association classification of the Stikine Area, Tongass National Forest. U.S. Dept. of Agriculture Forest Service Report R10-TP-72, Juneau, Alaska, 125.
- Pellatt, M.G., Mathewes, R.W., 1994. Paleoecology of postglacial tree line fluctuations on the Queen Charlotte Islands, Canada. *Ecoscience* 1(1), 71-81.
- Peteet, D.M., 1986. Modern pollen rain and vegetational history of the Malaspina Glacier District, Alaska. *Quaternary Research* 25(1), 100-120.
- Peteet, D. M., 1991. Postglacial migration history of lodgepole pine near Yakutat, Alaska. *Canadian Journal of Botany* 69, 786-796.
- Peteet, D.M., Mann, D.H., 1994. Late-glacial vegetational, tephra, and climatic history on southwestern Kodiak Island, Alaska. *Ecoscience* 1, 255-267.
- Praetorius, S. K., Mix, A. C., 2014. Synchronization of North Pacific and Greenland climates preceded abrupt deglacial warming. *Science* 345, 444-448.
- Robinson, G.D., 1946. Molybdenite Deposits on Baker Island, In: Molybdenite investigations in southeastern Alaska. US Government Printing Office, Washington, pp. 31-36.
- Simenstad, C.A., Wissmar, R.C., 1985. $\delta^{13}\text{C}$ evidence of the origins and fates of organic carbon in estuarine and nearshore food webs. *Marine Ecology Progress Series* 22, 141-152.
- Stuiver, M., Grootes, P. M., Braziunas, T. F., 1995. The GISP2 $\delta^{18}\text{O}$ climate record of the past 16,500 years and the role of the sun, ocean, and volcanoes. *Quaternary Research* 44, 341-354.
- Stuiver, M., Reimer, P.J., Reimer, R.W., 2013. CALIB 7.0. <http://calib.org> (accessed 15.08.13).
- Thompson, R., Battarbee, R.W., O'Sullivan, P.E., Oldfield, F., 1975. Magnetic susceptibility of lake sediments. *Limnology* 20(5), 687-698.
- Thompson, R.S., Anderson, K.H., Strickland, L.E., Shafer, S.L., Pelletier, R.T., Bartlein, P.J., 2006. Atlas of relations between climatic parameters and distributions of important trees and shrubs in North America: Alaska species and ecoregions. US Geological Survey Professional Paper 1650-D. US Dept. of the Interior, US Geological Survey.
- Traverse, A.T., 1988. *Paleopalynology*. Unwin Hyman, Boston.
- Vandenbergh, J., 1995. The climate of the Younger Dryas in the Netherlands. *Geologie en Mijnbouw* 74, 245-249.
- Van de Water, P.K., Leavitt, S.W., Betancourt, J.L., 2002. Leaf $\delta^{13}\text{C}$ variability with elevation, slope aspect, and precipitation in the southwest United States. *Oecologia* 132(3), 332-343.

Viereck, L.A., Little, E.L., 2007. Alaska trees and shrubs. University of Alaska Press, Fairbanks, AK.

Walker, M.J.C., 1995. Climatic changes in Europe during the last glacial/interglacial transition. *Quaternary International* 28, 63-76.

2.9 Figures

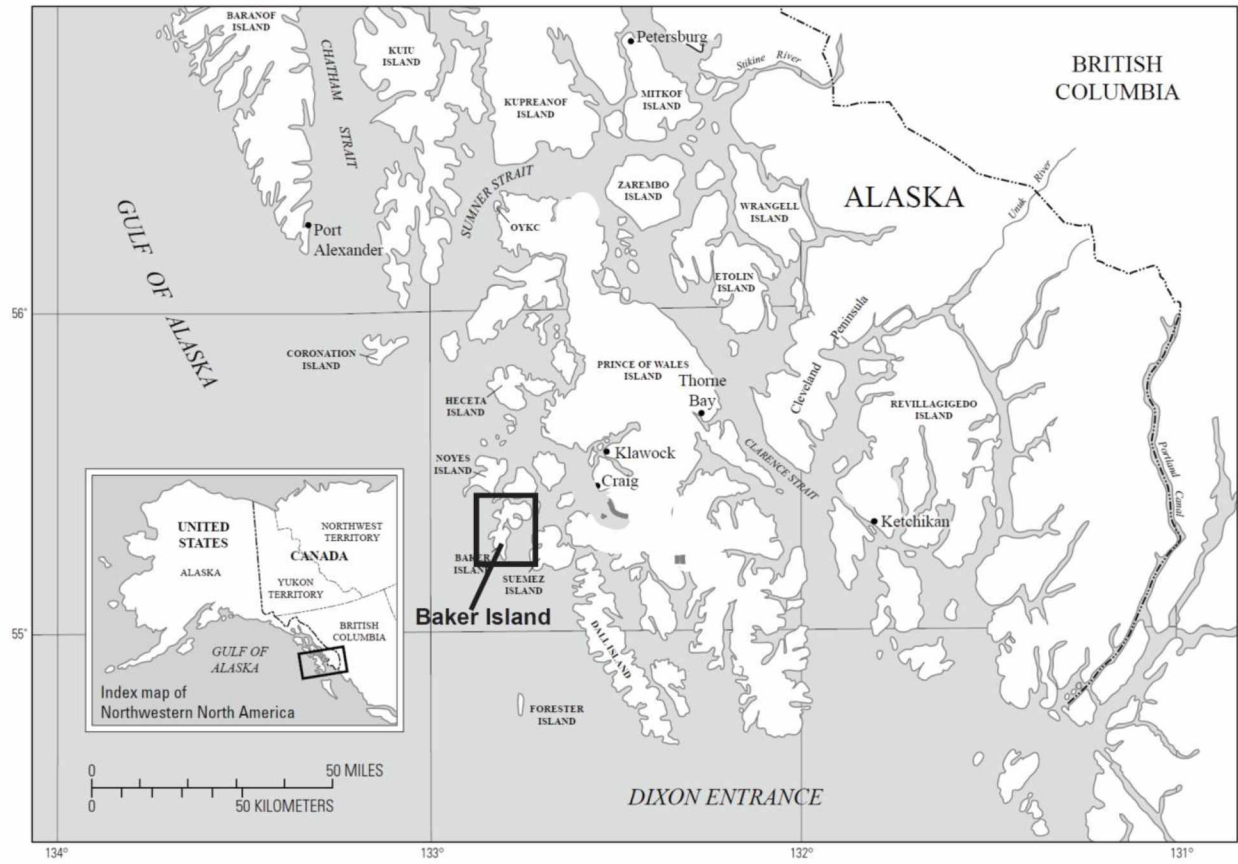


Figure 2.1: Map showing location of Baker Island Map showing location of Baker Island in Southeast Alaska's Alexander Archipelago.

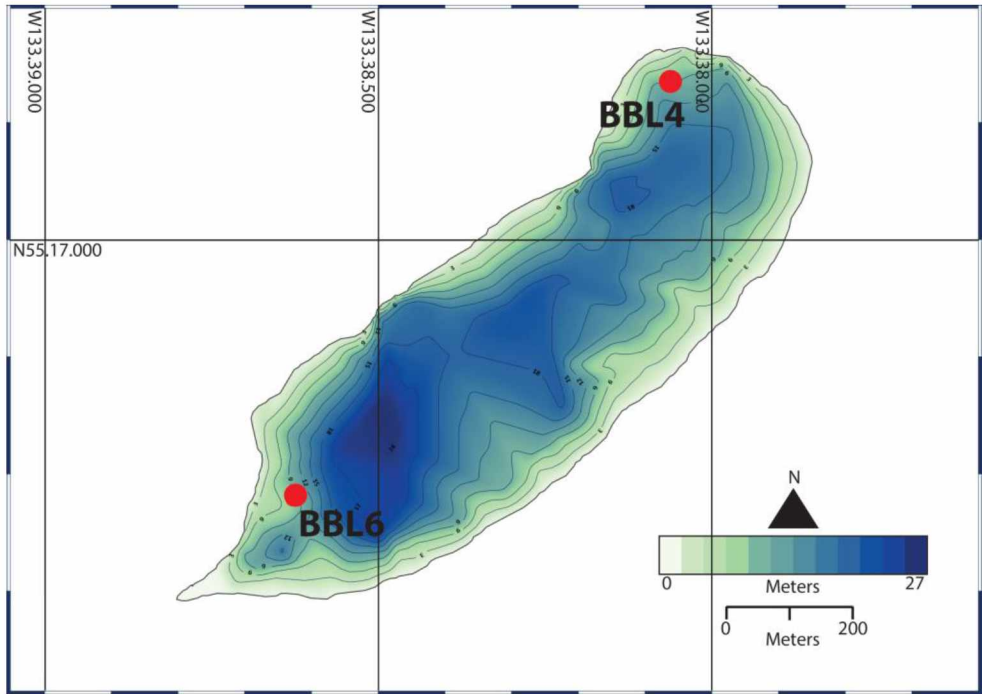


Figure 2.2: Bathymetry of Bonsai Lake. Bathymetry of 'Bonsai' Lake with core site locations. Due to close proximity of sites BBL1 and BBL4, only site BBL4 is shown. BBL2, BBL3, and BBL5 are not shown or mentioned in the text.

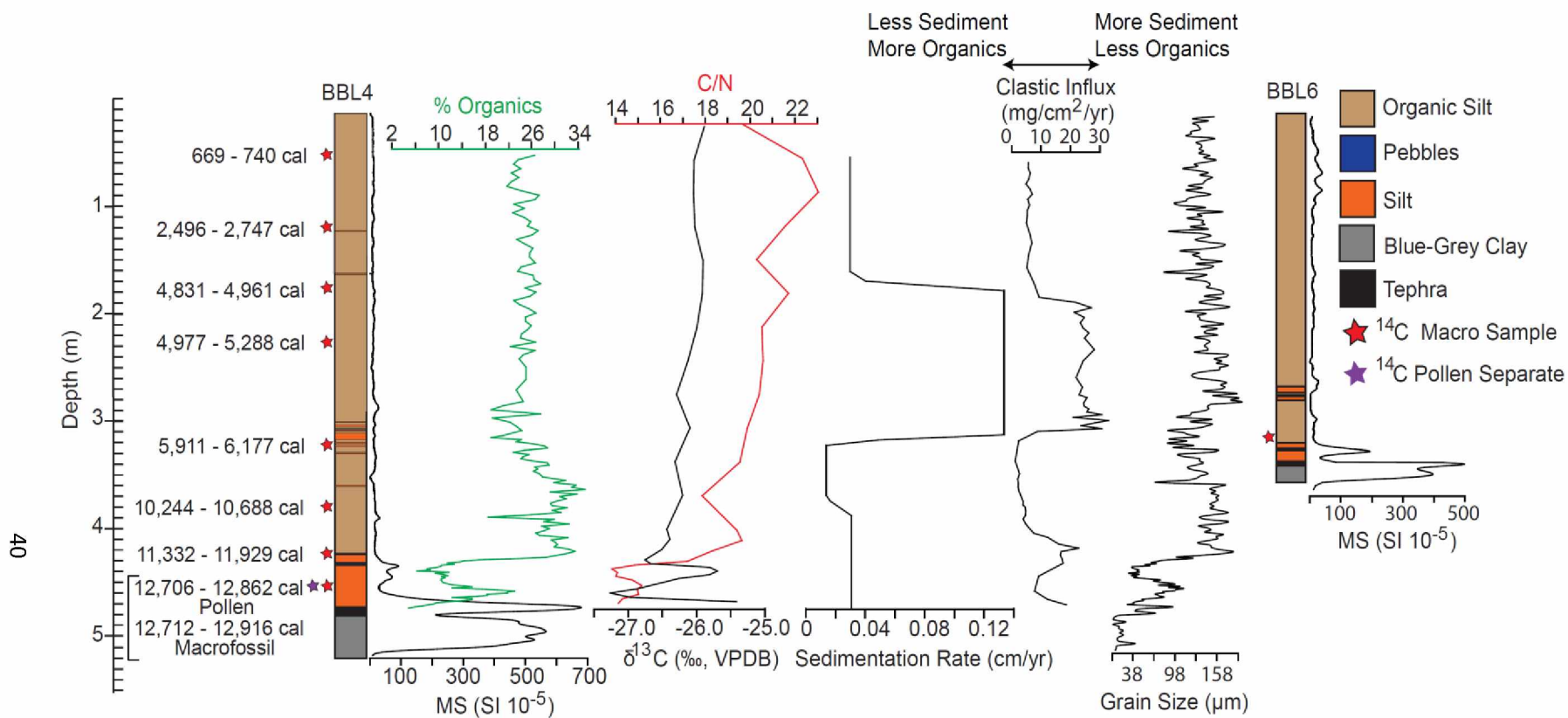


Figure 2.3: Baker Island sediment core analyses. Sediment core from Baker Island showing dated horizons, sediment units, magnetic susceptibility (MS), organic %, $\delta^{13}\text{C}$, C/N ratios, sedimentation rate, clastic Influx, and median grain size. Note that at 455 cm, there are both pollen and wood macrofossil AMS ages.

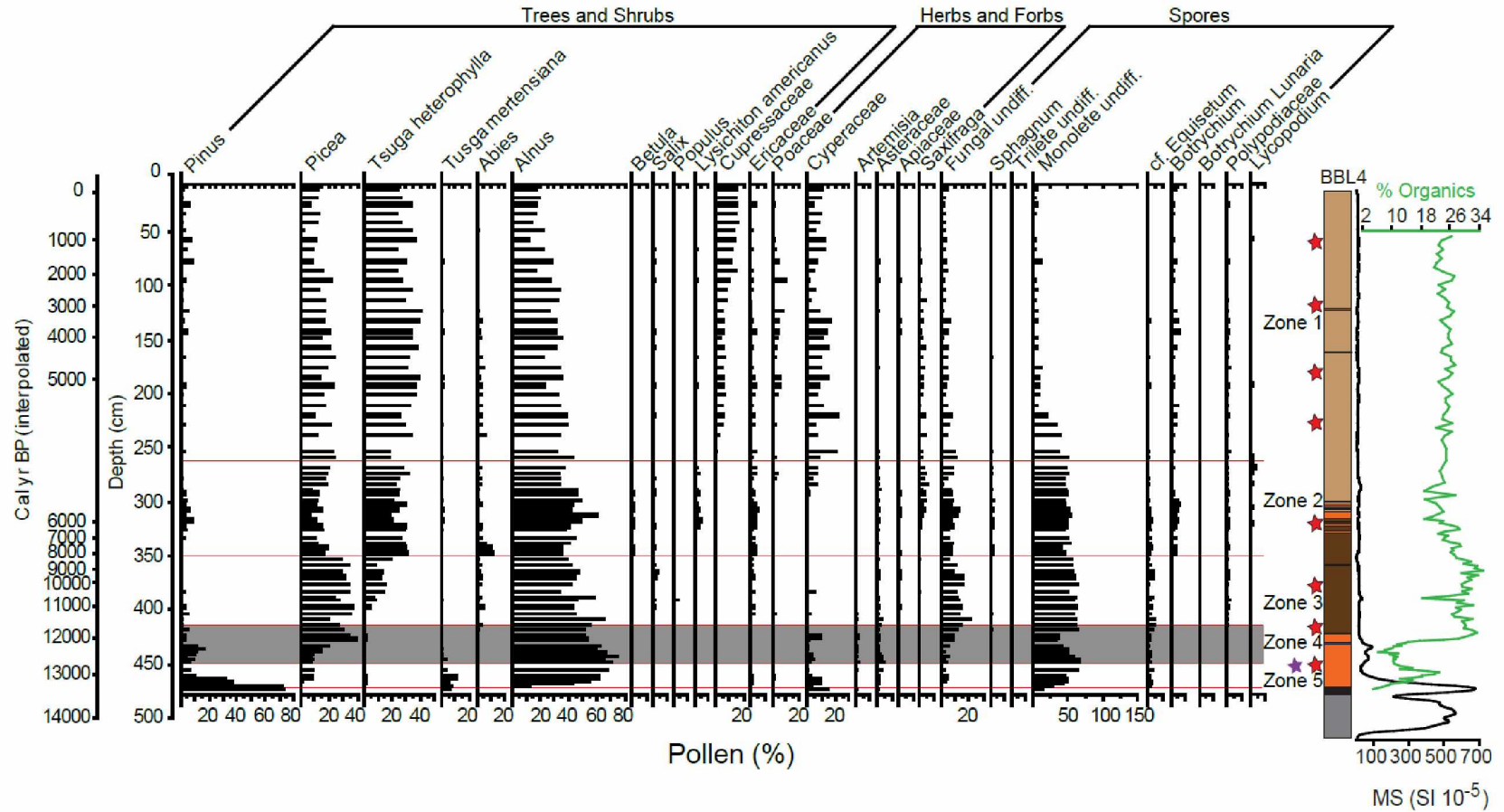


Figure 2.4: Pollen and spore percentage diagram from Baker Island. Red lines indicate zone boundaries. Gray shaded area highlights the Younger Dryas interval with respect to dates defined by Alley (2000). Lake core stratigraphy, magnetic susceptibility (black line), and percent sedimentary organic matter determined by loss-on-ignition (green line) are shown to the right of the diagram. Horizons sampled for radiocarbon dating are indicated by red and purple stars.

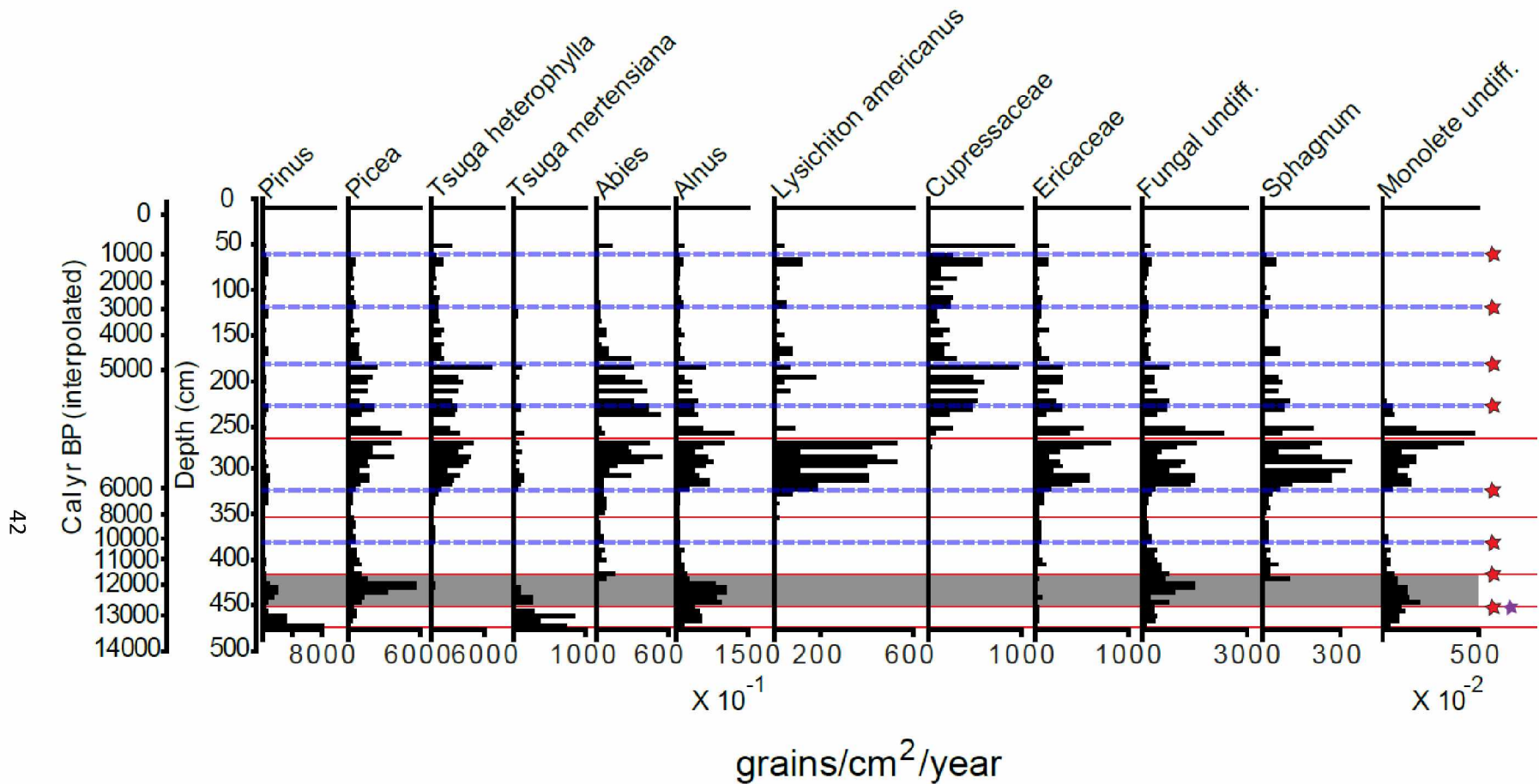


Figure 2.5: Pollen and spore influx from Baker Island. Pollen and spore influx (grains/cm²/year) for key taxa from Baker Island. Red lines indicate zone boundaries. Gray shaded area highlights the Younger Dryas interval with respect to bounding dates defined by Alley (2000). Horizons sampled for radiocarbon dating are indicated by red and purple stars and dashed blue lines. Note that influx values for Alnus and Monolete undifferentiable are $\times 10^{-1}$ and $\times 10^{-2}$, respectively.

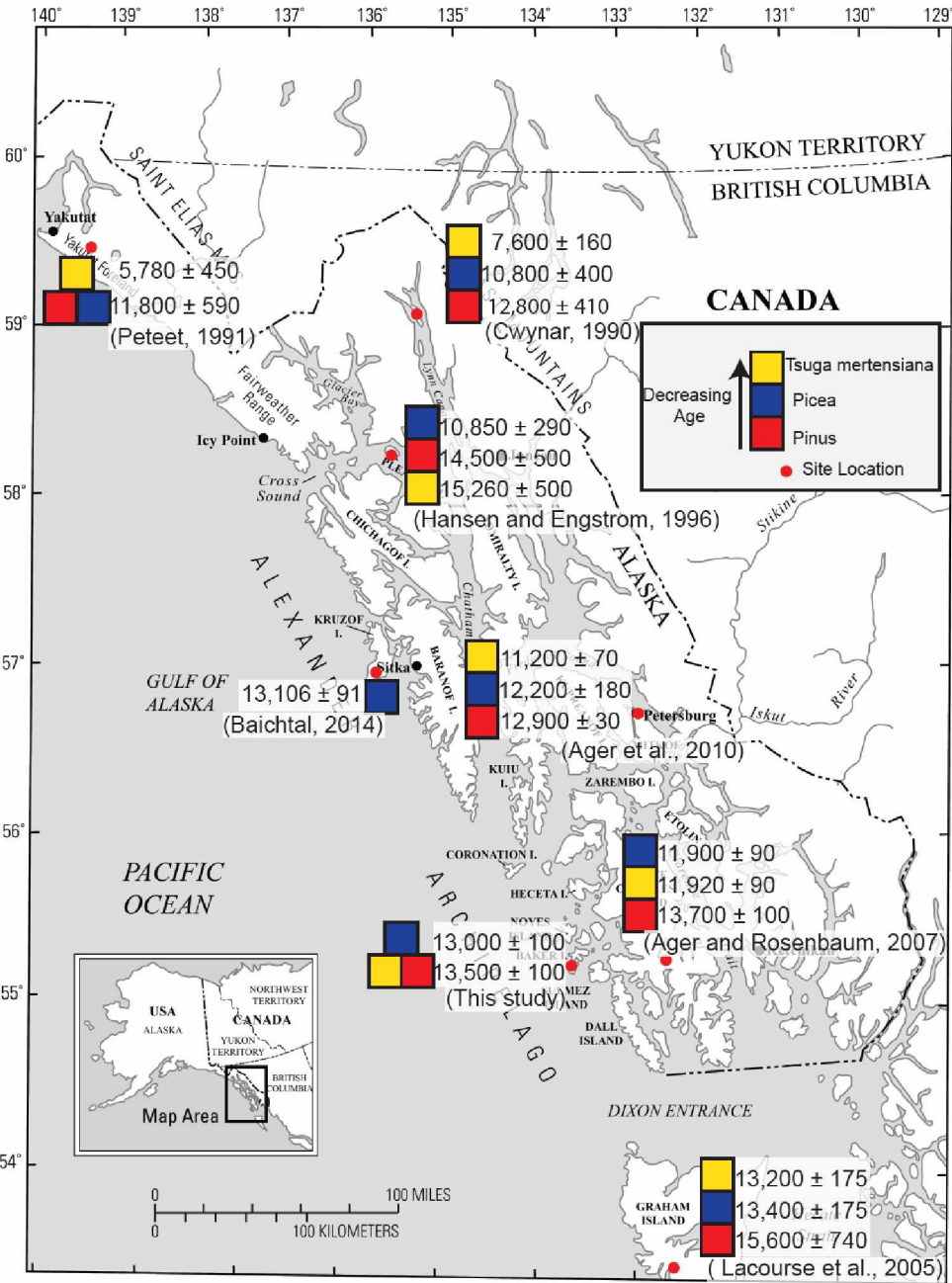


Figure 2.6: Map showing initial pollen arrival patterns. Map showing initial arrival patterns of *Pinus*, *Picea*, and *Tsuga mertensiana* pollen at sites in Southeast Alaska and British Columbia. Median ages were taken from CALIB 7.0 software using the median value of the relative area distribution curve. The Pleasant Island chronology (Hansen and Engstrom, 1996) is questionable due to large uncertainties in the ages of bulk samples.

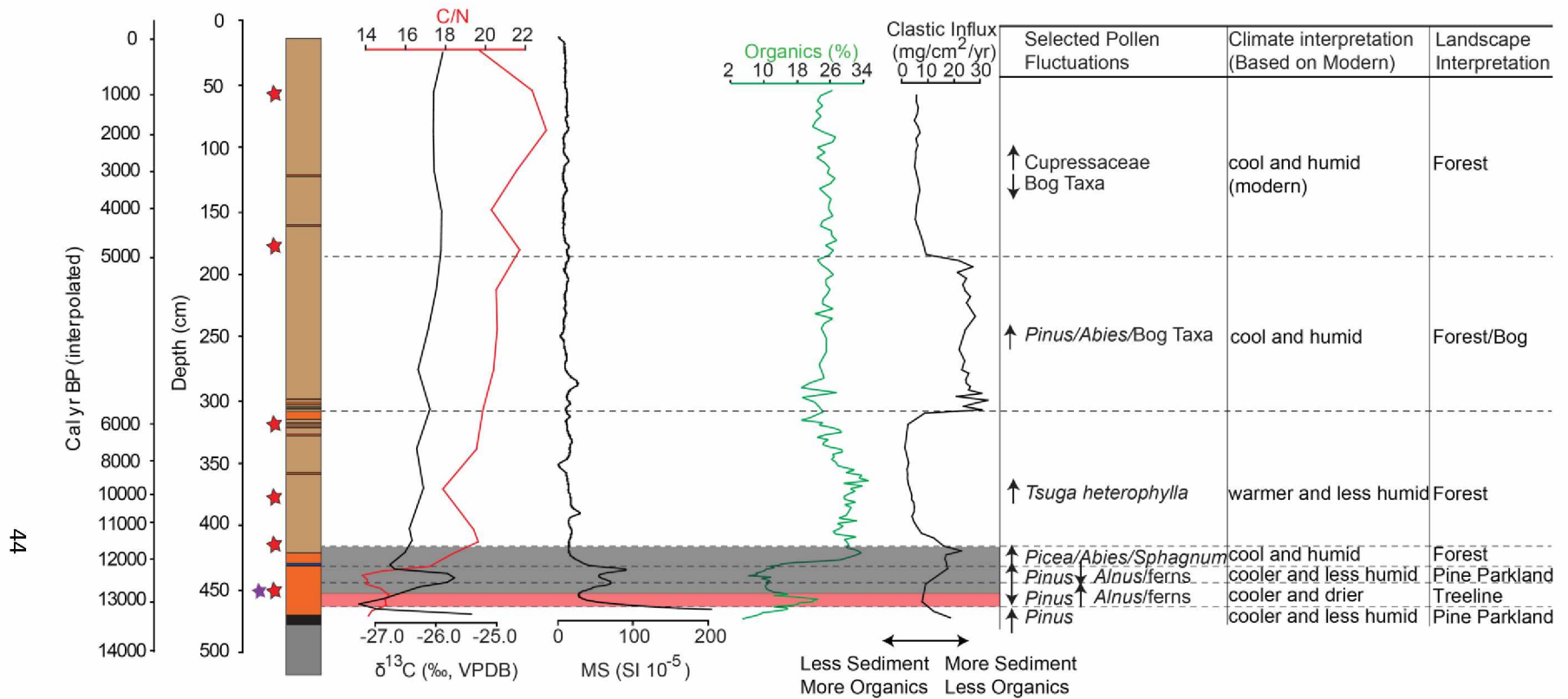


Fig. 2.7: Summary Figure. $\delta^{13}\text{C}$, C/N, MS, Organics, clastic Influx, selected pollen changes, climate interpretations, and landscape interpretations.

Gray shaded area highlights the Younger Dryas (YD) interval with respect to boundaries defined by Alley (2000). Red shaded area highlights apparent early local onset of the YD based on *Pinus* decline. Horizons sampled for radiocarbon dating are indicated by red and purple stars.

2.10 Tables

Table 2.1: List of radiocarbon dates used for chronology on Baker Island. Calibrated ages and median ages were calculated using 2σ range from CALIB 7.0 software. Macrofossils are composed of unidentified wood material.

Sample Location	Material	d ¹³ C	Fraction Modern	±	D ¹⁴ C	±	¹⁴ C age	±	Calibrated age	Median age (cal yr. BP)
BBL4 55 cm	Macrofossil	-25	0.9072	0.0032	-92.8	3.2	780	30	669-740	703
BBL4 120 cm	Macrofossil	-25	0.7290	0.0026	-271.0	2.6	2540	30	2496-2747	2630
BBL4 180 cm	Macrofossil	-25	0.5852	0.0024	-414.8	2.4	4305	35	4831-4961	4864
BBL4 227 cm	Macrofossil	-25	0.5730	0.0020	-427.0	2.0	4475	30	4977-5288	5173
BBL4 320 cm	Macrofossil	-25	0.5214	0.0028	-478.6	2.8	5230	45	5911-6177	5985
BBL4 380 cm	Macrofossil	-25	0.3152	0.0032	-684.8	3.2	9270	90	10244-10688	10451
BBL4 422 cm	Macrofossil	-25	0.2856	0.0016	-714.4	1.6	10065	50	11332-11929	11609
BBL6 307 cm	Macrofossil	-25	0.2766	0.0059	-723.4	5.9	10320	180	11404-12627	12099
BBL4 455 cm	Pollen	-25	0.2563	0.0010	-743.7	1.0	10935	35	12706-12862	12776
BBL4 455 cm	Macrofossil	-25	0.2558	0.0010	-744.2	1.0	10955	35	12712-12916	12789

2.11 Acknowledgments

Funding for this chapter was provided by National Geographic and the Hopkins Fellowship. I would like to the Lawrence Livermore National Laboratory for allowing me to personally process many of the radiocarbon dates found in this chapter.

2.12 Appendix

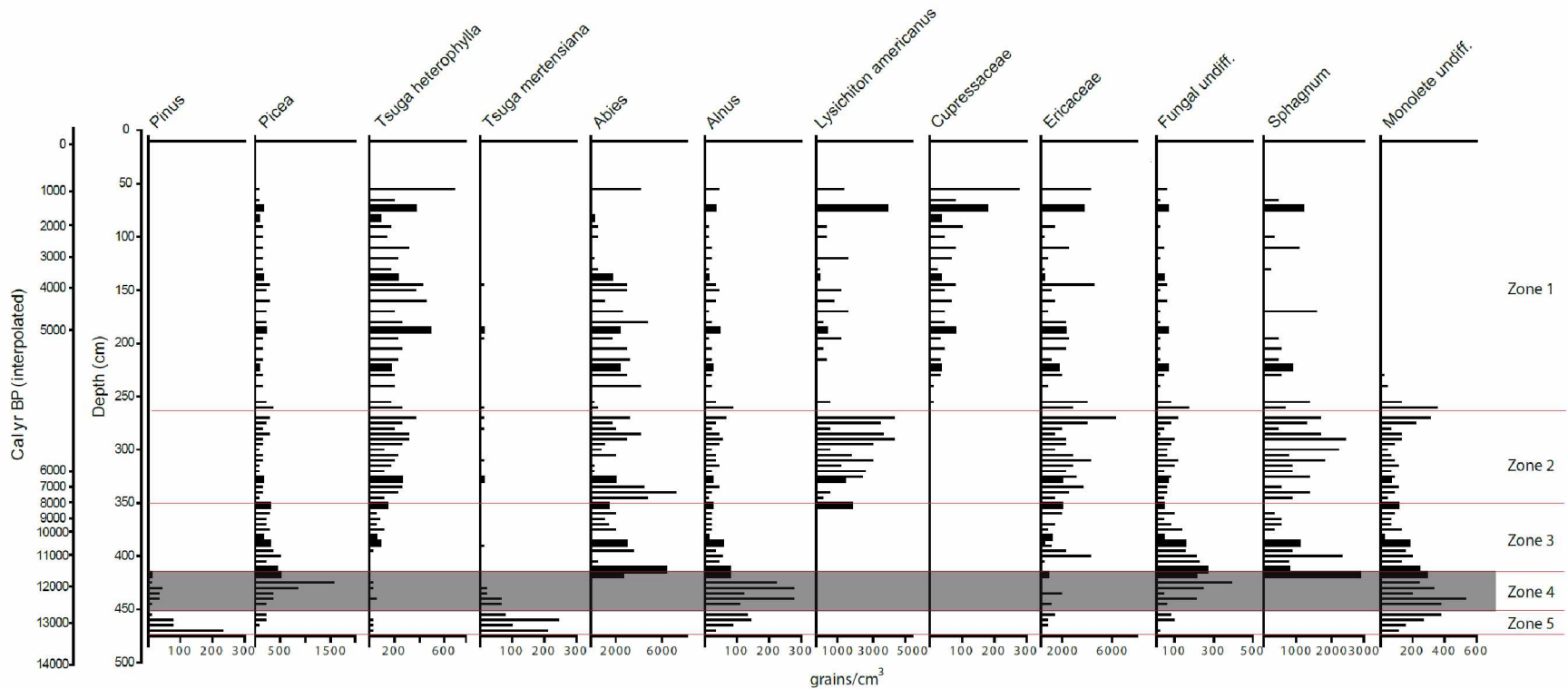


Figure A-1: Baker Island Pollen Concentration. Pollen and spore concentration (grains/cm³) for key taxa from Baker Island. Red lines indicate zone boundaries. Gray shaded area highlights the Younger Dryas interval with respect to ranges defined by Alley (2000).

3.1 Abstract

An eight cm-thick black tephra with nine discrete normally graded beds is present in cores from a lake on Baker Island in Southeast Alaska (N 55.281232° N, W 133.637559° W, 107 m above sea level). Based on interpolation of AMS dates on macrofossils and pollen separates, the age of the tephra is 13,500 ± 250 cal yr. BP (calibrated years before present). Although similar in age to the Mt. Edgecumbe tephra, which was deposited between 13,050 and 13,250 cal yr. BP, this black tephra is geochemically distinct. In addition, it is located 200 km outside of the southernmost limit of deposits from Mt. Edgecumbe. The evidence thus indicates that the black tephra is derived from a different volcanic source. Based on the thickness and the presence of multiple graded beds with median grain size ranging from 25 µm to 120 µm, we infer that the black tephra was emplaced by a large strombolian-style paroxysm. Because the dominant wind direction along this coast is from the west, the submerged Addington Volcanic Field on the continental shelf, which may have been subaerially exposed during the eruption, is a possible source. Consistent with this idea is the presence of a prominent maar feature within the Addington Volcanic Field. If the black tephra on Baker Island was derived from this source, the eruption that produced it may have been a strombolian phase of a maar eruption. The similarity in timing between this eruption and the Mt. Edgecumbe eruption suggests a shared trigger, possibly a response to crustal unloading caused by the retreat of the Cordilleran Ice Sheet.

² Wilcox, P.S., Fowell, S.J., Baichtal, J.F., Mann, D.H., Severin, K. 2017. 13,500 cal yr. BP Black Tephra from Baker Island, Southeast Alaska. Submitted to the Journal of Quaternary Research.

3.2 Introduction

The Late Glacial eruption of Mt. Edgecumbe has proven to be a useful tephrochronologic marker between sites in northern Southeastern Alaska, with deposits correlated from Lituya Bay (Mann and Ugolini, 1985), Juneau (Heusser, 1960), Glacier Bay (McKenzie, 1970) and Sitka (Yehle, 1974) based on tephra composition and decreasing thickness away from eruption site on Kruzof Island (Riehle et al., 1992). However, the fallout area from Mt. Edgecumbe does not extend to southern southeast Alaska (Begét and Motyka, 1998).

The Late Glacial is a period of drastic climate changes (Petit et al., 1999) when an interval of interstadial warming was followed by abrupt Younger Dryas cooling (Alley et al., 1993). As temperatures rose during the Bølling–Allerød interstadial, pollen of forest plants appeared in Southeast Alaska (Cwynar, 1990; Hansen and Engstrom, 1996; Ager and Rosenbaum, 2007; Ager et al., 2010). These early Late Glacial appearances are variously attributed to long distance transport along western Canada (Ritchie and MacDonald, 1986) or dispersal from multiple local refugia (Hansen and Engstrom, 1996; Wilcox et al., 2017, in prep). If a plant species survived in local refugium, its postglacial arrival should be nearly contemporaneous with the onset of favorable climate conditions (Brubaker et al., 2005). Simultaneous northward and southward migration patterns extending from a central location also suggest the presence of refugia (Hansen and Engstrom, 1996; Brubaker et al., 2005; Wilcox et al., 2017, in prep), but documentation of such patterns requires precise dating of first arrivals.

Dating of pollen records from Southeast Alaska relies primarily on radiocarbon dates of macrofossils and bulk samples from lake sediment cores (Cwynar, 1990; Hansen and Engstrom, 1996; Ager and Rosenbaum, 2007). However, certain sites in Southeast Alaska, such as Pleasant Island (Hansen and Engstrom, 1996) and Heceta Island (Ager, 2007), have questionable radiocarbon chronologies due to

possible reservoir effects from limestone bedrock. For example, Hanson and Engstrom (1996) attribute differences of 800 to 1,000 years between bulk dates and from ages of adjacent conifer needles to inputs of ^{14}C -depleted carbon from carbonate-rich tills in the Pleasant Island catchment. Correlation of dated tephra layers provides an additional calibration tool for radiocarbon chronologies, which can help to determine the relative timing of arrivals of plant taxa throughout the region.

A previously undescribed tephra found in a lake sediment core on Baker Island in southern Southeast Alaska was deposited during Late Glacial warming. Identification of this tephra in other records will facilitate accurate dating and clarify migration patterns of forest taxa in southern Southeast Alaska. Compilation of accurate dates of first arrivals will, in turn, provide a reliable test for the existence and relative locations of ice age refugia.

3.3 Material and Methods

Lake sediment cores were obtained from two sites (BBL4 and BBL6) in an unnamed lake (informally named 'Bonsai' Lake) on Baker Island (N 55.281232°, W 133.637559°, 107 m above sea level) (Fig. 3.1). Cores were collected from a modular raft using a Livingstone piston corer. The lake is in a granitic basin with no potential for a reservoir effect. The two cores have a basal age of ~14,500 cal yr. BP (Wilcox et al., 2017, in prep), and the black tephra occurs near the base of both cores immediately above a blue-grey clay interpreted as glacial flour (Fig. 3.2).

3.3.1 Chronology

Samples selected for radiocarbon dating were cleaned with de-ionized water and sent to Lawrence Livermore National Laboratory for Accelerator Mass Spectrometry (AMS) dating. The AMS dating was conducted on an HVEC 10 MV Model FN Tandem Van de Graaff Accelerator. AMS ages were calibrated

using CALIB 7.0 software with 2σ range (Stuiver et al., 2013). Median calibrated ages were calculated from CALIB 7.0 software.

The chronology is based on radiocarbon dates (Table 3.1) of eight wood macrofossils and one pollen separate from BBL4 (55 cm, 120 cm, 180 cm, 227 cm, 320 cm, 380 cm, 422 cm, and 455 cm) and one macrofossil from BBL6 (307 cm). The age of the tephra was determined by assuming a constant sedimentation rate between the median calibrated ages of the lowest two dated horizons (Fig. 3.3), and applying this rate to the 20 cm of sediment between the lowest dated horizon and the top of the tephra. Errors were determined by graphically extrapolating the maximum error range produced by Clam, version 2.2, between the lowest two dated horizons and the top of the tephra (see Fig. 3.3).

3.3.2 Analytical Methods

Tephra compositional analyses were acquired on a JEOL JXA-8530F Electron Microprobe. The beam energy was set to 15 keV, the beam current was set to 10 nA, and the beam diameter was set to ten microns. The standards were Basaltic Glass (BG-3), USNM 113716 for Si ka, Ilmenite, USNM 96189 for Fe ka, Scapolite (Meionite), USNM R6600-1 for Cl ka, KE12 for Na ka, OR10 CT for K ka, and Al ka, Wollastonite (CaSiO₃) for Ca ka, MgO for Mg ka, and ilmenite (68ILM) for Ti ka. Analyses were performed on Probe for EPMA version 5.1 (probesoftware.com). This work was conducted at the University of Alaska Fairbanks Advanced Instrumentation Laboratory (AIL).

We analyzed ten tephra grains from three different depths (475 cm, 480 cm, and 481 cm) for elemental composition (Table 3.2). The working standard was the Old Crow Tephra (provided by Dr. James Begét) because this was the standard used for the Mt. Edgecumbe tephra geochemistry (Addison et al., 2010). The Mt. Edgecumbe geochemistry was conducted on a Cameca microprobe (Addison et al., 2010).

Therefore, five Old Crow tephra grains were analyzed on the JEOL microprobe for comparison with the Old Crow tephra results analyzed on the Cameca microprobe, with each grain being probed once.

Grain size analyses were conducted on samples from 475 cm and 476 cm using a Beckman Coulter Counter LS 320. Tephra grains at 480 cm were imaged on a FEI Quanta 200 Environmental Scanning Electron Microscope.

3.4 Results

In cores from site BBL4, the black tephra is found at 475 cm and has a thickness of eight cm. In cores from site BBL6 the tephra is found at 320 cm and has a thickness of four cm (Fig. 3.2). The eight cm-thick tephra in BBL4 is composed of nine distinct, normally graded beds that range from 0.4 cm to 1.2 cm thick (Fig. 3.4). Median grain sizes within these beds range from medium silt to very fine sand (25 μm to 120 μm) based on the Wentworth grain size scale (Wentworth, 1922). A calculated sedimentation rate of 0.03 cm/yr between the lowest two dated horizons and the black tephra produces a date of $\sim 13,500 \pm 250$ cal yr. BP (Fig. 3.3) for the black tephra.

Geochemical analyses of the Old Crow standard are consistent between the JEOL microprobe and the Cameca microprobe (Table 3.2), meaning that analyses of the black tephra and the Mt. Edgecumbe tephra (Addison et al., 2010) can be compared with a high degree of confidence. Geochemical results indicate that the black tephra on Baker Island is composed of tephrite or trachybasalt (Fig. 3.5). Analysis with the scanning electron microscope reveals angular, vesicular fragments (Fig. 3.6).

3.5 Discussion

A chronology based on accelerator mass spectrometer (AMS) dates on plant macrofossils and pollen separates places the tephra at $13,500 \pm 250$ cal yr. BP, similar in timing to the eruption of Mt.

Edgecumbe at 13,050 - 13,250 cal yr. BP, 200 km to the north (Begét and Motyka, 1998). However, differences in the silica content between the two tephras indicate that they are the product of separate eruptive events.

Multiple late Pleistocene and Holocene tephra deposits in Southeast Alaska can be attributed to eruptions from Mt. Edgecumbe (Riehle et al., 1992; Begét and Motyka, 1998; Addison et al., 2010). The black tephra from Baker Island is similar to the Mt. Edgecumbe tephra with respect to age and grain size. Both tephras are composed of glass shards typically less than $<100 \mu\text{m}$ (Addison et al., 2010). The composition of tephra deposits from Mt. Edgecumbe ranges from basaltic to rhyolitic; however, the late Pleistocene ($\sim 13,250$ cal yr. BP) eruptions generally have high silica content and are rhyolitic (Addison et al., 2010). The black tephra from Baker Island consists of tephrite or trachybasalt (Fig. 3.5), both of which have $\sim 30\%$ less silica than rhyolite, distinguishing it from the Mt. Edgecumbe tephra. The hypothesis that these two tephras are the products of separate volcanic events is supported by their locations. The black tephra lies 200 km south of the documented limit of fallout from the 13,050 – 13,250 cal yr. BP Mt. Edgecumbe eruption (Fig. 3.7) (Begét and Motyka, 1998).

Other well-studied tephra deposits such as the White River, Bridge River, St. Helens, Redoubt, Spurr, Augustine, and Mazama tephras are also considered unlikely to be related to the black tephra as the fallout areas do not include Baker Island (Clague et al., 1995; Riehle et al., 1992; and Fierstein and Hildreth, 2000) (Fig. 3.7). Novarupta has the only volcanic plume that covers the study area (Fierstein

and Hildreth, 2000). However, this eruption occurred in 1912 (Fierstein and Hildreth, 2000), so it is far too young to be the source of the black tephra.

Dated lava flows from volcanic vents near Baker Island are not correlative with the black tephra. On Suemez Island, 10 km east of Baker Island, two rhyolitic domes yield ages of 842 ± 11 ka and 851 ± 17 ka (Karl et al., 2013). These are unlikely to be the source of the black tephra due to large differences in both silica content and age. On western Prince of Wales Island, 20 km east of Baker Island, a basalt flow overlies till and yields an age of 21.5 ± 3.8 ka (Karl et al., 2013). Both the black tephra and the western Prince of Wales flow have low silica content, but the difference in age suggests that these are products of separate eruptions. 32 km south of Baker Island, on northern Dall Island, a pahoehoe lava dates to 6.7 ± 3.3 ka (Karl et al., 2013), too young to be correlative with the black tephra. Middle Tertiary basaltic rocks of the Kuiu-Etolin volcanic belt on Kupreanof Island (Wood and Kienle 1990), 145 km to the north, are too old to be related to the black tephra. Near Ketchikan, 122 km to the east, a basalt flow yielding an age of 42 - 44 ka (Karl et al., 2013) is also too old.

Four sites near Baker Island may contain tephra from the same volcanic event that produced the black tephra. A three cm-thick black tephra bed with a graded top and sharp basal contact was identified in a marine core from the Gulf of Esquibel, 38 km North of Baker Island (Barron et al., 2009). Another tephra, similar to the Gulf of Esquibel tephra, was recovered in a core from Leech Lake on Heceta Island, 15 km to the northwest of the Gulf of Esquibel (Barron et al., 2009). Barron et al. (2009) indicate that the tephtras from the Gulf of Esquibel and Leech Lake are geochemically similar and potentially correlative. Geochemical analyses indicate that the tephtras from Leech Lake and the Gulf of Esquibel have a tephrite composition (unpublished analysis, Addison, 2010, pers. comm.) similar to the black tephra from Baker Island. A second tephra in the Gulf of Esquibel, immediately below the tephrite, has a Hawaiite composition (unpublished analysis, Addison, 2010, pers. comm.), possibly from an earlier phase of the

eruption. Using a linear age model assuming constant sedimentation between ^{14}C samples, the tephra from Leech Lake is estimated to be $16,042 \pm 343$ cal yr. BP (Addison, 2010, pers. comm.). Because of the similar composition of the tephra between Leech Lake and Gulf of Esquibel, the age of $16,042 \pm 343$ cal yr. BP was also applied to the Gulf of Esquibel tephra. A basaltic sandy tephra recovered from a peat core on Heceta Island's Bald Mountain, near Leech Lake, has an age of $15,689 \pm 214$ cal yr. BP (Ager, 2010, pers. comm.) and may be correlative to the Leech Lake and Gulf of Esquibel tephras.

The ages of the Gulf of Esquibel/Leech Lake/Bald Mountain tephras are well outside the age of the black tephra from Baker Island ($\sim 13,500 \pm 250$ cal yr. BP). The age difference may be attributable to Heceta Island's limestone geology (Soja, 1990), such that the older ages are the product of a reservoir effect. Alternatively, these older tephras may be the product of an earlier eruption from the same volcanic field.

It is difficult to decipher eruption style based on tephra alone. The tephritic/trachybasalt composition suggests that the black tephra could be the result of a Strombolian, Hawaiian, Subplinian, or Plinian eruption (Houghton and Gonnermann, 2008). However, the multiple distinct graded beds in the black tephra (Fig. 3.4) record discrete, short-lived events more typical of Strombolian explosivity (Houghton and Gonnermann, 2008), with sequences of explosions lasting a few seconds to tens of seconds (Barberi et al., 1993). Further evidence of Strombolian explosivity is provided by the grain size of the black tephra, which plots largely within the Strombolian eruption range (Fig. 3.8).

The broadly similar ages of the Mt. Edgecumbe tephra, Gulf of Esquibel/Heceta Island tephras, and black tephra may indicate a shared eruptive trigger. One possibility is that ice sheet retreat promoted volcanism through decompression melting in the shallow mantle or a reduction in crustal magma storage time (Praetorius et al., 2016). Based on the coeval onset of Bølling–Allerød interstadial warmth,

disappearance of ice-rafted detritus and rapid vertical land motion associated with regional isostatic rebound, Praetorius et al. (2016) hypothesize that ice sheet deterioration is responsible for volcanic activity at Mt. Edgecumbe. Because the black tephra overlies the blue clay interpreted as glacial flour (Fig. 3.4), we also infer a causal relationship between ice sheet deterioration and the onset of volcanism. Evidence of rapid warming is provided by high concentrations of *Pinus* and *Tsuga mertensiana* pollen that appear in the silt unit immediately above the tephra but are not present in the blue clay below (Wilcox et al., 2017, in prep). Rapid unloading of the crust may have resulted in isostatic rebound and increased volcanic activity (Praetorius et al., 2016).

Today, prevailing wind directions from the Cape Edgecumbe buoy (N 55.600, W 136.101), 220 km northwest of Baker Island, are from the south and west (National Data Buoy Center, 2017). Thus it is likely that the source of the black tephra also lay to the south or west, on the continental shelf. High resolution multibeam seafloor surveys of the continental shelf west of Baker Island reveal a well-defined hole or crater at a depth of ~74 m, surrounded by a low tephra ring and subtle volcanic cones. These features are collectively known as the Addington Volcanic Field (Greene et al., 2011) (Fig. 3.9).

A prominent crater surrounded by ejecta rings suggests that this may be a maar volcanic feature (White and Ross, 2011) and it is interpreted as a maar feature by Karl et al. (2012). Maar style eruptions are known to have variable eruptive phases, including strombolian (White and Ross, 2011). For example, during the 1977 eruption of the Ukinkrek Maar on the Alaska Peninsula, a strombolian phase of the maar eruption deposited 35 scoria fall layers (Kienle et al., 1980). At ~38 km from the Addington Volcanic Field, Baker Island is well within the known limits of strombolian-style paroxysm fallout, which deposits tephra with grain sizes of ~100 μm up to ~50 km from the source (Scasso et al., 1994). These paroxysms consist of violent cannon-like gas bursts typically lasting seconds to minutes and produce

fallout of coarse material over relatively large dispersal areas (Aiuppa et al., 2010). We therefore suggest that the black tephra was deposited by a maar eruption with a strombolian paroxysm phase.

Evidence for a regional glacial forebulge, with minimum uplift of 45 – 60 m between 16,700 and 11,100 cal yr. BP based on shell-bearing raised marine deposits, (Baichtal and Carlson, 2010; Carlson and Baichtal, 2015; Baichtal et al., 2017) led Karl et al. (2012) to suggest that volcanic features associated with the Addington Volcanic Field may have formed during the forebulge.

As no dates or geochemical analyses are available from the Addington Volcanic Field, a direct correlation with the black tephra cannot yet be tested. However, a rock sample of mugearite collected from the crater confirms a basalt-like composition (Greene et al., 2011) with low silica content, broadly similar to the black tephra.

If the Addington Volcanic Field is the source of the black tephra, then the eruption at ~13,500 cal yr. BP would have been subaerial, as regional sea level was up to 150 meters below present due to a combination of extensive inland glaciation (Hetherington et al., 2003) and the presence of a regional forebulge, with maximum uplift at ~13,700 cal yr. BP (Baichtal et al., 2017). Further evidence of a subaerial explosion is provided by tephra grain morphology. Scanning electron microscopy reveals angular, vesicular fragments (Fig. 3.6), typical of high-viscosity magmatic eruptions formed when expanding gases in the magma approach the ground surface (Heiken, 1972). If the black tephra layers from Heceta Island and the Gulf of Esquibel can be attributed to the same event, then the tephra fallout may have covered a limited regional area of southern Southeast Alaska (Fig. 3.10). However, we will not be able to confirm the Addington Volcanic Field as the source of the black tephra until samples from that field are available for geochemical and age analyses.

3.6 Conclusions

The Baker Island black tephra is a new tephro-chronological marker in Late Glacial deposits in southern Southeast Alaska. It is geochemically distinct from the Mt. Edgecumbe tephra in that it is silica poor, with a tephritic/trachybasalt composition, while the Mt. Edgecumbe tephra has a highly siliceous, rhyolitic composition. Further evidence of an alternate source for the black tephra is the fact that it appears to be too far south to be derived from Mt. Edgecumbe (Begét and Motyka, 1998). Based on thickness, presence of multiple distinct graded beds, and grain size, the black tephra is interpreted as the product of a large Strombolian eruption, possibly a paroxysm. Regardless of eruption style, the similarity in timing with the Mt. Edgecumbe eruption at ~13,500 cal yr. BP suggests that the two eruptions may share a trigger. Based on the Baker Island stratigraphy, deglaciation immediately preceded and may have triggered eruptions, as described by Praetorius et al. (2016). Prevailing westerly winds suggest that the source of the eruption may be on the continental shelf. Based on its location less than 50 km west of Baker Island and potential eruptive style, Addington Volcanic field, which contains a prominent maar feature (Greene et al., 2011), is considered a potential source for the black tephra. If the black tephra on Baker Island was derived from this source, the eruption may have been in a strombolian phase of a maar eruption. However, confirmation requires geochemical analyses of samples from the crater in the Addington Volcanic Field.

3.7 References:

- Addison JA, Begét JE, Ager TA, Finney, BP. 2010. Marine tephrochronology of the Mt. Edgecumbe volcanic field, southeast Alaska, USA. *Quaternary Research* **73**(2) : 277-292.
- Ager TA. 2007. Vegetation development on Heceta Island, southeastern Alaska during the late glacial and Holocene. In *Geological Society of America, Program with Abstracts* **39** : 17.
- Ager TA, Rosenbaum J.G. 2007. Late glacial-Holocene pollen-based vegetation history from Pass Lake, Prince of Wales Island, southeastern Alaska. US Geological Survey Professional Paper 1760-G. US Dept. of the Interior, US Geological Survey.
- Ager TA, Carrara PE, Smith JL, Anne V, Johnson J. 2010. Postglacial vegetation history of Mitkof Island, Alexander Archipelago, southeastern Alaska. *Quaternary Research* **73** : 259-268.
- Alley RB, Meese DA, Shuman CA, Gow AJ, Taylor KC, Grootes PM, White JWC, Ram M, Waddington ED, Mayewski PA, Zielinski GA. 1993. Abrupt increase in Greenland snow accumulation at the end of the Younger Dryas event. *Nature* **362** : 527-529.
- Aiuppa A, Burton M, Caltabiano T, Giudice G, Guerrieri S, Liuzzo M, Murè F, Salerno G. 2010. Unusually large magmatic CO₂ gas emissions prior to a basaltic paroxysm. *Geophysical Research Letters* **37**(17).
- Baichtal JF, Carlson RJ. 2010. Development of a Model to Predict the Location of Early Holocene Habitation Sites along the Western Coast of Prince of Wales Island and the Outer Islands, Southeast Alaska. *Current Research in the Pleistocene* **27** : 64-67.
- Baichtal JF, Carlson RJ, Smith JL, Landwehr DJ. 2017. Reconstructing Southeast Alaska's Relative Sea Level History from Raised Shell-bearing Strata and Narrowing the Timing of the Retreat of the Cordilleran Ice Sheet from the Archipelago to near 13,700 Cal. BP. In *47th International Arctic Workshop, Program with Abstracts*.
- Barberi F, Rosi M, and Sodi A. 1993. Volcanic hazard assessment at Stromboli based on review of historical data. *Acta Vulcanol* **3** : 173-187.
- Barron JA, Bukry D, Dean WE, Addison JA, Finney B. 2009. Paleooceanography of the Gulf of Alaska during the past 15,000 years: results from diatoms, silicoflagellates, and geochemistry. *Marine Micropaleontology* **72**(3) : 176-195.
- Begét JE, Motyka RJ. 1998. New dates on late Pleistocene dacitic tephra from the Mount Edgecumbe volcanic field, southeastern Alaska. *Quaternary Research* **49**(1) : 123-125.
- Blaauw, 2010. Clam version 2.2. <http://www.chrono.qub.ac.uk/blaaauw/clam.html> [11 November 2016]

- Brubaker LB, Anderson PM, Edwards ME, Lozhkin AV. 2005. Beringia as a glacial refugium for boreal trees and shrubs: new perspectives from mapped pollen data. *Journal of Biogeography* **32** : 833-848.
- Carlson RJ, Baichtal JF. 2015. A Predictive Model for Locating Early Holocene Archaeological Sites Based on Raised Shell-Bearing Strata in Southeast Alaska, USA. *Geoarchaeology* **30**(2) : 120-138.
- Clague JJ, Evans SG, Rampton VN, Woodsworth GJ. 1995. Improved age estimates for the White River and Bridge River tephras, western Canada. *Canadian Journal of Earth Sciences* **32**(8) : 1172-1179.
- Cwynar LC. 1990. A late Quaternary vegetation history of Lily Lake, Chilkat Peninsula, southeast Alaska. *Canadian Journal of Botany* **68** :1106-1112.
- Fierstein J, Hildreth W. 2000. Preliminary volcano-hazard assessment for the Katmai volcanic cluster, Alaska. US Geological Survey Professional Paper 2000-489. US Dept. of the Interior, US Geological Survey.
- Greene HG, O'Connell VM, Brylinsky CK. 2011. Tectonic and glacial related seafloor geomorphology as possible demersal shelf rockfish habitat surrogates—examples along the Alaskan convergent transform plate boundary. *Continental Shelf Research* **31**(2) : 39-53.
- Hansen BCS, Engstrom DR. 1996. Vegetation history of Pleasant Island, southeastern Alaska, since 13,000 yr B.P. *Quaternary Research* **46** : 161-175.
- Heiken G. 1972. Morphology and petrography of volcanic ashes. *Geological Society of America Bulletin* **83**(7) : 1961-1988.
- Hetherington R, Barrie JV, Reid RG, MacLeod R, Smith DJ, James TS, Kung R. 2003. Late Pleistocene coastal paleogeography of the Queen Charlotte Islands, British Columbia, Canada, and its implications for terrestrial biogeography and early postglacial human occupation. *Canadian Journal of Earth Sciences* **40**(12) : 1755-1766.
- Heusser CJ. 1960. Late-Pleistocene environments of North Pacific North America. *American Geographical Society Special Publication* **35**.
- Houghton BF, Gonnermann HM. 2008. Basaltic explosive volcanism: constraints from deposits and models. *Chemie der Erde-Geochemistry* **68**(2) : 117-140.
- Karl SM, Baichtal JF, Calvert AT, Layer PW. 2012. Pleistocene to Recent volcanoes bracket glacial advances and retreats in southeast Alaska. In *IAVCEI-IACS meeting, program with abstracts*.
- Karl SM, Baichtal JF, Calvert AT, Layer PW. 2013. Pliocene to Recent Alkaline Volcanic Centers in Southeast Alaska: Western Component of the Northern Cordilleran Volcanic Province. *Alaska Geology. Newsletter of the Alaska Geological Society* **44** : 1-2.

- Kienle J, Kyle PR, Self S, Motyka R, Lorenz V. 1980. Ukinrek Maars, Alaska, I. Eruption sequence, petrology and tectonic setting. *Journal of Volcanology and Geothermal Research* **7** : 11-37.
- Mann DH, Ugolini FC. 1985. Holocene glacial history of the Lituya District, southeast Alaska. *Canadian Journal of Earth Sciences* **22** : 913-928.
- McKenzie GD. 1970. Some properties and age of volcanic ash in Glacier Bay National Monument. *Arctic* **23** : 46-49.
- National Data Buoy Center. 2017. http://ndbc-load.nws.noaa.gov/station_history.php?station=46084 [4 May 2017]
- Petit JR, Jouzel J, Raynaud D, Barkov NI, Barnola JM, Basile I, Bender M, Chappellaz J, Davis M, Delaygue G, Delmotte M. 1999. Climate and atmospheric history of the past 420,000 years from the Vostok ice core, Antarctica. *Nature* **399**(6735) : 429-436.
- Praetorius S, Mix A, Jensen B, Froese D, Milne G, Wolhowe M, Addison J, Prahf F. 2016. Interaction between climate, volcanism, and isostatic rebound in Southeast Alaska during the last deglaciation. *Earth and Planetary Science Letters* **452** : 79-89.
- Riehle JR, Mann DH, Peteet DM, Engstrom DR, Brew DA, Meyer CE. 1992. The Mount Edgecumbe tephra deposits, a marker horizon in southeastern Alaska near the Pleistocene-Holocene boundary. *Quaternary Research* **37**(2) : 183-202.
- Ritchie JC, MacDonald GM. 1986. The patterns of post-glacial spread of white spruce. *Journal of Biogeography* **13** : 527-540.
- Scasso RA, Corbella H, Tiberi P. 1994. Sedimentological analysis of the tephra from the 12–15 August 1991 eruption of Hudson volcano. *Bulletin of Volcanology* **56**(2) : 121-132.
- Soja CM. 1990. Island arc carbonates from the Silurian Heceta Formation of southeastern Alaska (Alexander terrane). *Journal of Sedimentary Research* **60**(2).
- Stuiver M, Reimer PJ, Reimer RW. 2013. CALIB 7.0. <http://calib.org>. [15 August 2013]
- Wentworth C.K. 1922. A scale of grade and class terms for clastic sediments. *The Journal of Geology* **30**(5) : 377-392.
- White JD, Ross PS. 2011. Maar-diatreme volcanoes: a review. *Journal of Volcanology and Geothermal Research* **201**(1) : 1-29.
- Wilcox, P.S., Fowell, S.J., Bigelow, N.H., Baichtal, J.F., Raphael Dreier. 2017. Variable Younger Dryas Based on Palynological and Sedimentological Analyses of Lacustrine Cores from Baker Island, Southeast Alaska. Prepared for submission in the *Journal of Palaeogeography, Palaeoclimatology, Palaeoecology*.

Wood CA, Kienle J. 1990. Volcanoes of North America. Cambridge University Press: Cambridge.

Yehle LA. 1974. Reconnaissance Engineering Geology of Sitka and Vicinity, Alaska, with Emphasis on Evaluation of Earthquake and Other Geologic Hazards. U.S. Geological Survey Open-File Report 74-53.

3.8 Figures

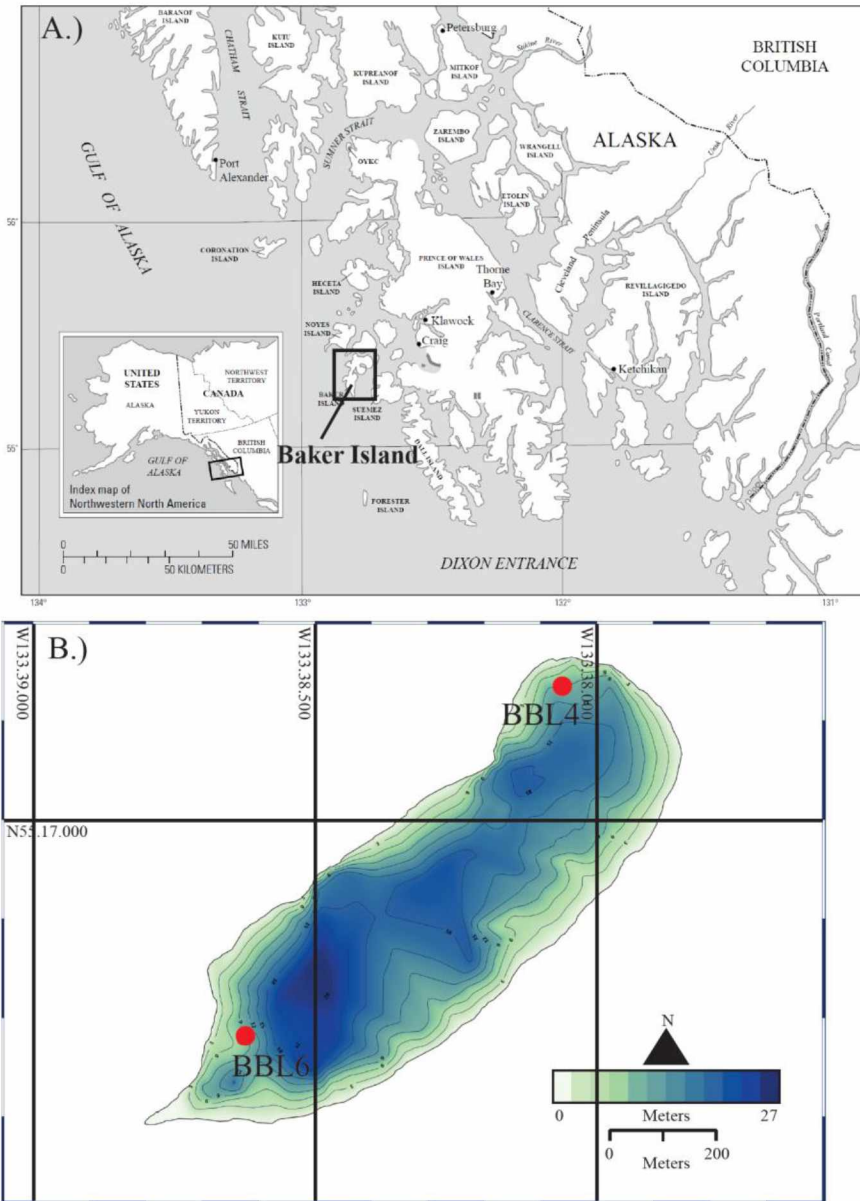


Fig. 3.1: Map showing location of Baker Island/Bathymetry A.) Location of Baker Island in Southeast Alaska's Alexander Archipelago. B.) Bathymetry of 'Bonsai' Lake with core site locations. Due to close proximity of sites BBL1 and BBL4, only site BBL4 is shown. BBL2, BBL3, and BBL5 are not shown or mentioned in the text.

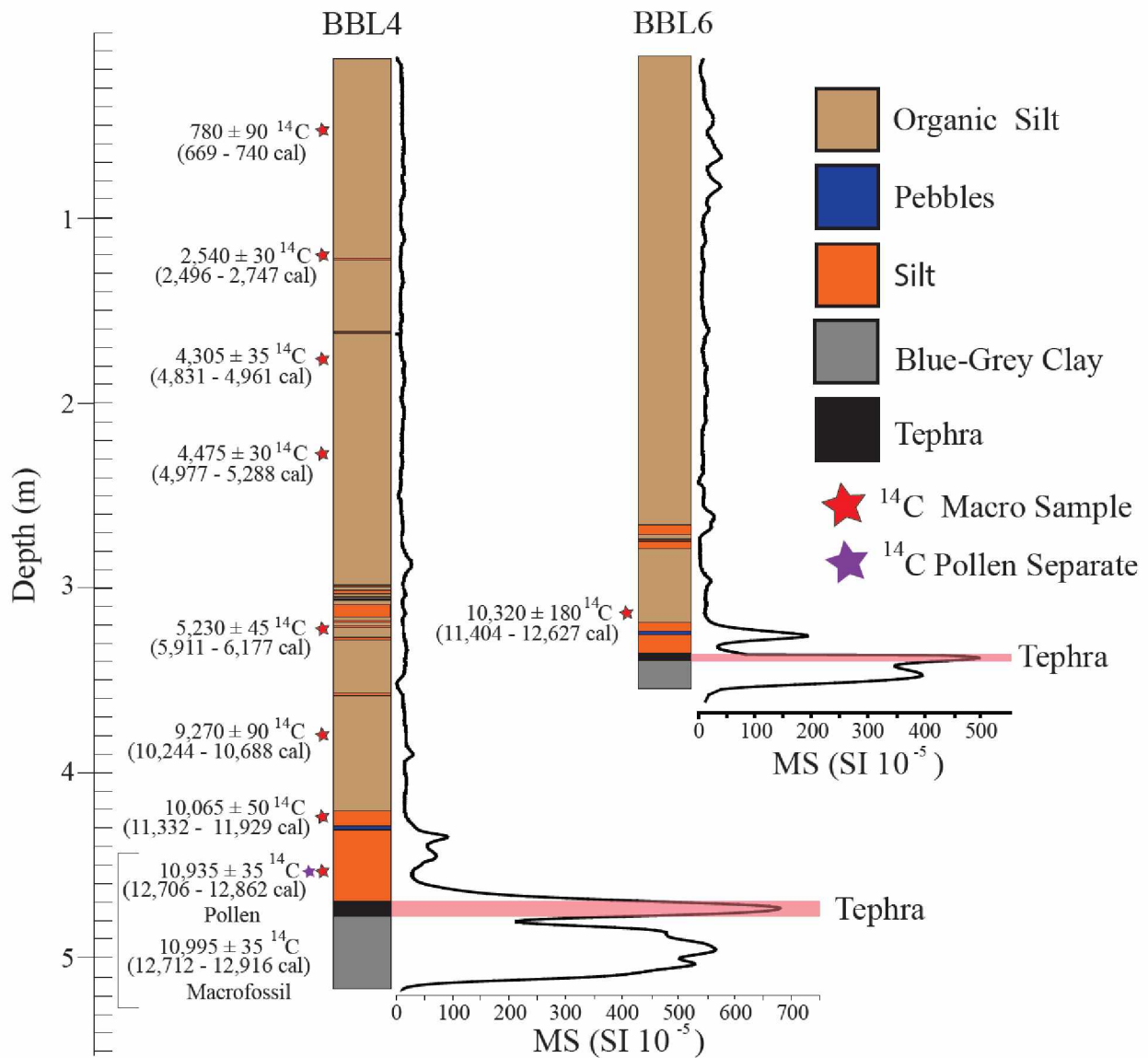


Fig. 3.2: Baker Island core stratigraphy. Baker Island core stratigraphy with tephra unit highlighted in red. Note that at 455 cm, there are both pollen and macrofossil AMS ages.

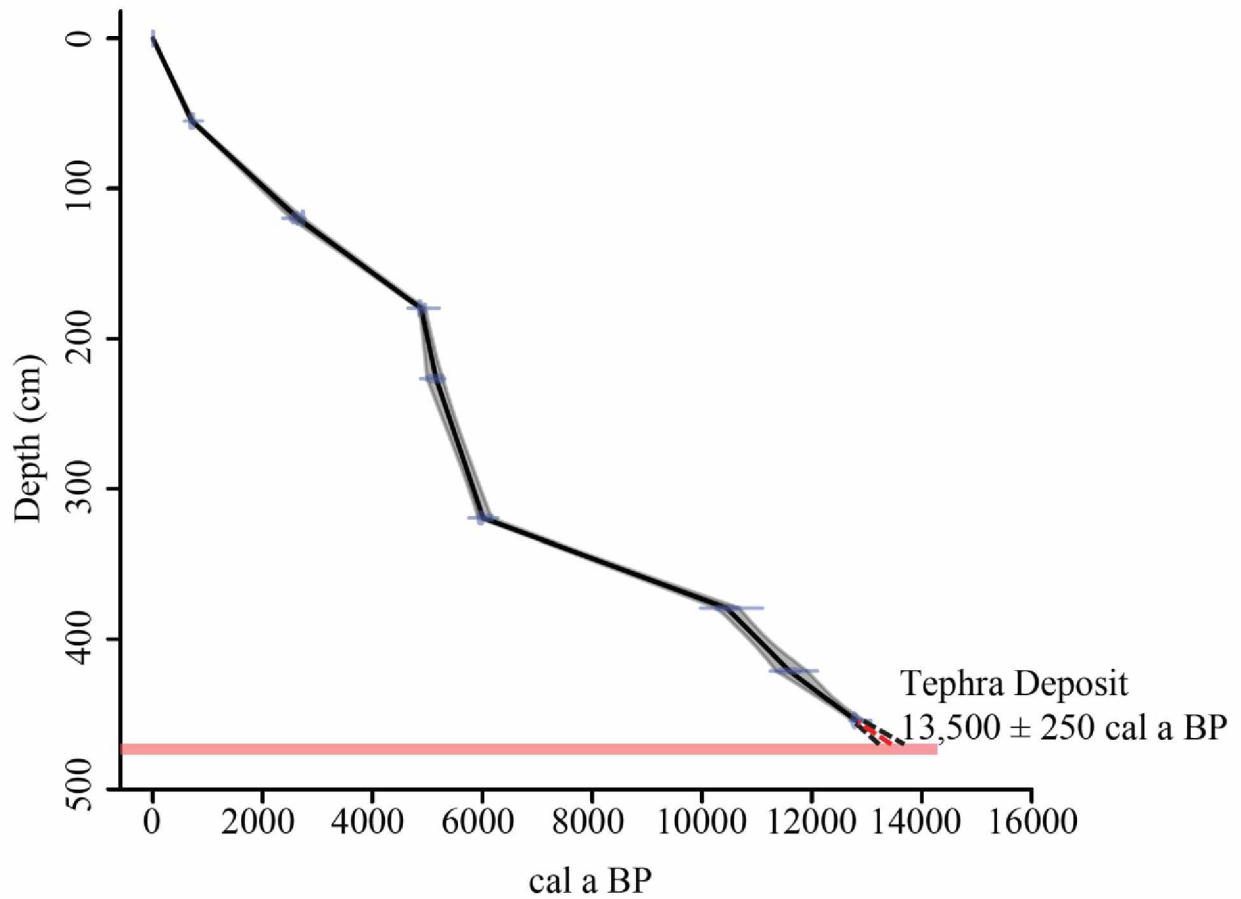


Fig. 3.3: Age-depth diagram of cores from Baker Island. Red highlighted area is depth of tephra and the extrapolated age. Diagram constructed using Clam, version 2.2 (Blaauw, 2010).

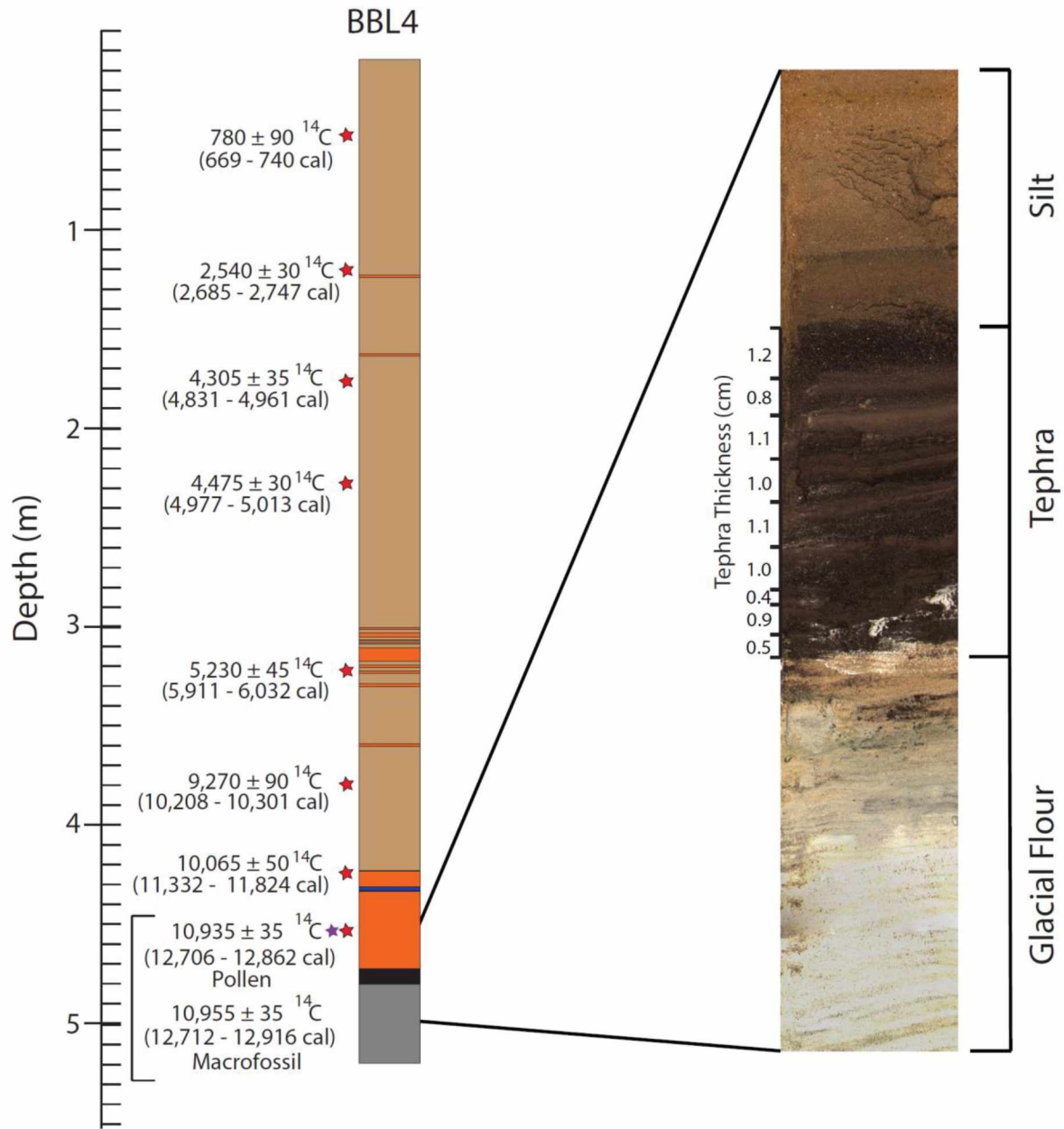


Fig. 3.4: Sediment core with tephra unit magnified and highlighted. High resolution photo of sediment core BBL4 from Baker Island at selected depth to highlight abrupt shift from blue clay to tephra and abrupt termination of tephra deposition. Tephra thickness on photo of core illustrates the multiple graded beds observed in the tephra. Note that at 455 cm, there are both pollen and macrofossil AMS ages.

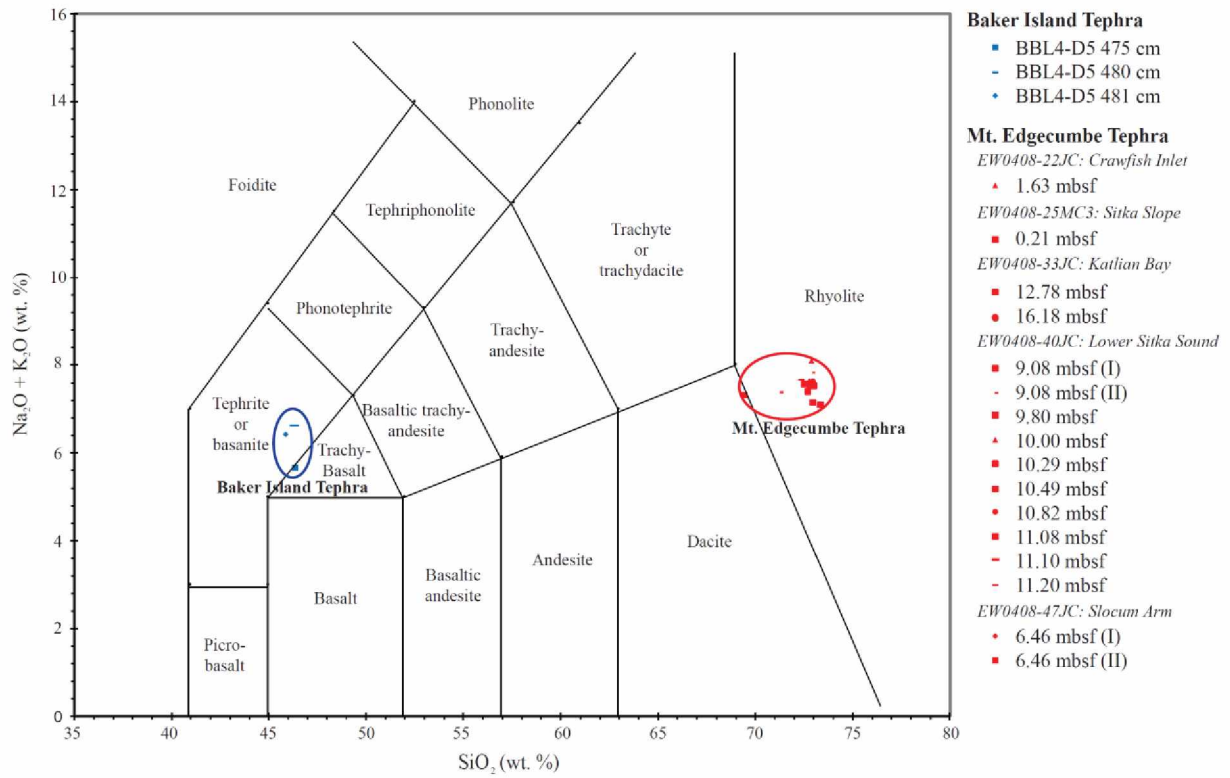


Fig. 3.5: Na₂O + K₂O vs. SiO₂ of black tephra. Na₂O + K₂O vs. SiO₂ of black tephra (Blue) and Mt.

Edgecumbe Tephra (Red) from Addison et al. (2010). Only geochemical analyses from Mt. Edgecumbe tephtras deposited during the last 13,500 cal yr. BP are plotted.



Fig. 3.6. Scanning electron image of black tephra. Scanning electron microscope image of black tephra revealing angular, vesicular fragments.

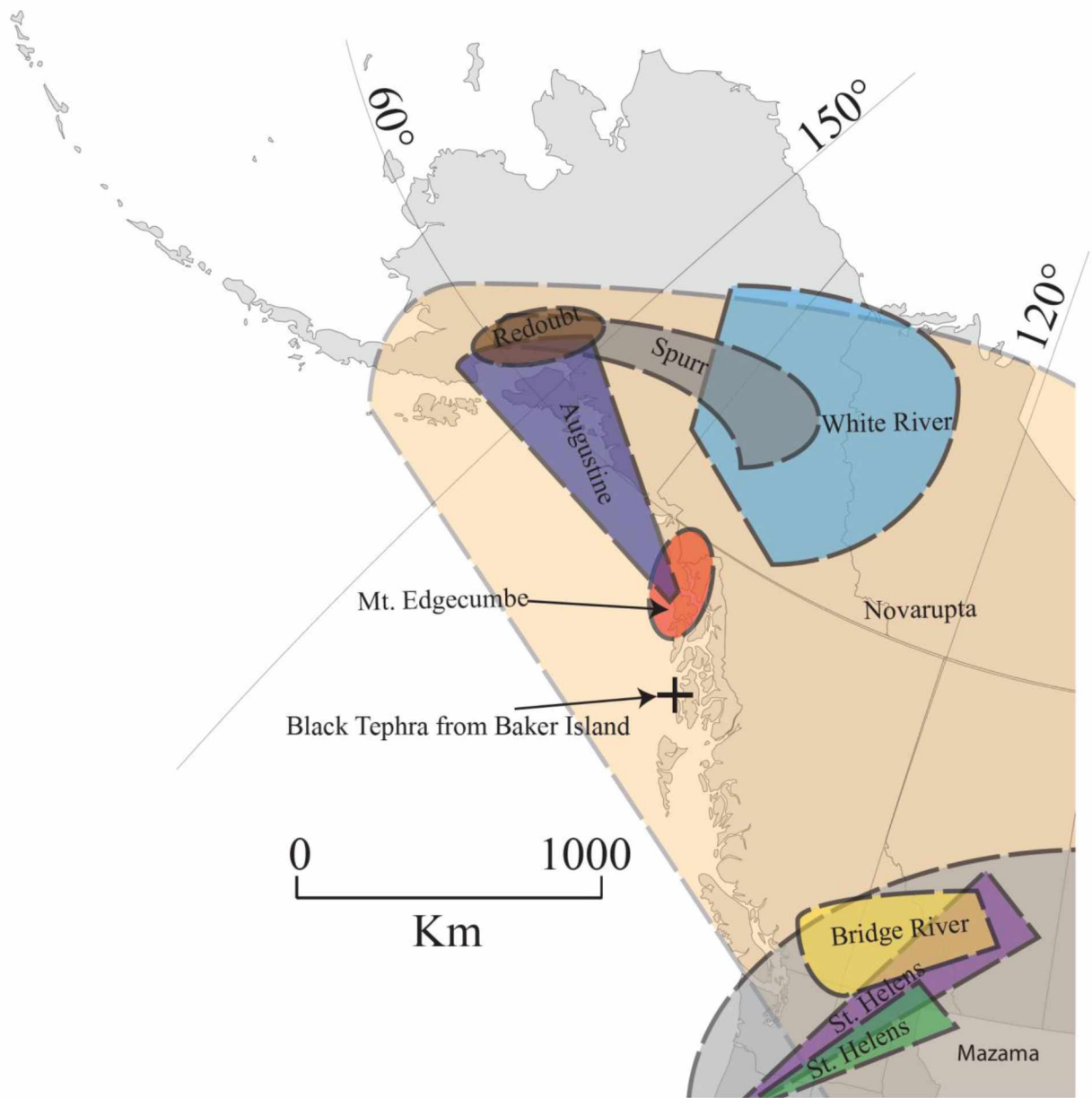


Figure 3.7: Distribution map of tephras in western Canada and Alaska. Distribution of tephras in western Canada and Alaska (modified from Clague et al., 1995; Riehle et al., 1992; and Fierstein and Hildreth, 2000).

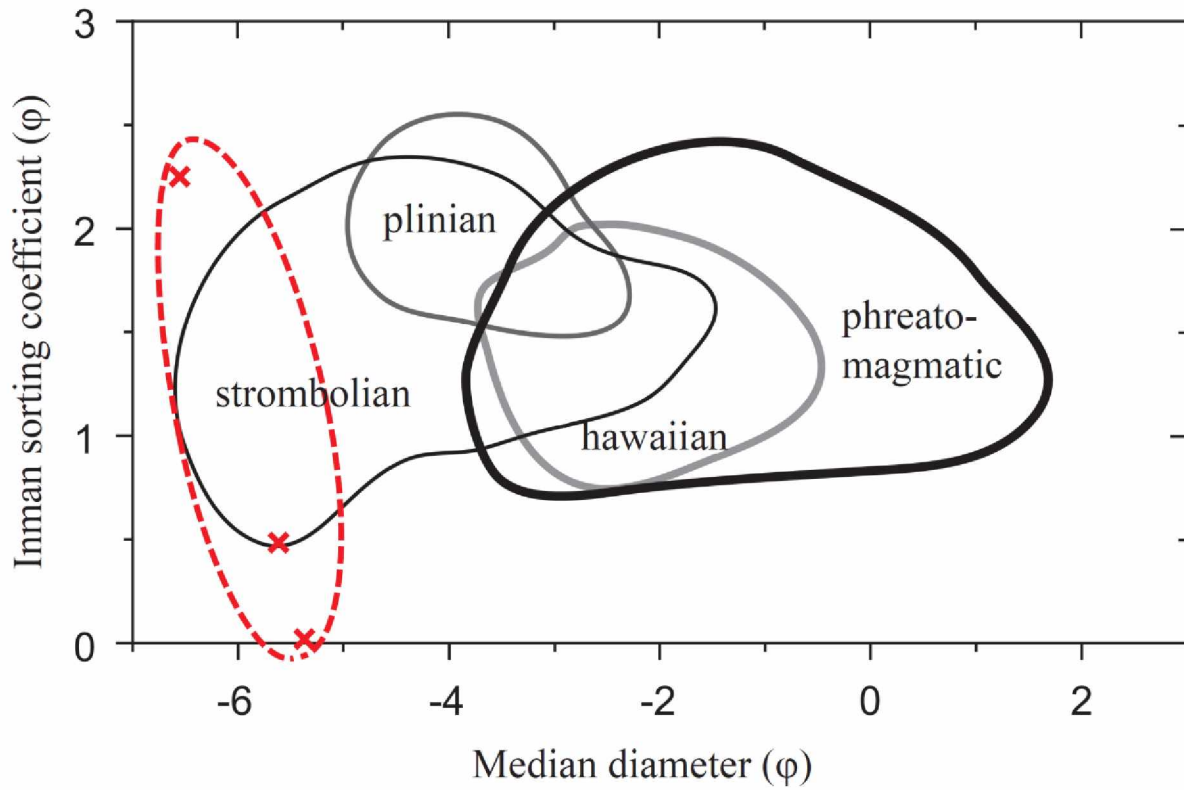


Fig. 3.8. Plot of median diameter versus sorting coefficient. Plot of median diameter versus sorting coefficient for fall deposits from basaltic explosive eruptions (modified from Houghton Gonnermann, 2008). Results from the black tephra fall within the red dashed circle.

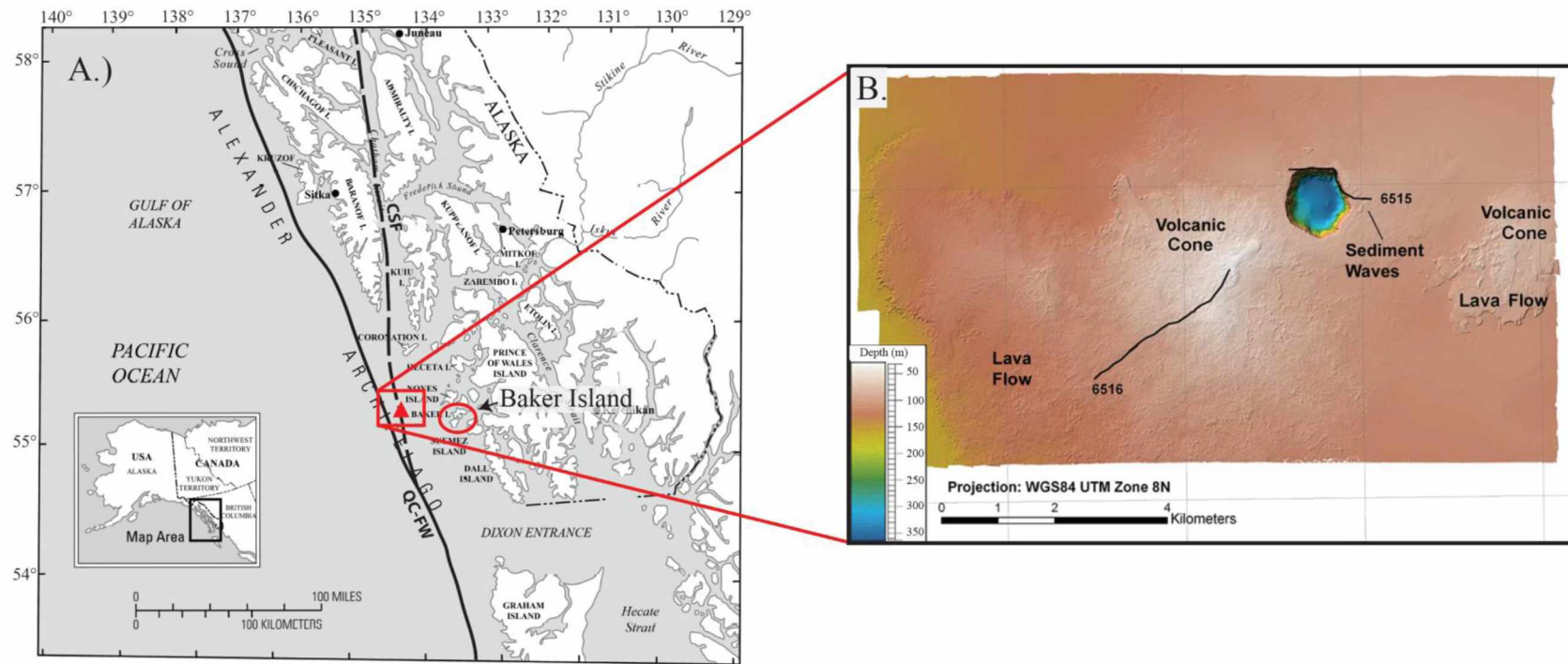


Fig. 3.9. Location of Addington volcanic field/artificial sun-illuminated seafloor map A.) Location of Addington volcanic field (modified from Greene et al., 2011). B.) Artificial sun-illuminated seafloor of the offshore Cape Addington area showing the volcanic lava field with maar crater, volcanic cones, lava flows, and 2005 *Delta* submersible dive transects (from Greene et al., 2011). CSF=Chatham Strait Fault, QC-FW=Queen Charlotte-Fairweather fault system.

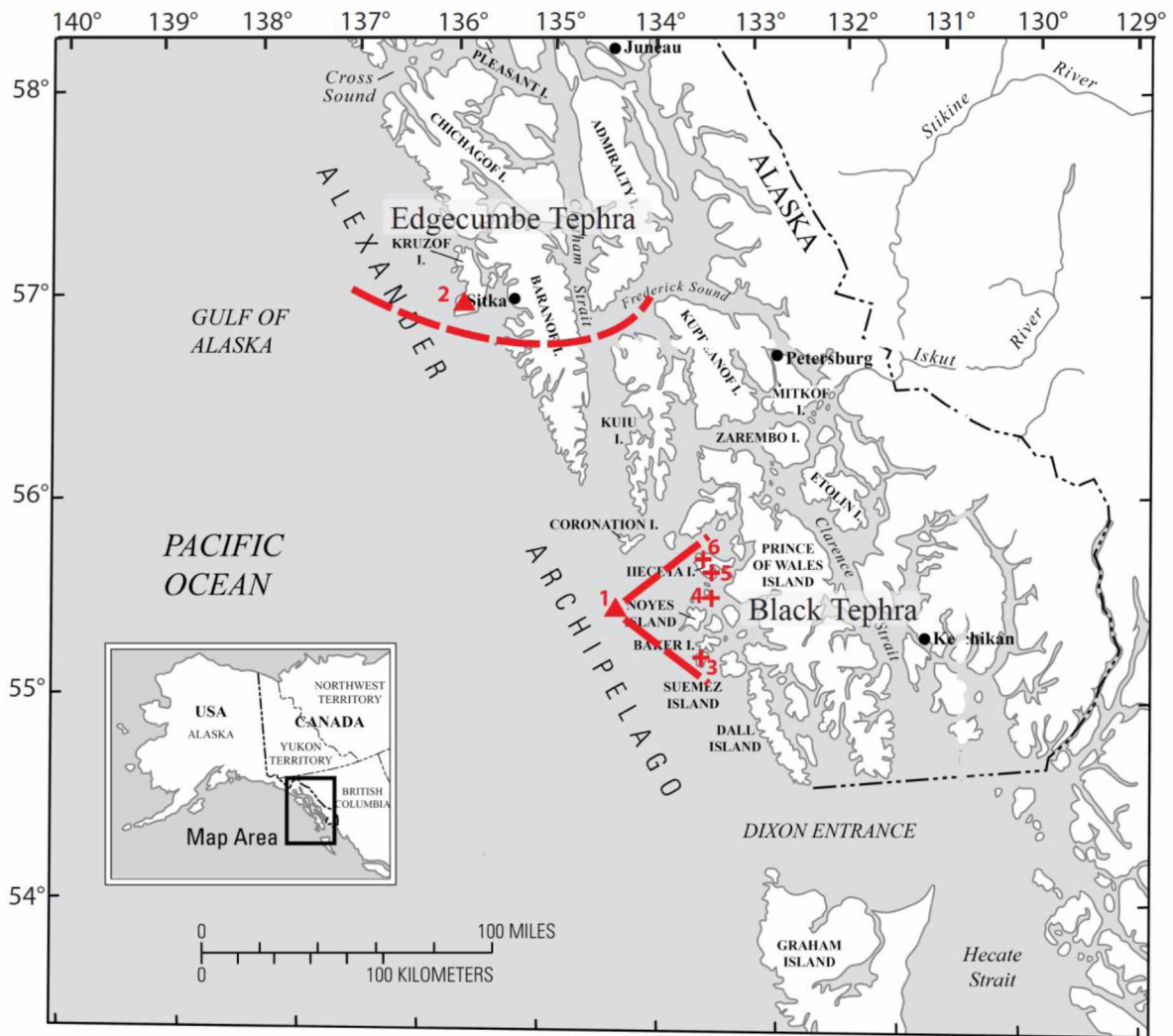


Fig. 3.10: Map of proposed tephra limits. Southern limit of fallout area from Mt. Edgumbe tephra and proposed fallout area of black tephra. 1. Addington Volcanic Field 2. Mt. Edgumbe 3. Baker Island 4. Gulf of Esquibel 5. Bald Mountain 6. Leech Lake.

3.9 Tables

Table 3.1: List of radiocarbon dates used for chronology on Baker Island. Calibrated ages and median ages were calculated using 2σ range from CALIB 7.0 software. Macrofossils are composed of unidentified wood material.

Sample Location	Material	d ¹³ C	Fraction Modern	±	D ¹⁴ C	±	¹⁴ C age	±	Calibrated age	Median age (cal yr. BP)
BBL4 55 cm	Macrofossil	-25	0.9072	0.0032	-92.8	3.2	780	30	669-740	703
BBL4 120 cm	Macrofossil	-25	0.7290	0.0026	-271.0	2.6	2540	30	2496-2747	2630
BBL4 180 cm	Macrofossil	-25	0.5852	0.0024	-414.8	2.4	4305	35	4831-4961	4864
BBL4 227 cm	Macrofossil	-25	0.5730	0.0020	-427.0	2.0	4475	30	4977-5288	5173
BBL4 320 cm	Macrofossil	-25	0.5214	0.0028	-478.6	2.8	5230	45	5911-6177	5985
BBL4 380 cm	Macrofossil	-25	0.3152	0.0032	-684.8	3.2	9270	90	10244-10688	10451
BBL4 422 cm	Macrofossil	-25	0.2856	0.0016	-714.4	1.6	10065	50	11332-11929	11609
BBL6 307 cm	Macrofossil	-25	0.2766	0.0059	-723.4	5.9	10320	180	11404-12627	12099
BBL4 455 cm	Pollen	-25	0.2563	0.0010	-743.7	1.0	10935	35	12706-12862	12776
BBL4 455 cm	Macrofossil	-25	0.2558	0.0010	-744.2	1.0	10955	35	12712-12916	12789

Table 3.2: Geochemical results from tephra from Baker Island. Geochemical results (weight percent) of tephra from Baker Island analyzed on a JEOL microprobe (Blue) and the Old Crow standard analyzed on Cameca microprobe (Green).

Sample	Na2O	MgO	Al2O3	SiO2	Cl	K2O	CaO	TiO2	Fe2O3	Na2O+K2O
BBL4-D5 475 cm	4.81	4.63	14.70	45.87	0.09	1.62	9.78	4.35	14.55	6.43
BBL4-D5 480 cm	4.17	4.74	15.10	46.37	0.08	1.50	10.32	4.48	14.64	5.67
BBL4-D5 481 cm	5.04	4.50	15.22	46.32	0.08	1.59	9.95	4.48	14.48	6.62
Old Crow Working Standard	0.27	1.46	1.20	0.24	2.91	0.26	11.76	67.30	2.15	0.53
Old Crow Standard	0.28	1.73	1.35	0.29	3.65	0.28	12.50	72.40	3.65	0.28

3.10 Acknowledgements

Research reported in this chapter was supported by the National Institute of General Medical Sciences of the National Institutes of Health under Award Numbers UL1GM118991, TL4GM118992, or RL5GM118990. The content is solely the responsibility of the authors and does not necessarily represent the official views of the National Institutes of Health. The authors gratefully acknowledge use of the UAF-AIL electron microprobe acquired with support from the National Science Foundation, Major Research Instrumentation Program Award Number 1126898.

Chapter 4: A Speleothem Paleoclimate Record of Southeast Alaska from 60 to 11 ka³

4.1 Abstract

A paleoclimate record, based on $\delta^{13}\text{C}$ and $\delta^{18}\text{O}$ stable isotope values, from ~60,000 yr. BP to ~11,150 yr. BP, is reconstructed from a speleothem from El Capitan Cave in Southeast Alaska. The data show multiple oscillations in $\delta^{13}\text{C}$ probably related to vegetation changes on the landscape above the cave. Positive $\delta^{13}\text{C}$ values in EC-16-5-F are interpreted to indicate the presence of gymnosperms above the cave, while more negative $\delta^{13}\text{C}$ values indicate a predominance of angiosperms. The data suggest limited or no ice cover above El Capitan Cave, indicating that the area around the cave was a nunatak during glacial periods.

4.2 Introduction

Paleoclimate records containing and/or pre-dating the Last Glacial Maximum (LGM) from coastal terrestrial locations in Washington, British Columbia and Southeast Alaska are rare. The LGM took place during the latest part of marine isotope stage (MIS) 2, ~20,000 cal yr. BP (Hughes et al., 2013). Besides peat beds exposed in a seacliff near Kalaloch, Washington with a basal age of ~55,000 yr. BP (Heusser, 1985), there are few other records that penetrate the LGM in this region. However, records that incorporate MIS 2 and MIS 3 are vital as they represent the largest temperature swings in recent geologic history (Petit et al., 1999); During MIS 2, mean annual temperature reductions of at least ~3 °C are reconstructed from beetle assemblages from the Kalaloch sea cliffs (Cong and Ashworth, 1996). Obtaining a climate record that extends further back in time will elucidate the magnitude and timing of climate perturbations during and prior to the LGM. This is important for regional and worldwide

³ Wilcox, P.S., Dorale, J.A., Fowell, S.J., Baichtal, J.F., Kovarik, J., Shakun, J., Mix, A., Cheng, H., Edwards, L. 2017. Prepared for submission in the Journal of Quaternary Research.

comparison and for constraining climate parameters for model simulation used to predict future climate scenarios.

The presence of biological refugia in Southeast Alaska and northern British Columbia has been proposed by various authors (Warner et al., 1982; Hansen and Engstrom, 1996; Heaton et al., 1996). Such refugia would have allowed a habitat suitable for animals and plants to survive the encroachment of the vast Cordilleran Ice Sheet during the height of the ice age and possibly facilitate human migration through the region (Fagundes et al., 2008). Ancient bones from bears found on Prince of Wales Island with genetically distinct DNA from mainland bears have been dated to ~30,000 years BP and to ~13,000 years BP, which hints that refugia existed (Heaton et al., 1996). In addition, pollen evidence collected from Pleasant Island, which was covered under the Cordilleran Ice Sheet during the LGM, indicates that pine woodland was present immediately after deglaciation. This suggests that pine trees survived the ice age within a refugium (Hansen and Engstrom, 1996). Furthermore, a palynological record from sea-cliff exposures of late Pleistocene sediment and peat from the Queen Charlotte Islands spans the last ~18 ka and indicates that at least a portion of Queen Charlotte Island was ice free throughout the late Wisconsin (Warner et al., 1982; Mathewes et al. 1993). Beyond these hints, there is no definitive evidence that such a refugium existed in the region.

Caves are well suited for paleoclimate and paleovegetation reconstructions because climatic signals can be captured in speleothems due to variations in $\delta^{18}\text{O}$ and $\delta^{13}\text{C}$ isotopes, which are driven by changes in temperature/precipitation and vegetation cover, respectively (Hudson, 1977; Dorale et al., 1992). As speleothem studies are rare in the cave-rich region of Southeast Alaska, this speleothem record provides a unique climate and vegetation record during a time interval unattainable by other methods.

4.3 Site Location

Speleothems were collected from El Capitan Cave (N 56.162°, W 133.319°, 74 m above sea level) in southern Southeast Alaska on Prince of Wales Island (Fig. 4.1). Land above the cave reaches an elevation of ~700 meters a.s.l. The cave is found in Silurian Heceta limestone, a unit that contains locally thick lenses of polymictic conglomerate, limestone breccia, sandstone, and argillaceous rocks (Ovenshine and Webster, 1970). Present day mean annual temperature in El Capitan Cave is 5 °C (Baichtal, 2017, pers. comm.). Speleothem EC-16-5-F, used in this study, was found broken on the cave floor just beyond a formation known as Hot Fudge Sundae, approximately 90 meters inside the cave entrance (Fig. 4.1b). There is no evidence of active speleothem formation in the passageway where the speleothem was collected. A younger speleothem sample, collected in 2008, from Goliath's Wake Cave (N 56.029°, W 133.530°) on nearby Kosciusko Island, was used to assist interpretations of the record from El Capitan. The Goliath's Wake speleothem is also found in Heceta limestone and the speleothem ranges in age from modern to 1,200 yr. Old growth forest grows on the landscape above both caves.

4.4 Climate and Vegetation

Today, Prince of Wales Island has a maritime climate characterized by cool, generally wet conditions. Mean annual temperature and precipitation from Craig, Alaska, 33 km South of El Capitan Cave, are 7.2°C and 2500 mm, respectively (Western Regional Climate Center, 2017). Storms associated with the Aleutian low-pressure system are especially common in autumn and winter. Most annual precipitation falls as rain at low altitudes, but snowfall is heavy at higher elevations, and snow can accumulate intermittently even at sea level during the winter (Ager et al., 2010).

Most of Prince of Wales Island is covered by Pacific coastal rainforest interspersed with muskeg (Ager et al., 2010), containing only C₃ vegetation (Thompson et al., 2006). Modern tree taxa in the region include

Picea sitchensis (Sitka Spruce), *Tsuga* (Fir), *Alnus* (alder), *Sphagnum* (moss), and *Pinus contorta* ssp. *contorta* (Shore Pine). Among these vegetation types, $\delta^{13}\text{C}$ values range from -26‰ to -31‰ (DeLucia et al., 1988; DeLucia and Schlesinger 1991; Lajtha and Barnes 1991; Marshall and Zhang 1994; Van de Water et al., 2002; McCallister and Giorgio, 2008).

Cool maritime temperatures of the region result in slow biotic activity and the thick accumulation of an organic mat from 15 to 25 cm thick on the forest floor (Stephens, 1969), with muskegs containing up to 12 meters of peat (Stephens et al., 1970). This results in high CO_2 concentrations in the soils with acidic pH values as low as 3.2 (Fellman et al., 2008).

4.5 Methods

Speleothem EC-16-5-F was cut in half, polished, cleaned with an alcohol solution, and drilled for U-Th dates and carbon/oxygen stable isotopes at the University of Iowa. Four U-Th samples were collected at 4mm, 63 mm, 67 mm, and 123 mm. Subsamples weighing 150 to 300 mg were analyzed for U-Th content and dated at the University of Minnesota Trace Metal Isotope Geochemistry Laboratory. We collected 103 stable isotope samples at 2 mm increments along the central growth axis of the stalagmite. Stable isotope samples were analyzed at the University of Missouri-Columbia Stable Isotope Laboratory using a Finnigan Delta-V mass spectrometer and a Kiel III device. Carbon and oxygen isotopes are reported in per mil relative to VPDB with an analytical precision better than 0.1 per mil. Ages of isotopes between dated horizons are estimated via linear interpolation (Fig. 4.3).

4.6 Results

4.6.1 Uranium-Series Dating

U-Th dating of speleothem EC-16-5-F produced dates of $11,146 \pm 258$ (4 mm depth), $43,045 \pm 183$ (63 mm depth), $46,236 \pm 209$ (67 mm depth), and $59,523 \pm 427$ (123 mm depth) yr BP (Fig. 4.2 and Fig. 4.3). Six unconformities are tentatively identified based on visual identification of abrupt changes in color and growth direction (Fig. 4.2). To test if these visual features represent gaps in age, U-Th samples were collected below and above a possible unconformity at 65 mm. The resulting dates of $43,045 \pm 183$ and $46,236 \pm 209$ suggest that a possible unconformity exists because the growth rate between these sites is half the average growth rate between $11,146 \pm 258$ (4 mm) and $59,523 \pm 427$ (123 mm). Further dates are needed to determine whether other visual features are unconformities.

4.6.2 Stable Isotopes

$\delta^{13}\text{C}$ values in speleothem EC-16-5-F range from -1.42‰ to -8.74‰ (Fig. 4.3). $\delta^{13}\text{C}$ is at -3.83‰ early in the record at $\sim 62,000$ yr. BP. It decreases to -5.47‰ by $\sim 60,000$ yr. BP, followed by an increase to -3.89‰ at $\sim 58,000$ yr. BP. $\delta^{13}\text{C}$ remains at approximately -4‰ until $\sim 53,000$ yr. BP where it decreases to approximately -8‰ . More negative $\delta^{13}\text{C}$ values of approximately -8‰ persist until $\sim 46,000$ yr. BP where values increase to -2.81‰ . $\delta^{13}\text{C}$ values remain at approximately -3‰ until $\sim 22,000$ yr. BP where they decrease to -6.57‰ , followed by an increase to -2.49‰ at $\sim 20,000$ yr. BP. Afterward, $\delta^{13}\text{C}$ values level off at approximately -3‰ and then increase to -1.42‰ at $\sim 13,000$ yr. BP. $\delta^{13}\text{C}$ values decrease to -3.60‰ at $\sim 11,800$ yr. BP, followed by an increase to -2.37‰ at $\sim 11,400$ yr. BP.

To help interpret speleothem $\delta^{13}\text{C}$ values, the parent host rock was analyzed for $\delta^{13}\text{C}$. Two samples contain $\delta^{13}\text{C}$ values of 1.04‰ and 1.54‰ .

$\delta^{18}\text{O}$ values in speleothem EC-16-5-F range from -8.01‰ to -10.01‰ (Fig. 4.3). $\delta^{18}\text{O}$ is at -9.26‰ early in the record at ~62,000 yr. BP. It increases to -8.01‰ at ~58,000 yr. BP, followed by a decrease to -9.52‰ at ~57,000 yr. BP. $\delta^{18}\text{O}$ remains at approximately -9.1‰ until ~45,000 yr. BP where it increases to -8.63‰. Between ~46,000 yr. BP and ~31,000 yr. BP, there are fluctuations in $\delta^{18}\text{O}$ from -9.54‰ to -8.59‰. At ~30,000 yr. BP, $\delta^{18}\text{O}$ values begin to decrease, reaching the most negative value in the record, -10.01‰, at ~22,000 yr. BP. $\delta^{18}\text{O}$ values increase to -8.76‰ at ~20,000 yr. BP. Values further increase to -8.16‰ by ~13,000 yr. BP, followed by a decrease to -9.58‰ at ~11,800 yr. BP. $\delta^{18}\text{O}$ values then rise to -8.04‰ at ~11,400 yr. BP.

4.7 Discussion

Speleothem EC-16-5-F has bounding ages of ~11,150 and ~60,000 yr. BP, spanning parts of MIS 1 through MIS 3. Additional dates are needed to determine whether unconformities formed during glacial periods, when ice cover may have inhibited water movement and halted speleothem precipitation. Much of the Holocene is not present in the speleothem, which appears to have been broken by activity in the main passageway of the cave. Therefore the speleothem cannot be directly calibrated by modern records. Instead, a record previously obtained from nearby Goliath's Wake Cave is used to facilitate interpretation by providing isotope results during a time interval when modern climate and vegetation exists.

In addition, a pollen and $\delta^{13}\text{C}$ record from Baker Island (100 km southwest) has ages ranging from modern to ~13,500 cal yr. BP, overlapping with the record of speleothem EC-16-5-F between ~11,150 cal yr. BP and ~13,500 cal yr. BP. This core provides additional evidence of regional vegetation and climate changes during that interval. The overlapping interval includes the Younger Dryas (YD) cold event between 12,800 cal yr. BP and 11,500 cal yr. BP, and part of the warm Bølling-Allerød (BA) interstadial between 14,700 cal yr. BP and 13,000 cal yr. BP (Alley et al., 1993).

4.7.1 $\delta^{13}\text{C}$ Record

Our data show multiple large oscillations in speleothem $\delta^{13}\text{C}$ values of up to 4‰. These changes in $\delta^{13}\text{C}$ are derived from cave seepage waters. The waters contain the $\delta^{13}\text{C}$ signature of soil CO_2 which is related to the type of vegetation occupying the land surface and the composition of the bedrock (Hudson, 1977; Dorale et al., 1992). Bedrock $\delta^{13}\text{C}$ values are not expected to change on timescales of thousands of years. Therefore, the changes in $\delta^{13}\text{C}$ in this record are interpreted as the result of transitions in dominant vegetation type between gymnosperms and angiosperms. Gymnosperms have $\delta^{13}\text{C}$ values between -26‰ and -27‰ (Kloppel et al., 1998; Choi et al., 2005) while angiosperms $\delta^{13}\text{C}$ values range between -29.2 and -31‰ (Simenstad and Wissmar, 1985). Therefore, a change from gymnosperms to angiosperms would drive $\delta^{13}\text{C}$ toward more negative values.

When the host rock contains sulfides, speleothems could continue to grow during glacial intervals from sulfide oxidation (Spötl and Mangini, 2007). However, because the host rock at this site contains no sulfides, speleothem growth is probably due to a biogenic carbon source, which requires a moderately well-developed soil above the cave (Spötl and Mangini, 2007). Values approaching or exceeding the parent host rock (due to lack of soil-derived biogenic carbon), could indicate overlying glaciers (Spötl and Mangini, 2007). However, as $\delta^{13}\text{C}$ values in speleothem EC-16-5-F do not approach or exceed values of the parent host rock, it seems unlikely that glaciers overrode El Capitan Cave.

4.7.2 $\delta^{18}\text{O}$ Record

Whereas speleothem $\delta^{13}\text{C}$ is sensitive to vegetation, soil, and related climatic conditions, $\delta^{18}\text{O}$ is linked to meteoric water (Lachniet, 2009). The $\delta^{18}\text{O}$ value of mean annual precipitation (MAP) is observed to be largely a function of mean annual atmospheric temperature (MAT), and it tends to decrease with decreasing ambient temperature and increasing latitude (Dansgaard, 1964). Cave temperatures, and

hence mean annual temperature at the ground surface, may also affect $\delta^{18}\text{O}$ values, with colder cave temperatures resulting in greater fractionation and more positive $\delta^{18}\text{O}$ values, and warmer temperatures resulting in less fractionation (O'Neil et al., 1969).

We note a general trend in speleothem EC-16-5-F where negative $\delta^{18}\text{O}$ values correspond to cold conditions while positive $\delta^{18}\text{O}$ values correspond to warm conditions, agreeing with the MAP-MAT relationship. For example, most negative $\delta^{18}\text{O}$ values occur at $\sim 22,000$ cal yr. B.P., consistent with cold conditions during the LGM described by Blaise et al. (1990) along the west coast of Canada sometime after 24,500 cal yr. BP. Negative $\delta^{18}\text{O}$ values are also found at $\sim 12,000$ yr. BP, consistent with the Younger Dryas cold interval (Alley et al., 1993). Positive $\delta^{18}\text{O}$ values are found at $\sim 13,000$ yr. BP, consistent with warming during the BA interstadial (Alley et al., 1993).

Other factors may obscure the MAP $\delta^{18}\text{O}$ – MAT relationship. For example, precipitation derived from different air masses typically contains distinct $\delta^{18}\text{O}$ signatures, and the $\delta^{18}\text{O}$ value of precipitation varies seasonally (Gat, 1996; Dorale et al., 1998). Additionally, glacial/interglacial cycles may also obscure this signal as moisture sources may be different than modern and/or ocean $\delta^{18}\text{O}$ values may be variable due to ice sheet decay and growth (Gat, 1996). Therefore, paleotemperature reconstruction assumes that neither the moisture source, the seasonality of precipitation, nor the $\delta^{18}\text{O}$ of seawater has varied significantly through time.

4.7.3 Overlapping records of EC-16-5-F and Baker Island lake core

Throughout the speleothem EC-16-5-F record, negative $\delta^{13}\text{C}$ values correspond to more negative $\delta^{18}\text{O}$ values. This suggests that vegetation with more negative $\delta^{13}\text{C}$ values occur during periods with cooler temperatures. Conversely, intervals with more positive $\delta^{13}\text{C}$ and $\delta^{18}\text{O}$ occur during periods with warmer temperatures.

Palynological data from the Baker Island lake sediment core (Wilcox et al., 2017, in prep) indicates that the BA interval between 13,500 cal yr. BP and 13,000 cal yr. BP was warmer and wetter than the previous glacial period based on increases in *Pinus*, which occupies modern humid maritime climate in Southeast Alaska (Hebda, 1983; Thompson et al., 2006). High clastic influx is interpreted to be from increased precipitation. The corresponding $\delta^{13}\text{C}$ values is the most positive in the record (Wilcox et al., 2017, in prep).

The beginning of the YD period, between 13,000 cal yr. BP and 12,500 cal yr. BP, is dryer and cooler than the BA based on the decline of *Pinus* and *Tsuga mertensiana* pollen, increases in *Alnus* pollen and fern spores, and a decrease in clastic influx. Because *Alnus* and ferns dominate modern tree line vegetation in the Malaspina Glacier District near Yakutat (Peteet, 1986), it is suggested that YD cooling lowered tree line and allowed *Alnus* and ferns to replace *Pinus* and *Tsuga mertensiana*. The corresponding $\delta^{13}\text{C}$ values are the most negative in the record.

The middle segment of the YD, between 12,400 cal yr. BP and 11,800 cal yr. BP, appears to be warmer and wetter than the first half based on increasing *Pinus* pollen, decreasing percentages of *Alnus* pollen and fern spores, and increasing clastic influx. We infer that warming temperatures resulted in an increase in the elevation of tree line and reestablishment of *Pinus*. Corresponding $\delta^{13}\text{C}$ values are more positive, approaching BA levels. Pollen fluctuations from Baker Island during the period between 13,500 cal yr. BP and ~11,000 cal yr. BP are in good agreement with vegetation cover interpreted from pollen fluctuations from nearby Pass Lake on Prince of Wales Island ~ 60 km east of Baker Island and ~100 km southeast of El Capitan Cave (Ager and Rosenbaum, 2007), indicating that the changes seen on Baker Island are consistent with the regional vegetation history.

More typical coniferous vegetation of modern coastal Alaska, such as Sitka spruce (*Picea sitchensis*) and western hemlock (*Tsuga heterophylla*), do not appear in the region until after ~11,000 cal yr. BP, and

therefore are not expected to contribute to the $\delta^{13}\text{C}$ values captured in speleothem EC-16-5-F. The only tree/shrub species present during the interval in which the Baker Island record and speleothem EC-16-5-F record overlap are *Pinus*, *Alnus*, and small amounts of *Tsuga mertensiana*.

The interpretations from the Baker Island sediment core suggests that the sharp decline in $\delta^{18}\text{O}$ values from speleothem EC-16-5-F, around $\sim 13,000$ yr. BP, reflect cooling associated with the first part of the YD (Fig. 4.4). In turn, the corresponding decline in $\delta^{13}\text{C}$ in speleothem EC-16-5-F may indicate the presence of alder shrubland (Fig. 4.4). Conversely, increases in $\delta^{18}\text{O}$ in at $\sim 13,500$ yr. BP and $\sim 12,400$ yr. BP in speleothem EC-16-5-F may be warming associated with the BA and middle segment of the YD, respectively. Corresponding increases in $\delta^{13}\text{C}$ (Fig. 4.4) suggest dominance of conifers and may indicate establishment of pine parkland vegetation during these warmer intervals.

4.7.4 EC-16-5-F $\delta^{13}\text{C}$ Extrapolation

Based on the correlative intervals of the Baker Island and speleothem records, we can interpret the $\delta^{13}\text{C}$ signal for remainder of the EC-16-5-F (Fig. 4.5) record. More negative $\delta^{13}\text{C}$ values record dominance of angiosperms above the cave. Conversely, more positive values correspond to an increase in gymnosperms. The more negative $\delta^{13}\text{C}$ values found in the modern Goliath's Wake record is puzzling, as conifers in the coastal rainforest would be expected to have more positive $\delta^{13}\text{C}$ values. The differences may be due to a more scattered, pine parkland setting being represented in EC-16-5-F, resulting in more positive $\delta^{13}\text{C}$ values than modern, closed canopy coniferous forests. This trend is observed in studies by Ehleringer et al. (1986) and Medina et al. (1991), which show that closed-canopy forests have increased recycling of plant-respired CO_2 and reduced light intensity, shifting plant tissues toward more negative $\delta^{13}\text{C}$ values compared to a more open setting.

Alternately, changes in bedrock between caves may have altered the $\delta^{13}\text{C}$ signal. However, as both sites are located in Heceta limestone with very similar geochemistry (Mass et al., 1995), we suggest changes in $\delta^{13}\text{C}$ values are more likely a result of vegetation changes above the cave.

4.7.5 Evidence for Refugia

If speleothem formation was continuous, it seems that there was limited or no ice cover throughout the entire record and persistent vegetation during stadials. However, possible unconformities in the record could represent time intervals where glacial conditions were present, inhibiting water movement and halting speleothem growth. Because $\delta^{13}\text{C}$ values never approach or exceed host bedrock $\delta^{13}\text{C}$ values, it is possible that ice age forest refugia existed along the coast of Southeast Alaska. As the entrance to El Capitan is 74 m above sea level, and the land above it reaches over 700 m a.s.l., it is possible that this region was a nunatak, allowing vegetation to persist during periods when glaciers were flowing nearby. Previous attempts to acquire records of the LGM from lake sediment may have been unsuccessful because most lakes in the region lie in geographically low areas which were probably overridden by glaciers during the LGM. Even in areas that were not under ice, local alpine glaciers may have deposited glacial flour, inhibiting the extraction of long sediment records. Additional speleothems from the region are needed for comparison with this speleothem record to further validate these interpretations.

4.8 Conclusions

$\delta^{13}\text{C}$ and $\delta^{18}\text{O}$ stable isotope values from a speleothem recovered from El Capitan Cave in Southeast Alaska, spanning from ~60,000 to ~11,150 yr. BP, are used to reconstruct the vegetation and climate history of the region. More positive $\delta^{13}\text{C}$ values in EC-16-5-F may indicate gymnosperms, and correspond to interstadials. More negative $\delta^{13}\text{C}$ values may indicate more angiosperms, and correspond to stadials.

This record provides a rare glimpse of climate and vegetation during and prior to the LGM. The data obtained can, in turn, be used as parameters for climate modeling. Furthermore, $\delta^{13}\text{C}$ values may suggest continual vegetation above El Capitan Cave, possibly indicating that the region above the cave acted as a nunatak during glacial periods. These results, therefore, suggest a new location for regional refugia, as previous work focuses on areas along the outer coast and continental shelf (Warner et al., 1982; Hansen and Engstrom, 1996; Wilcox et al., 2017, in prep).

Because speleothems extend further back in time than other proxies in the region, these records provide crucial constraints on the timing and magnitude of events for regional and worldwide comparison. By collecting and correlating additional speleothem records, applying different techniques for paleotemperature and paleovegetation interpretations (such as clumped isotope sampling and speleothem pollen extraction), and implementing long term cave monitoring, a more robust temperature and vegetation reconstructions can be obtained.

4.9 References:

- Ager, T.A., Rosenbaum, J.G., 2007. Late glacial-Holocene pollen-based vegetation history from Pass Lake, Prince of Wales Island, southeastern Alaska. US Geological Survey Professional Paper 1760-G. US Dept. of the Interior, US Geological Survey.
- Ager TA, Carrara PE, Smith JL, Anne V, Johnson J. 2010. Postglacial vegetation history of Mitkof Island, Alexander Archipelago, southeastern Alaska. *Quaternary Research* **73**(2) : 259-268.
- Alley RB, Meese DA, Shuman CA, Gow AJ, Taylor KC, Grootes, PM, White JWC, Ram M, Waddington ED, Mayewski PA, Zielinski GA. 1993. Abrupt increase in Greenland snow accumulation at the end of the Younger Dryas event. *Nature* **362**(6420) : 527-529.
- Blaise B, Clague JJ, Mathewes RW. 1990. Time of maximum Late Wisconsin glaciation, west coast of Canada. *Quaternary Research* **34** : 282-295.
- Choi WJ, Chang SX, Curran MP, Ro HM, Kamaluddin M, Zwiazek JJ. 2005. Foliar $\delta^{13}\text{C}$ and $\delta^{15}\text{N}$ response of lodgepole pine and Douglas-fir seedlings to soil compaction and forest floor removal. *Forest Science* **516** : 546-555.
- Cong S, Ashworth AC. 1996. Palaeoenvironmental interpretation of middle and late Wisconsinan fossil coleopteran assemblages from western Olympic Peninsula, Washington, USA. *Journal of Quaternary Science* **11**(5) : 345-356.
- Dansgaard W. 1964. Stable isotopes in precipitation. *Tellus* **16**(4) : 436-468.
- DeLucia EH, Schlesinger WH, Billings WD. 1988. Water relations and the maintenance of Sierran conifers on hydrothermally altered rock. *Ecology* **69** : 303-311.
- DeLucia EH, Schlesinger WH. 1991. Resource-use efficiency and drought tolerance in adjacent Great Basin and Sierran plants. *Ecology* **72** : 51-58.
- Dorale JA, González LA, Reagan MK, Pickett DA, Murrell MT, Baker RG. 1992. A high-resolution record of Holocene climate change in speleothem calcite from Cold Water Cave, Northeast Iowa. *Science* **258** : 1626-1630.
- Dorale JA, Edwards RL, Gonzalez L, Ito E. 1998. Climate and vegetation history of the midcontinent from 75 to 25 ka: a speleothem record from Crevice Cave, Missouri, USA. *Science* **282** : 1871-1874.
- Ehleringer JR, Field CB, Lin ZF, Kuo CY. 1986. Leaf carbon isotope and mineral composition in subtropical plants along an irradiance cline. *Oecologia* **70**(4) : 520-526.
- Fagundes NJ, Kanitz R, Bonatto SL. 2008. A reevaluation of the Native American mtDNA genome diversity and its bearing on the models of early colonization of Beringia. *PLoS One* **3**(9) : 3157.

- Fellman JB, D'Amore DV, Hood E, Boone RD. 2008. Fluorescence characteristics and biodegradability of dissolved organic matter in forest and wetland soils from coastal temperate watersheds in southeast Alaska. *Biogeochemistry* **88**(2) : 169-184.
- Gat JR. 1996. Oxygen and hydrogen isotopes in the hydrologic cycle. *Annual Review of Earth and Planetary Sciences* **24**(1) : 225-262.
- Hansen BCS, Engstrom DR. 1996. Vegetation history of Pleasant Island, southeastern Alaska, since 13,000 yr B.P. *Quaternary Research* **46** : 161-175.
- Heaton TH, Talbot SL, Shields GF. 1996. An ice age refugium for large mammals in the Alexander Archipelago, southeastern Alaska. *Quaternary Research* **46** : 186-192.
- Hebda RJ. 1983. Late-glacial and postglacial vegetation history at Bear Cove Bog, northeast Vancouver Island, British Columbia. *Canadian Journal of Botany* **61** : 3172-3192.
- Heusser CJ. 1985. Quaternary pollen records from the Pacific Northwest coast-Aleutians to the Oregon-California boundary, in Bryant, V.M., Jr., and Holloway, R.G., eds., *Pollen records of Late-Quaternary North American sediments*: Dallas, American Association of Stratigraphic Palynologists Foundation, 141-165.
- Hudson JD. 1977. Stable isotopes and limestone lithification. *Journal of the Geological Society* **133**(6) : 637-660.
- Hughes PD, Gibbard PL, Ehlers J. 2013. Timing of glaciation during the last glacial cycle: evaluating the concept of a global 'Last Glacial Maximum'(LGM). *Earth-Science Reviews* **125** : 171-198.
- Kloppel BD, Gower ST, Treichel IW, Kharuk S. 1998. Foliar carbon isotope discrimination in *Larix* species and sympatric evergreen conifers: a global comparison. *Oecologia* **114**2 : 153-159.
- Lachniet MS. 2009. Climatic and environmental controls on speleothem oxygen-isotope values. *Quaternary Science Reviews* **28**(5) : 412-432.
- Lajtha K, Barnes FJ, 1991. Carbon gain and water use in pinyon pine-juniper woodlands of northern New Mexico: field versus phytotron chamber measurements. *Tree Physiology* **9** : 59- 67.
- Marshall JD, Zhang J. 1994. Carbon isotope discrimination and water-use efficiency in native plants of the north-central Rockies. *Ecology* **75** : 1887-1895.
- Mass KM, Bittenbender PE, Still JC. 1995. Mineral Investigations in the Ketchikan Mining District, Southeasten Alaska. U.S. Department of the Interior, Bureau of Mines, Open file Report 11-95.
- Mathewes RW, Heusser LE, Patterson RT. 1993. Evidence for a Younger Dryas-like cooling event on the British Columbia coast. *Geology* **21** : 101-104.

- McCallister SL, Giorgio PAD. 2008. Direct measurement of the $\delta^{13}\text{C}$ signature of carbon respired by bacteria in lakes: Linkages to potential carbon sources, ecosystem baseline metabolism, and CO₂ fluxes. *Limnology and oceanography* **53**(4) : 1204.
- Medina E, Sternberg L, Cuevas E. 1991. Vertical stratification of $\delta^{13}\text{C}$ values in closed natural and plantation forests in the Luquillo mountains, Puerto Rico. *Oecologia* **87**(3) : 369-372.
- O'Neil JR, Clayton RN, Mayeda TK. 1969. Oxygen isotope fractionation in divalent metal carbonates. *The Journal of Chemical Physics* **51**(12) : 5547-5558.
- Ovenshine AT, Webster GD. 1970. Age and stratigraphy of the Heceta Limestone in northern Sea Otter Sound, southeastern Alaska. US Geological Survey Professional Paper 700, 170-174. US Dept. of the Interior, US Geological Survey.
- Peteet DM. 1986. Modern pollen rain and vegetational history of the Malaspina Glacier District, Alaska. *Quaternary Research* **25**(1) : 100-120.
- Petit JR, Jouzel J, Raynaud D, Barkov NI, Barnola JM, Basile I, Bender M, Chappellaz J, Davis, M, Delaygue, G, Delmotte M. 1999. Climate and atmospheric history of the past 420,000 years from the Vostok ice core, Antarctica. *Nature* **399**(6735) : 429-436.
- Simenstad CA, Wissmar RC. 1985. $\delta^{13}\text{C}$ evidence of the origins and fates of organic carbon in estuarine and nearshore food webs. *Marine Ecology Progress Series* **22** : 141-152.
- Spötl C, Mangini A. 2007. Speleothems and paleoglaciers. *Earth and Planetary Science Letters* **254**(3) : 323-331.
- Stephens FR. 1969. Source of cation exchange capacity and water retention in southeast Alaskan spodosols. *Soil Science* **108**(6) : 429-431.
- Stephens FR, Gass CR, Billings RF. 1970. Muskegs of southeast Alaska and their diminished extent. *Northwest science* **44** : 123-130.
- Thompson RS, Anderson KH, Strickland LE, Shafer SL, Pelltier RT, Bartlein PJ. 2006. Atlas of relations between climatic parameters and distributions of important trees and shrubs in North America: Alaska species and ecoregions. US Geological Survey Professional Paper 1650-D. US Dept. of the Interior, US Geological Survey.
- Van de Water PK, Leavitt SW, Betancourt JL. 2002. Leaf $\delta^{13}\text{C}$ variability with elevation, slope aspect, and precipitation in the southwest United States. *Oecologia* **132**(3) : 332-343.
- Warner BG, Mathewes RW, Clague JJ. 1982. Ice-free conditions on the Queen Charlotte Islands, British Columbia, at the height of late Wisconsin glaciation. *Science* **218**(4573) : 675-677.
- Western Regional Climate Center, 2017. Craig Alaska Climate Summary. Retrieved from <http://www.wrcc.dri.edu/cgi-bin/cliMAIN.pl?ak2227> [4 March 2016].

Wilcox, P.S., Fowell, S.J., Bigelow, N.H., Baichtal, J.F., Raphael Dreier. 2017. Variable Younger Dryas Based on Palynological and Sedimentological Analyses of Lacustrine Cores from Baker Island, Southeast Alaska. Prepared for submission in the Journal of Palaeogeography, Palaeoclimatology, Palaeoecology.

4.10 Figures

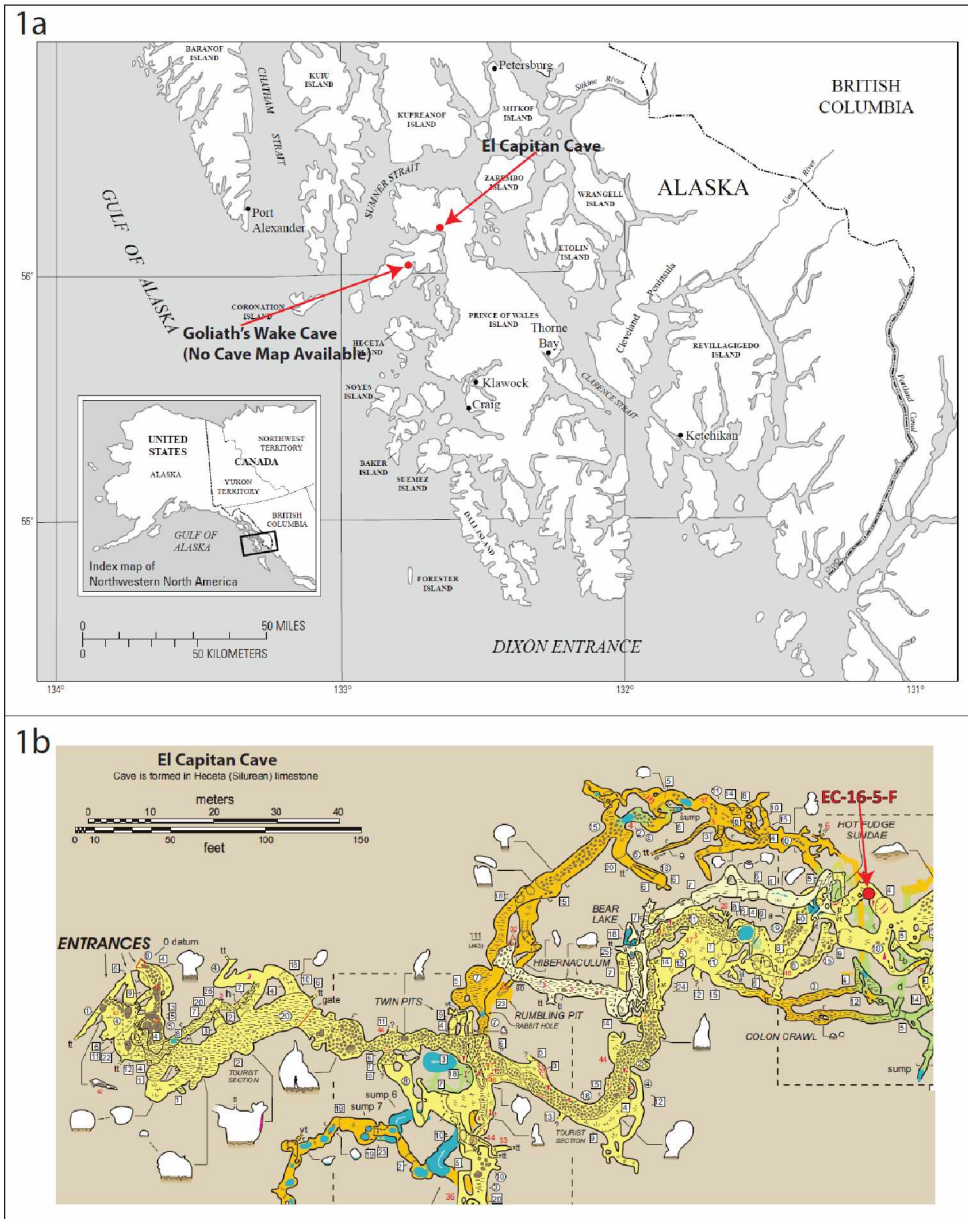


Figure 4.1: Site Location of El Capitan Cave and Goliath's Wake Cave/map of El Capitan Cave. a.) Site Location of El Capitan Cave on Prince of Wales Island and Goliath's Wake Cave on Kosciusko Island in Southeast Alaska. b.) Map of El Capitan Cave with speleothem sample location.

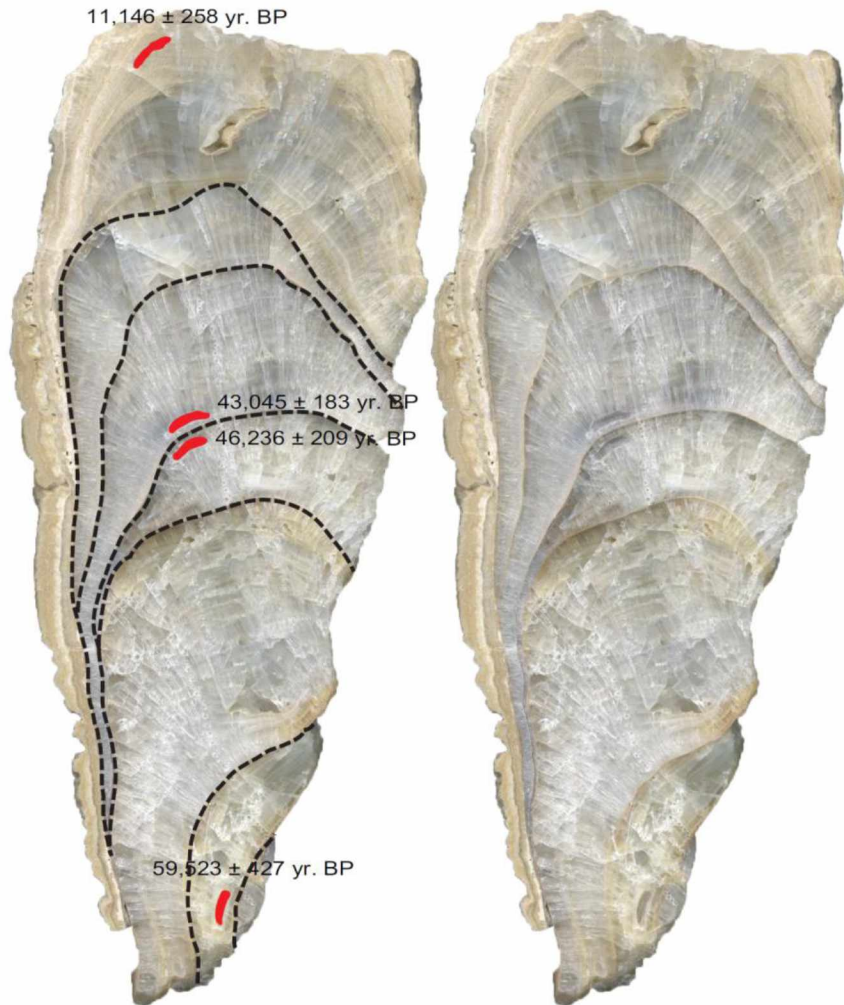


Fig. 4.2: Photo of speleothem with U/Th sampling sites and possible unconformities. Photo of speleothem EC-16-5-F with U/Th sampling sites (red ovals). Dashed lines indicate possible unconformities based on color and growth direction changes. Unedited photo of speleothem EC-16-5-F also shown.

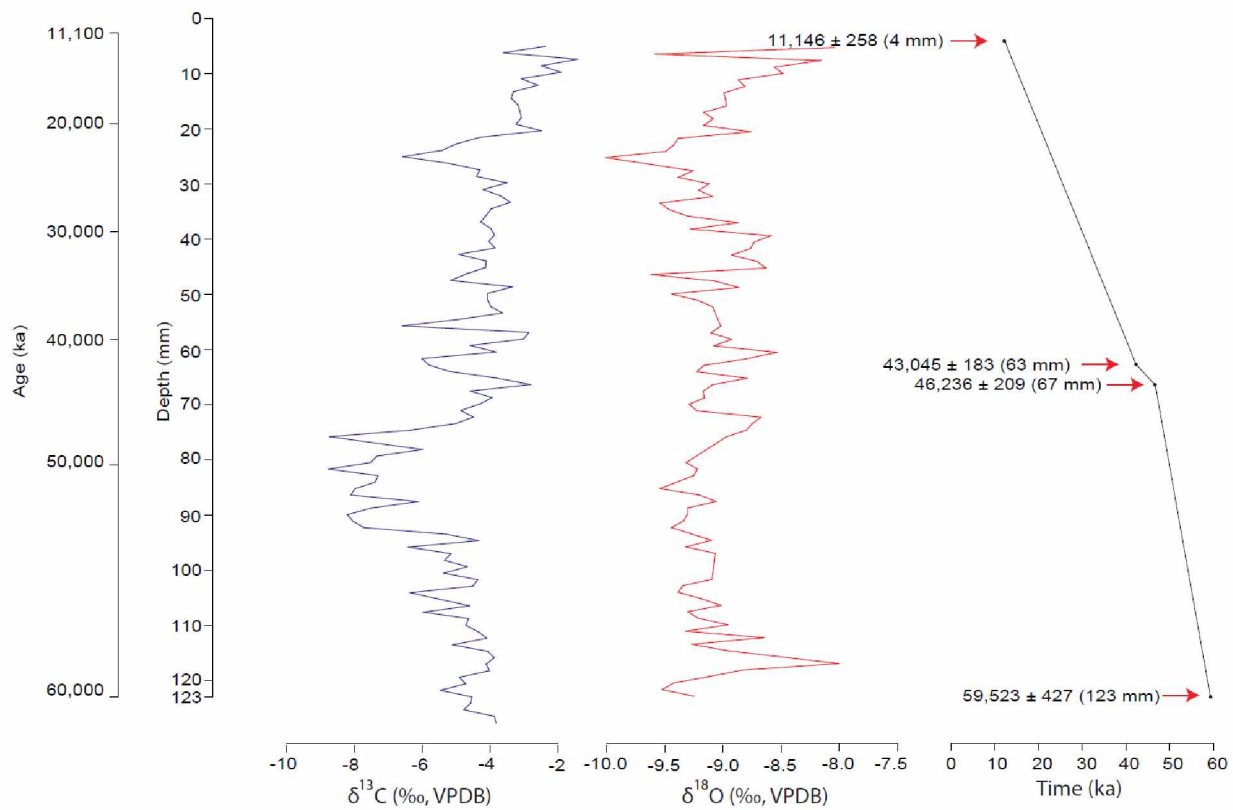


Fig. 4.3: Age and depth of $\delta^{13}\text{C}$ and $\delta^{18}\text{O}$ samples.

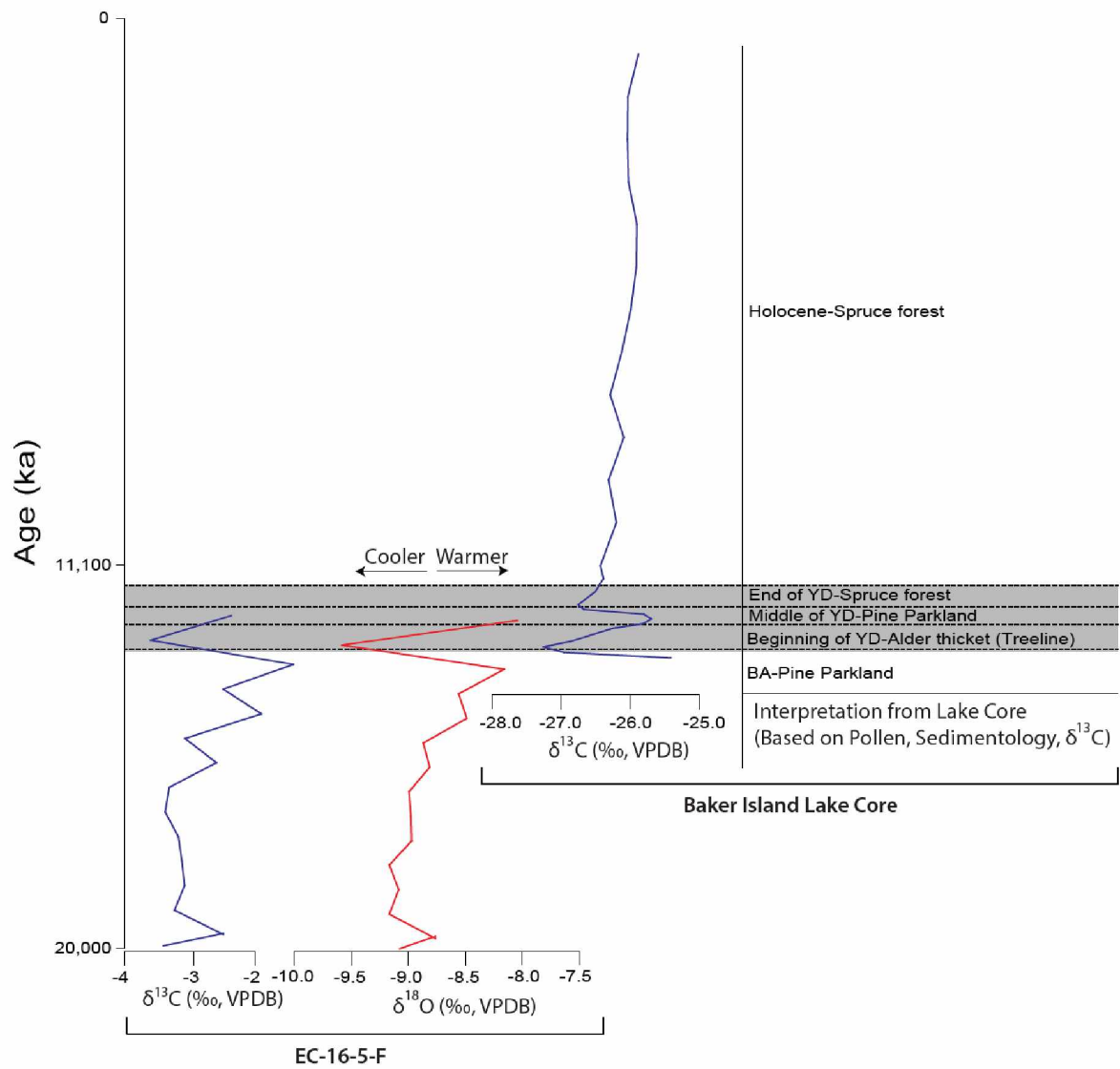
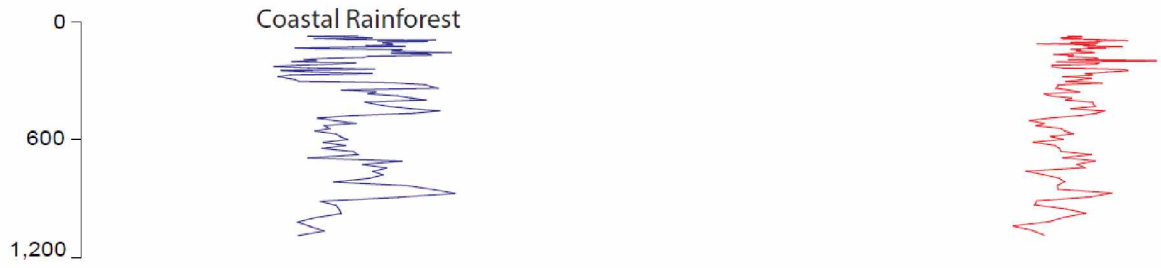


Fig. 4.4. Overlapping records of EC-16-5-F and Baker Island lake core. $\delta^{13}\text{C}$ and $\delta^{18}\text{O}$ from speleothem EC-16-5-F plotted next to $\delta^{13}\text{C}$ and vegetation interpretations from Baker Island lake core. EC-16-5 is cropped at 20,000 yr. BP to focus on the interval where the two records overlap. Gray shaded area represents YD interval.

Goliath



EC-16-5-F

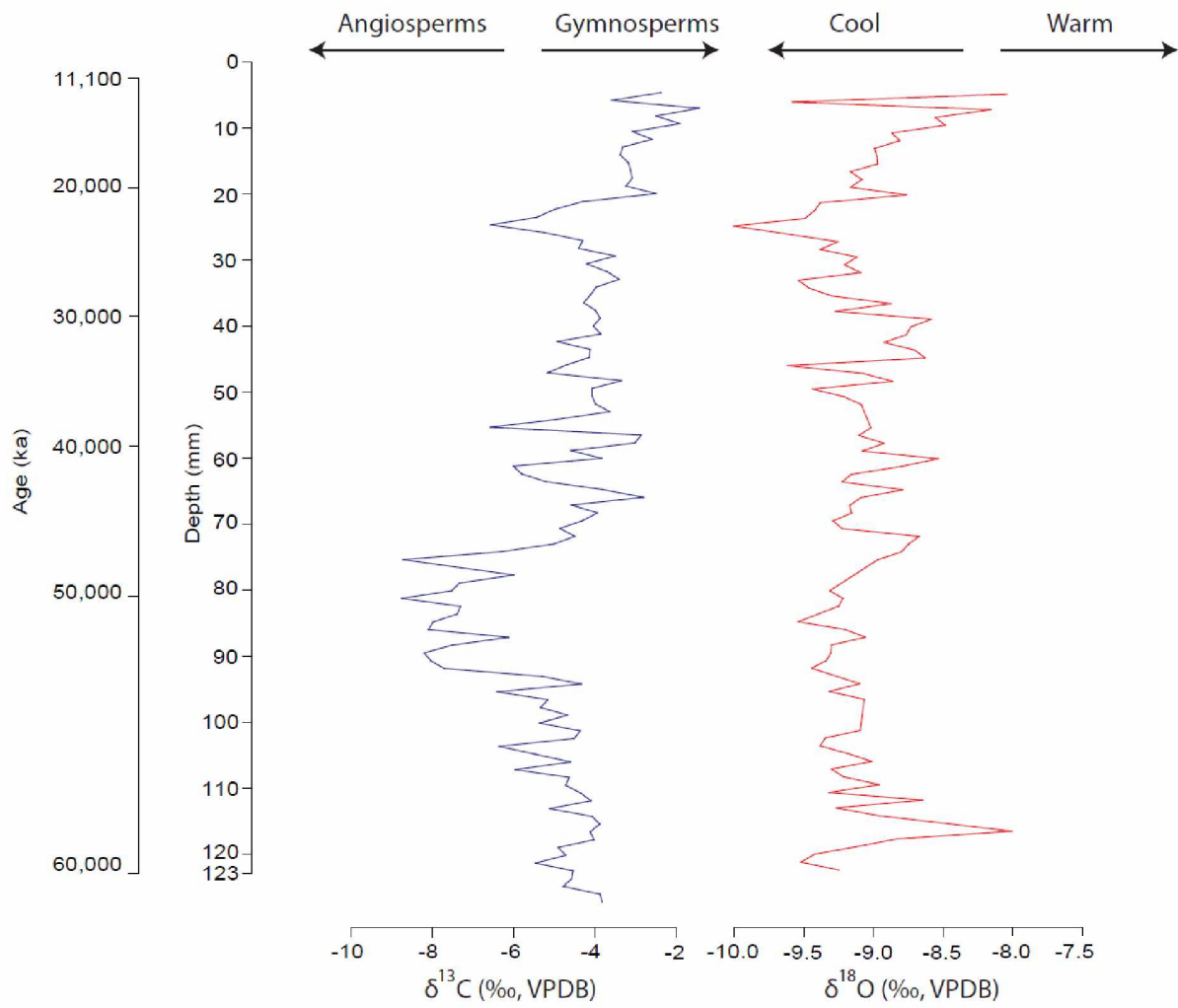


Fig. 4.5: Vegetation interpreted from $\delta^{13}\text{C}$ in EC-16-5-F and Goliath's Wake Cave.

4.11 Acknowledgments

This work was funded by the University of Alaska Global Change Grant, The University of Alaska Geist Fund, the Alaska Geological Society, and the Alaska Space Grant. I thank Dr. Jeff Dorale for allowing me to use his lab at the University of Iowa for isotope and uranium/thorium sampling.

Chapter 5: Conclusion

This research provides new insights on past climate and vegetation in Alaska over the past ~60,000 years. Palynological and sedimentological results from sediment cores retrieved from Baker Island extend to ~13,500 cal yr. BP. The palynological record hints at nearby refugia, as pollen of *Pinus* and *Tsuga mertensiana* appeared immediately after glacial retreat at ~13,500 cal yr. BP. The palynological and sedimentological results also indicate a variable Younger Dryas (YD) interval, beginning cool and dry, but becoming warmer and more humid during the latter half.

Future work should focus on higher resolution palynology/sedimentology of the Late Glacial in Southeast Alaska to better constrain the timing of YD and quantify climate fluctuations within the YD. This is important for calibration of climate models, which can then be used to help predict future climate scenarios in the region.

Speleothems collected from El Capitan Cave on Prince of Wales Island span the interval from ~11,100 yr. BP to ~60,000 yr. BP and show multiple glacial/interglacial periods defined by $\delta^{13}\text{C}$ and $\delta^{18}\text{O}$ isotopes. Changes in $\delta^{13}\text{C}$ values are thought to be driven by fluctuations in the abundance of angiosperms and gymnosperms in the local vegetation. Palynological records from Baker Island are used to help interpret vegetation changes in the speleothem $\delta^{13}\text{C}$ record. If the speleothem record is continuous, it indicates limited to no glaciation above the cave and the presence of continuous vegetation. In this case, the speleothem supports the palynological/sedimentological interpretation from Baker Island for glacial refugia in the region.

Much more future work needs to focus on speleothem reconnaissance and reconstruction because results from this research have shown that speleothems are a very powerful tool for climate reconstructions in the region. A quantitative approach for paleoclimate reconstruction should be used in

future studies. Typically, $\delta^{18}\text{O}$ of dripwater must be identified to determine paleotemperatures. This is achieved by either knowing the groundwater age and isotopic composition near the studied cave, or using fluid inclusions within the speleothem calcite. Carbonate clumped isotope thermometry can also be used to calculate paleotemperatures and does not require the $\delta^{18}\text{O}$ of precipitating fluid.

For more detailed paleovegetation and temperature reconstructions, a speleothem extending throughout the entire Holocene and into the Pleistocene must be attained. Pollen from lake cores can then be used to compare and interpret $\delta^{13}\text{C}$ values from the speleothem, and the youngest portion of the record can be compared to modern climate data.

In addition to climate/vegetation interpretations, a ~13,500 cal yr. BP tephra was identified and examined from the Baker Island sediment core. Geochemical analyses indicates that it has a tephritic/trachybasalt composition and erupted from a large strombolian style eruption, possibly a paroxysm. It is distinct from other eruptions in the region, such as Mt. Edgecumbe with respect to both composition and location. The Addington Volcanic Field, 38 km West of Baker Island, is a potential source area. Coeval eruptions in the region may have been caused by ice sheet retreat (Praetorius et al., 2016). The tephra can be used to help calibrate radiocarbon chronologies in the region and, thereby, help establish migration patterns of postglacial vegetation.

Additional work needs to be done to confirm if the Addington Volcano Field is the source for the black tephra on Baker Island and surrounding islands by sampling tephra at the Addington Volcano Field for geochemical analyses. Additionally, the age of the Addington Volcano Field would need to be determined to confirm if it was the source of the tephra from Baker Island. A sea core would need to be collected from the Addington Volcano Field to determine its geochemical composition and age.

5.1 References

Praetorius, S., Mix, A., Jensen, B., Froese, D., Milne, G., Wolhowe, M., Addison, J., Prah, F., 2016. Interaction between climate, volcanism, and isostatic rebound in Southeast Alaska during the last deglaciation. *Earth and Planetary Science Letters* 452, 79-89.